INVESTIGATING THE INACTIVATION, PHYSIOLOGICAL CHARACTERISTICS AND TRANSCRIPTOMIC RESPONSES OF BACTERIA EXPOSED TO IONIZING RADIATION

A Dissertation

by

ANNE-SOPHIE CHARLOTTE HIEKE

Submitted to the Office of Graduate and Professional Studies of
Texas A&M University
in partial fulfillment of the requirements for the degree of

DOCTOR OF PHILOSOPHY

Chair of Committee,	Suresh D. Pillai
Committee Members,	Stephen H. Safe
	Timothy D. Phillips
	Leslie A. Braby
	Ivan V. Ivanov
Interdisciplinary Faculty Chair,	Timothy D. Phillips

December 2015

Major Subject: Toxicology

ABSTRACT

Ionizing radiation is used for many different applications that require a reduction in microbial bioburden. Yet, the scientific literature remains unsettled when it comes to the relative biological effectiveness or kill efficiency of the different types of ionizing radiation, electron beam, gamma, and x-ray. The first objective of this study was to determine if the inactivation kinetics and D_{10} values (dose required to kill 90% of the population) of *Escherichia coli* and *Salmonella* are different for six different ionizing radiation sources under the same experimental conditions and using the same dosimetry system. The results indicate that there is no difference in the relative biological effectiveness of different ionizing radiation sources. Furthermore, the physiological characteristics as well as the transcriptomic responses of bacteria exposed to lethal (no bacterial replication) ionizing radiation doses was investigated. *Salmonella* Typhimurium and *E. coli* cells were irradiated and the following physiological characteristics were examined: membrane integrity, DNA damage, metabolic activity, ATP levels, and overall cellular functionality. The results showed that the membrane integrity of *S.* Typhimurium and *E. coli* cells was maintained and that the cells remained metabolically active when stored at 4°C. The ATP levels in lethally irradiated cells were similar to non-irradiated (control) cells. Extensive DNA damage was also visualized and overall cellular functionality was confirmed via bacteriophage propagation. To investigate the transcriptomic response of *S.* Typhimurium following a lethal ionizing radiation dose, total RNA was extracted and RNA Sequencing (RNA-Seq) analysis was

performed. The results of this study show that post-irradiation incubation in PBS buffer at 4°C results in minimal differential gene expression in irradiated cells. When incubated in growth media (TSB) at 37°C, the transcriptomic response for irradiated cells is markedly different from non-irradiated (control) cells. In general, lethally irradiated cells focus on repairing DNA and membrane damage. Major, long-term metabolic pathways, such as the citric acid cycle, are down-regulated, presumably to redirect the energy expenditure to focus on DNA and membrane repair. In essence, lethal ionizing radiation creates senescent bacterial cells that are no longer capable of dividing but are still alive and metabolically active for an extended period of time after irradiation.

DEDICATION

To my family.

ACKNOWLEDGEMENTS

I would like to express my gratitude to my advisor, Dr. Suresh D. Pillai. Thank you for your support and guidance throughout the years. I would also like to thank my committee members, Dr. Timothy D. Phillips, Dr. Stephen H. Safe, Dr. Leslie A. Braby, and Dr. Ivan V. Ivanov. Your advice, support and kindness greatly helped me in my pursuit of earning my doctorate. I would also like to thank Dr. Giri Athrey for kindly substituting at my defense.

I would like to thank the staff at the National Center for Electron Beam Research as well as the staff at the Nuclear Science Center for helping me perform my irradiation experiments.

I would like to thank my past and present lab members. I am grateful to have had the opportunity to share this experience with you. I will always cherish our intellectual discussions, long days in the lab and our extracurricular activities. I would like to thank Dr. Noushin Ghaffari for her technical assistance with the RNA-Seq data analysis. Thanks also go to my friends and colleagues and the department faculty and staff for making my time at Texas A&M University a great experience. And finally, I would like to thank my family for their support throughout this process.

TABLE OF CONTENTS

Page

LIST OF FIGURES

Page

LIST OF TABLES

Page

CHAPTER I

INTRODUCTION

Ionizing radiation has been used for decades to sterilize medical equipment and reduce the bioburden on food products such as mangoes (1). There are three major types of ionizing radiation, namely electron beam (eBeam), gamma rays, and x-rays. All three types are used for commercial radiation processing. Historically, gamma rays, produced by radioactive isotopes, such as Cobalt-60, have been used predominantly in commercial radiation processing. A large part of the ionizing radiation research has focused on gamma and x-rays (2-8). In the early days (1930s-1970s), the effects of ionizing radiation in terms of kill efficiency were of interest (2, 9-18). At this time, the science of radiation dosimetry was still in its infancy and microbiological as well as molecular techniques were not as advanced as they are today. This led to discrepancies in the results and left the radiation field unsettled with regards to the relative biological effectiveness (RBE) or kill efficiency of the different ionizing radiation sources. In recent years, one area of interest has been the development of vaccines through ionizing radiation (19-21). All of these studies have shown that lethally irradiated bacteria impart an immune response similar to live vaccines, indicating that the epitopes' structure and functionality are preserved (19-22). However, no one has investigated the transcriptomic response of lethally irradiated bacteria.

Relevance of Research

Ionizing radiation is used to sterilize medical devices, reduce the bioburden in food products, and crosslink polymers. Investigating the relative biological effectiveness (RBE) or kill efficiency of the different types of ionizing radiation under the same experimental conditions and with the same dosimetry system will help clarify if the RBE is different for different ionizing radiation sources. This research will be useful for the radiation processing community. Investigating the physiological and transcriptomic responses of lethally irradiated bacteria will contribute to the general knowledge base of the effects of lethal ionizing radiation.

Rationale

In order to delineate the RBE of different ionizing radiation sources, the inactivation kinetics of two bacteria were studied, namely *Escherichia coli*, a prototypical gram-negative bacterium and *Salmonella enterica* serovar Typhimurium, a common foodborne pathogen. In addition, we chose to focus on eBeam, gamma and x-ray radiation since these three types are commonly used in commercial sterilization and pasteurization applications.

In order to elucidate the physiological responses of lethally irradiated bacteria, the following characteristics were examined: cellular membrane integrity, DNA damage, metabolic activity, ATP levels, and the ability to propagate bacteriophages. To gain a

better understanding of the global transcriptomic response of *S.* Typhimurium to lethal ionizing radiation, RNA Sequencing (RNA-Seq) experiments were performed.

Major Objectives

The first major objective was to determine if the inactivation kinetics and D_{10} values (dose required to kill 90% of the population) of bacteria are different for different ionizing radiation sources. The second major objective was to characterize *S.* Typhimurium and *E. coli* cells exposed to lethal gamma and electron beam (eBeam) irradiation. The third major objective was to determine if there is a difference in gene expression in lethally eBeam irradiated and lethally gamma irradiated *S.* Typhimurium cells compared to each other as well as non-irradiated (control) cells.

Specific Objectives

1. Determine the D_{10} values for *E. coli* and *Salmonella* spp. for the six different ionizing radiation sources.
2. Characterize the cellular membrane integrity of lethally irradiated cells.
3. Visualize the DNA Double-Strand Breaks (DSBs) in lethally irradiated cells using the neutral comet assay.
4. Monitor the metabolic activity in lethally irradiated cells over time.
5. Monitor the ATP levels in lethally irradiated cells over time.
6. Study the overall cellular functionality of lethally irradiated cells via bacteriophage propagation.

7. Study the global transcriptomic response of *S*. Typhimurium to lethal eBeam and gamma irradiation when incubated in buffer at 4°C and growth media at 37°C at three different time points (0, 4, 24 hours) after irradiation.

CHAPTER II

LITERATURE REVIEW

Ionizing Radiation

Ionizing radiation is characterized by its ability to excite and ionize atoms in matter (23). It carries enough energy, at least 4-25 electron volts (eV), to liberate a valance electron from an atom or molecule (23). The important types of ionizing radiation are gamma rays, x-rays, fast electrons, heavy charged particles, and neutrons (23). Since only gamma rays, x-rays, and fast electrons are used in commercial radiation processing, only these three types of ionizing radiation will be discussed in greater detail. Gamma rays (photons) are electromagnetic radiation that is emitted from a nucleus or in annihilation reactions between matter and antimatter (23). The practical range of photon energies emitted by radioactive atoms is 2.6 keV – 7.1 MeV (23). X-rays are electromagnetic radiation that is emitted by charged particles, usually electrons, in changing atomic energy levels (characteristic or fluorescence x-rays) or by slowing down in a Coulomb force field (continuous or Bremsstrahlung x-rays) (23). An x-ray photon and a gamma-ray photon of a given quantum energy have identical properties, differing only in mode of origin (23). Fast electrons can be emitted from a nucleus (beta-rays) or be the result of a charged particle collision (delta-rays) (23). Pulsed electron beams of high energies (i.e. 10 MeV) are available from linear accelerators ("linacs"), betatrons, and microtrons (23). The kinetic or photon energies most frequently used in research and commercial applications of ionizing radiation ranges from 10 keV to 10 MeV (23).

Ionizing radiation is typically divided into two categories: directly ionizing and indirectly ionizing. Directly ionizing radiation consists of fast charged particles (mainly electrons), which deliver their energy to matter directly, through many small Coulomb-force (electrostatic) interactions along the particle's track (23). Indirectly ionizing radiation consists of x- or gamma-ray photons or neutrons (uncharged particles), which first transfer their energy to charged particles (mainly electrons) in the matter through which they pass (23). An individual photon may pass through matter with no interactions at all, hence no loss of energy. Or it may interact and lose its energy in one or a few interactions. From a stochastic viewpoint, it is impossible to predict even crudely how far an individual photon will penetrate through matter, since only one or a few randomly occurring interactions are needed to dissipate all of its energy (23). The absorbed energy is given by the SI unit "Gray", where 1 Gray (Gy) is equal to 1 Joule (J) per kilogram (kg) of mass (23). X- and gamma-ray photons can interact with matter in five different ways: Compton effect (dominates at medium photon energies), photoelectric effect (dominates at lower photon energies), pair production (dominates at higher photon energies), Rayleigh (coherent) scattering, and photonuclear interactions (23). The first three are the most important, as they result in the transfer of energy to electrons, which then impart that energy to matter in many (usually small) Coulomb-force interactions along their tracks (23). During a Compton interaction, a photon, carrying a certain energy and forward momentum, collides with a target electron (assumed to be unbound (free) and stationary) that has no initial energy or momentum. After the collision, the electron departs at a certain angle with a certain energy and forward momentum. The

photon scatters at a different angle and with a new, lower energy and momentum. During a Compton collision, the photon cannot give up all of its energy (23). At low photon energies, the photoelectric effect dominates over the Compton effect, particularly with respect to the energy transferred to secondary electrons (23). During a photoelectric interaction, an incident photon, carrying a certain energy, interacts with an atomic-shell (tightly-bound) electron and is totally absorbed and ceases to exist. This interaction can only take place if the energy of the photon is greater than the potential energy of the tightly-bound electron. The electron departs from this interaction at a certain angle carrying momentum. When an electron is removed from an inner atomic shell by any process (i.e. photoelectric effect, charged particle hard collision), the resulting vacancy is immediately filled by another electron falling from a less tightly bound shell (i.e. higher energy orbital) (23). Pair production is an absorption process in which a photon disappears and gives rise to an electron and a positron. It can only occur in a Coulomb force field, usually that near an atomic nucleus. The electron and positron do not necessarily receive equal kinetic energies (23).

Other than photons, charged particles (mainly electrons) interact directly with matter. A charged particle (i.e. an electron), being surrounded by its Coulomb electric force field, interacts with one or more electrons or with the nucleus of practically every atom it passes. The probability of a charged particle passing through matter without any interaction is zero. For example, a 1 MeV charged particle (i.e. electron) would typically undergo 10^5 interactions before losing all of its kinetic energy (23). Charged particles

can interact with matter in three different ways: “soft” collisions, “hard” (or “knock-on”) collisions, and Coulomb-force (electrostatic) interactions with the external nuclear field. During “soft” collisions, a charged particle passes an atom at a considerable distance. The influence of the charged particle’s Coulomb force field affects the atom as a whole, thereby distorting it, exciting it to a higher energy level, and sometimes ionizing it by ejecting a valence-shell electron. The net effect is the transfer of a very small amount of energy (a few eV) to an atom of the absorbing medium. “Soft” collisions are by far the most numerous type of charged-particle interaction, and they account for roughly half of the energy transferred to the absorbing medium (23). During “hard” (or “knock-on”) collisions, the incident charged particle interacts primarily with a single atomic electron, which is then ejected from the atom with considerable kinetic energy. This kinetically energetic electron is called a delta (δ) ray. Delta rays are energetic enough to undergo additional Coulomb-force (electrostatic) interactions on their own. Although “hard” collisions are few in number compared to “soft” collisions, the fractions of the primary charged particle’s energy that are spent by these two processes are generally comparable. Whenever an inner-shell electron is ejected from an atom by a “hard” collision, characteristic x-rays will be emitted (23). When a charged particle passes an atom at a close distance, Coulomb-force (electrostatic) interactions take place mainly with the nucleus. In 97-98% of all encounters, the electron is scattered elastically and does not emit an x-ray photon or excite the nucleus. It loses just the insignificant amount of kinetic energy necessary to satisfy conservation of momentum for the collision. Hence this is not a mechanism for the transfer of energy to the absorbing medium, but it is an

important means of deflecting electrons. This is why electron backscattering increases with the atomic number (Z). This means that a thin foil of high Z material (i.e. tantalum, tungsten, or lead) may be used as a scatterer to spread out an electron beam while minimizing energy loss. In the other 2-3% of interactions in which the electron passes near the nucleus, an inelastic radiative interaction occurs in which an x-ray photon is emitted. The electron is not only deflected in this process, but gives a significant fraction (up to 100%) of its kinetic energy to the photon, slowing down in the process. Such x-rays are referred to as Bremsstrahlung. Bremsstrahlung production is relatively insignificant in low-Z (tissue-like) materials for electrons below 10 MeV. Not only is its probability of occurring low, but the resulting photons are penetrating enough so that most of them can escape from objects several centimeters in size. Thus they usually carry away their energy rather than expending it in the medium through further interactions (23). The expected rate of energy loss, or stopping power, by an electron traveling through matter depends on the particle's energy and the medium's atomic number (Z). The more energetic the electron, the lower its stopping power. In other words, high energy electrons move so fast that they only interact with the medium in "soft" collisions, hence not giving away much of their energy (23).

Applications of Ionizing Radiation

Ionizing radiation is used for a wide variety of applications such as the sterilization of medical devices and pharmaceutical products, food irradiation, insect pest control, flue gas treatment, wastewater purification, sludge treatment, curing of composite materials,

and polymer crosslinking (24-30). Many of these applications require a reduction in microbial bioburden. Commercially, ionizing radiation is most successful in the field of medical device sterilization. The use of ionizing radiation as a sterilization method for medical devices was developed in the 1950s-1960s, even though the ability of ionizing radiation to kill microorganisms had been known since the 1920s (10). Between 1960-1970, extensive research was conducted on the physical, chemical, and (micro)biological aspects of medical device sterilization. These efforts were mainly driven by the International Atomic Energy Agency (IAEA) (10). By the 1970s, sterilization of medical products (in their final packaging) by ionizing radiation, almost exclusively from gamma sources (i.e. Cobalt-60), had been widely accepted within the industry (10). A minimum dose of 25 kilo gray (kGy) was established in the early 1970s. This dose was largely based on bioburden reduction studies (10). Even in those early days, there was already controversy surrounding the minimum dose requirement and how microbial resistance to ionizing radiation was determined (10). Different researchers reached different conclusions when it came to the inactivation kinetics of microorganisms (10). These discrepancies were not only a result of inter-laboratory variability in terms of microbiological methods used, but also of different dosimetry systems employed (10). This issue was only intensified when electron beam technology was introduced as an ionizing radiation source in the medical device industry. This led to the scientific literature being unsettled with regards to the Relative Biological Effectiveness (RBE) or kill efficiency of the different ionizing radiation sources (2, 9-18).

Food irradiation is over 100 years old and is one of the most extensively studied food preservation methods (31, 32). However, it has been greatly underutilized commercially due to a number of reasons including psychological and political factors (31, 32). In recent years, there has been a renewed interest in commercial food irradiation, especially for phytosanitary treatment (insect pest control) of fruits and vegetables to facilitate international trade (24). Nonetheless, food irradiation has been endorsed as a safe and effective food preservation method by numerous international organizations such as the IAEA, the Food and Agriculture Organization (FAO), the World Health Organization (WHO), and the Codex Alimentarius. Worldwide, food irradiation has been approved in over 55 countries and is used commercially to irradiate fresh and frozen meats, spices, fresh produce, seafood, and food ingredients (28, 31, 32). In the U.S., food irradiation has been approved by the Food and Drug Administration (FDA) and the Department of Agriculture (USDA) (32). It is estimated that in the U.S. approximately 175 million pounds of spices, 18 million pounds of ground beef, and 8 million pounds of produce (for phytosanitary treatment) are currently irradiated (33). The volume of agricultural commodities imported into the U.S. that are treated by ionizing radiation has also increased significantly from 195,000 kg in 2007 to 12,853,000 kg in 2013 (34).

Numerous environmental applications for ionizing radiation have also been identified, such as wastewater purification and sludge treatment (29), but most of them are still in the research & development phase. In recent years, research focusing on irradiated microorganisms for use as killed vaccines has also been forthcoming (19-21).

Ionizing Radiation Dose Rate and Energy Effects on the Inactivation Kinetics of Microorganisms

Research on the inactivation kinetics of microorganisms exposed to ionizing radiation was largely conducted from the 1930s to the 1970s. However, to this day the relative biological effectiveness (RBE) of the different ionizing radiation sources is questioned (2, 8, 9, 11-15, 18, 35-37). Early radiation research focused on the dose rate and energy effects of ionizing radiation. In 1958, Howard-Flanders found that x-ray radiation was more effective in inactivating plant and mammalian cells if delivered quickly (6). A study from the same year showed that the lower the dose rate of Cobalt-60 gamma irradiation, the lower the dose required to completely sterilize *E. coli* and *Bacillus subtilis* (17). Yet another study from the same year showed that the higher the dose rate of x-rays, the more effective the inactivation of *Bacillus megaterium* (38). A comparative study between x-rays and eBeam found that *B. megaterium* was more resistant to eBeam than to x-rays (11). Another study comparing 1.5 MeV x-rays and electrons found a dose rate effect due to oxygen depletion for the inactivation of *Serratia marcescens*. For low dose rate x-rays (10 Gy/min), a 1% oxygen concentration was sufficient to produce 60-70% of the full (100%) oxygen effect in terms of inactivation. On the other hand, for high dose rate eBeam (750 Gy/μs), a 1% oxygen concentration produced the same radiosensitivity as anoxic conditions (nitrogen), making *S. marcescens* more resistant to high dose rate eBeam (36). When investigating the inactivation kinetics of *B. megaterium* with 12 MeV electrons, Purdie et. al. (1974) found that the higher the instantaneous dose rate, the more sensitive the organism (12).

When *B. megaterium* was studied under pulsed electrons, it was found that the higher the dose rate (18-72 Gy/min), the more resistant the organism (39). Saleh found that when *B. megaterium* was exposed to pulsed electrons at a dose rate of 10 Gy/µs, the organism's response was the same as for gamma radiation (40). Between dose rates of 10-200 Gy/µs *B. megaterium* was more radiosensitive and past 200 Gy/µs the organisms was most resistant (40). It is evident from these studies that there is no consensus among researchers even when a dose rate and/or energy effect was detected.

Other researchers found no dose rate or energy effect of ionizing radiation on the inactivation kinetics of microorganisms. When investigating the effect of x-rays and oxygen on *E. coli*, no dose rate effect was observed in the absence of dissolved oxygen (4, 5). Tarpley et. al. studied the effects of Cobalt-60 gamma radiation on vegetative and spore-forming organisms and found that only the total dose rather than the dose rate mattered (8). Other studies, investigating the inactivation kinetics of *E. coli* and *B. subtilis* with x-rays and electrons also observed no dose rate effect (3, 35, 41, 42). After the 1970s, the research focus shifted from the RBE of the different ionizing radiation sources to the effects of ionizing radiation on the organism itself, i.e. DNA damage. This shift in research focus was accompanied by advancements in the field of molecular biology.

Effects of Ionizing Radiation on Microorganisms

Research studying the effects of ionizing radiation on bacterial cells has been exclusively focused on sub lethal doses. This is not surprising since it was assumed that only viable cells are able to mount a physiological response to radiation stress. However, more recent studies have shown that lethal ionizing radiation stress leaves bacterial membranes intact and cells metabolically active (19-21). The majority of cellular damage due to ionizing radiation is actually caused by reactive oxygen species (ROS) formed in the cell during irradiation rather than the incident electrons (43). The creation of hydroxyl radicals (OH*), hydrogen peroxide (H_2O_2), and superoxide radical anions (O_2-*) leads to oxidative protein damage in irradiated cells (44). Hydroxyl radicals, created through the radiolysis of water, cause global, indiscriminate damage within the cell. However, they are short lived and can only damage molecules in their immediate surroundings (44). The superoxide radical is thought to create more severe and targeted protein damage because firstly, it does not easily cross the bacterial membrane and hence accumulates in the cell and secondly, it specifically targets enzymes with exposed iron-sulfur clusters (44).

Since the 1960s, "death by DNA damage" has been the central dogma in radiobiology (45). Ionizing radiation causes both DNA single-strand breaks as well as DNA double-strand breaks (DSBs) (46). DSBs are the most lethal form of DNA damage and most organisms can generally tolerate only a few of them (47). It has been estimated that 100 Gy of ionizing radiation cause approximately 1 DSB per one million base pairs (Mbp)

(48). Since the ultimate fate of a cell depends on its ability to preserve and replicate its genome, most studies have focused on how DNA is damaged by ionizing radiation and subsequently repaired by the cell (43, 49-51). Over the past several decades, researchers have tried to answer the question of radio-resistance. Why are some organisms more radio-resistant to ionizing radiation than others, considering both radio-resistant and radio-sensitive cells experience the same amount of DNA damage? The most logical answer was that radio-resistant organisms are better at repairing the DNA damage caused by ionizing radiation. Reports of homologous recombination in radio-resistant organisms soon followed (50-54). However, subsequent genome mapping revealed that radio-resistant bacteria did not possess unique DNA repair genes or a novel chromosome alignment that would facilitate homologous recombination (49, 55, 56). This led researchers to question the "death by DNA damage" dogma. In 2009, a new model was introduced: "death by protein damage" (44). In this model, proteins are the most important target of ionizing radiation. Since proteins are needed for all cellular functions, including DNA repair, protecting a cell's proteome is of utmost importance for the cell's survival. Studies have shown that radio-sensitive bacteria are more susceptible to oxidative protein damage than radio-resistant bacteria (57). It appears that radio-resistant bacteria protect their proteins through the accumulation of manganese complexes, which prevent the production of iron-dependent reactive oxygen species (44, 48). Researchers found that the radiation-resistant bacterium *Deinococcus radiodurans* contains far greater concentrations of manganese than radiation-sensitive bacteria (44). Furthermore, it was discovered that manganese forms complexes with ligands that act as

scavengers of superoxide radicals and other related ROSs and shield iron-sulfur cluster containing proteins from oxidative damage (48). It should be noted that in this "death by protein damage" model, the fate of a cell does not rest solely on the level of oxidative protein damage but also on the number of genome copies present and the genome size. Since DSBs are also occurring due to the radiation stress, the cell still needs systems that can rejoin random DSB ends (52). If the irradiated cell is overwhelmed by the sheer number of DSBs, it will ultimately be killed by the ionizing radiation stress, regardless of its ability to protect its proteome.

CHAPTER III

INACTIVATION KINETICS OF BACTERIA EXPOSED TO IONIZING RADIATION[*]

Overview

Ionizing radiation is used for many different applications that require a reduction in microbial bioburden. Yet, the scientific literature remains unsettled when it comes to the relative biological effectiveness of the different types of ionizing radiation, electron beam (eBeam), gamma, and x-ray. This is in large part due to the fact that researchers used many different dosimetry systems over the years. The inactivation kinetics of microbial cells exposed to ionizing radiation have been the key benchmark in comparing the effectiveness of the different ionizing radiation technologies as well as comparing the radiation sensitivity of different organisms. The objective of this study was to determine the inactivation kinetics of four different bacteria exposed to six different ionizing radiation sources using the same experimental conditions and the same dosimetry system. Overall, the results of our study indicate that the inactivation kinetics for *E. coli* and *Salmonella* are very similar for the different ionizing radiation sources. A statistically significant difference was detected between the different ionizing radiation sources for *E. coli* but not for *Salmonella*. This statistical difference is based on a rather small difference in absorbed dose (tens of Grays). Such a small difference in dose is

[*] Parts of this chapter are reprinted with permission from Hieke, A.-S. C. and S. D. Pillai. 2015. Attenuation of 10 MeV electron beam energy to achieve low doses does not affect *Salmonella* spp. inactivation kinetics. Radiation Physics and Chemistry 110: 38-41. Copyright 2015 Elsevier.

absorbed by the 5% margin of error in dose delivery by the radiation equipment and the 4-8% uncertainty in dosimetry under normal commercial radiation processing conditions (for any source type). Our results indicate that the radiation sensitivity of micro-organisms is the same for different ionizing radiation sources.

Introduction

Commercial radiation processing is used to reduce the microbial bioburden of a wide variety of products, such as food items, medical devices, blood bags, plastics, and polymers. In the United States, approximately 18 million pounds of frozen ground beef and about 175 million pounds of spices are irradiated every year for the purpose of pathogen reduction (33). The volume of agricultural commodities imported into the U.S. that are treated by ionizing radiation has increased significantly from 195,000 kg in 2007 to 12,853,000 kg in 2013 (34). Almost 50% of all medical devices and products are sterilized by ionizing radiation today. Whole blood is irradiated by gamma rays to destroy leukocytes to protect against transfusion associated diseases (58). Even though commercial irradiation services to reduce (or eliminate) bioburden are relatively common place, and the effectiveness of ionizing radiation to inactivate organisms has been studied for many decades, the scientific literature is still unsettled with regards to the Relative Biological Effectiveness (RBE) or kill efficiency of the different ionizing radiation sources (2, 9, 11, 12, 16-18, 59, 60). This disagreement is in large part due to the fact that a wide variety of dosimetry systems have been used. For example, Powers et.al. (38) used a windowless air-ionization chamber, Titani et.al. (17) used ferrous

dosimetry and Epp et.al. (36) used thermoluminescent dosimeters. Some studies even used two different dosimetry systems (37, 60), while others did not mention the use of a dosimetry system at all (59). Furthermore, almost all the articles dealing with the effects of ionizing radiation on microorganisms were published between 1930 and 1970. In those early days, the dosimetry systems were not as advanced as they are today and it is very likely that errors in the dosimetry occurred (A. Tallentire, pers. comm.). It is generally accepted that dosimetry systems carry a 4-8% uncertainty level inherent in their measurements (61). How the absorbed dose is measured can have an impact on experimental results and may lead to erroneous conclusions. Taking all of these factors into consideration, it is not surprising that the literature is unsettled. Hence, in our experiments we used the same dosimetry system (alanine) to measure the absorbed dose for all the different ionizing radiation sources to eliminate errors that could have been introduced by using different dosimetry systems. The alanine dosimetry system was chosen because it is considered the "gold standard" among dosimetry systems due to its accuracy in measuring absorbed dose over a wide dose range (10 Gy -100+ kGy) (61). Alanine dosimetry is based on the irradiation of L-α-alanine followed by free radical detection with an Electron Paramagnetic Resonance (EPR) spectrometer (61). EPR measures the absorbed energy due to the transition of unpaired electrons between different energy levels (61). Besides using only one dosimetry system, our study had the unique advantage that all ionizing radiation sources were located on the Texas A&M University campus, making it possible to maintain the same experimental conditions for all of them.

In order to delineate the RBE of different ionizing radiation sources, the inactivation kinetics of *Escherichia coli*, a prototypical experimental organism, and *Salmonella*, a prototypical foodborne pathogen, were studied. The primary objective of this study was to determine if the inactivation kinetics and D_{10} values (dose required to kill 90% of the population) of two *E. coli* strains and multiple *Salmonella enterica* serovars are different for different ionizing radiation sources. For the ionizing radiation sources, we focused on eBeam, gamma and x-ray since these three types are commonly used in commercial sterilization and pasteurization applications.

Materials and Methods

Target microorganisms

E. coli (ATCC 25922), *E. coli* (#5-an environmental isolate), *Salmonella* Typhimurium (ATCC 14028) (kindly provided by Dr. Robert Alaniz, Texas A&M University), *Salmonella* 4,[5],12:i:-, and a *Salmonella* cocktail consisting of *Salmonella* 4,[5],12:i:-, *Salmonella* Heidelberg, *Salmonella* Newport, and *Salmonella* Enteritidis were employed. (The serovars for the cocktail were kindly provided by Dr. James A. Byrd, USDA-ARS, College Station, TX).

Preparation of bacterial cultures

Overnight cultures of the various bacterial strains/serovars were grown in Tryptic Soy Broth (TSB) at 35°C in a shaking water bath. Cultures were centrifuged at 4000 x g for 10 minutes at Room Temperature (RT), the growth media removed and the cell pellets

washed once in Phosphate Buffered Saline (PBS). After washing, the cell pellets were resuspended in PBS to an OD_{600} of ca. 1.0, resulting in approximately $1x10^8$ Colony Forming Units (CFU)/ml. For the *Salmonella* cocktail, equal amounts of the individual cell suspensions were combined. Aliquots from the various cell suspensions were packaged for irradiation.

Packaging samples for irradiation

In order to comply with the biosafety regulations of Texas A&M University, aliquots of the cell suspensions were placed in heat-sealed double-bagged Whirl Pak bags (Nasco, New York, NY). These heat-sealed bags were then placed inside 95 kPa specimen transport bags (Therapak, Buford, GA). Previous studies in our laboratory have shown that irradiating cell suspensions in flat plastic bags produced a Dose Uniformity Ratio (DUR) close to 1.0. A DUR of 1.0 indicates complete dose uniformity throughout the sample. Samples were held at 4°C for less than 3 hours prior to irradiation and transported on ice in a Saf-T-Pak transport box (Saf-T-Pak, Hanover, MD). Non-irradiated samples (0 Gy) were used as controls. They were packaged the same way as samples destined for irradiation and were taken along to the irradiation facility to eliminate any differences in survival due to transport and holding conditions.

Radiation sources

Table 1 provides an overview of the six different ionizing radiation sources used in this study along with their respective energies and dose rates.

Table 1. Overview of the different ionizing radiation sources used in the study.

Radiation Source	Energy	Dose Rate
Electron Beam	10 MeV	ca. 3000 Gy/sec
	8.5 MeV	ca. 3000 Gy/sec
Gamma	1.59 MeV (Lanthanum-140)	ca. 4-7 Gy/min
	0.7-0.97 MeV (reactor core)	ca. 13 Gy/min
X-Ray	5 MeV (high energy)	ca. 100 Gy/sec
	100 keV (low energy)	ca. 0.6 Gy/min

Irradiation protocol

The eBeam irradiations were carried out at the National Center for Electron Beam Research (NCEBR) at Texas A&M University in College Station, TX using a 10 MeV and a 8.5 MeV, 15 kW eBeam linear accelerator. All eBeam irradiations were carried out at ambient temperature (ca. 25°C). Defined doses were targeted (ranging from 100 Gy to 1500 Gy, depending on the organism) and delivered by conveying the samples across the incident eBeam. Due to the high eBeam energy and conveyor belt speed limitations, it was necessary to attenuate the incident eBeam to achieve the low doses required for bacterial inactivation curves. The attenuated eBeam doses were obtained by placing eight 0.48 cm (3/16 inch) sheets of High Density Polyethylene (HDPE) (density: 0.95g/cm3) over the test samples and by varying the conveyor belt speed. To estimate the beam energy underneath the HDPE attenuators, 3 independent aluminum wedge tests (62) were performed. A comparison study was performed to determine whether or not attenuation alters the inactivation kinetics of bacteria. Non-attenuated eBeam doses were obtained by exposing the samples directly to the 10 MeV electron beam without any attenuation.

The gamma irradiations were carried out at the Nuclear Science Center (NSC) at Texas A&M University in College Station, TX using either an activated 1.59 MeV Lanthanum-140 (La-140) source or the nuclear reactor core (average gamma energy: 0.7-0.97 MeV) with a boron plate to shield neutron flux. It was determined that neutrons contributed less than 0.1 Gy to the overall absorbed gamma dose. For a more detailed explanation see Appendix A. All gamma irradiations were carried out at ambient temperature (ca. 25°C). Defined doses were targeted (ranging from 100 Gy to 1500 Gy, depending on the organism) and delivered by securing the samples to a cardboard holder, which in turn was taped to the exposure window.

The 5 MeV x-ray irradiations were carried out at the NCEBR using a 5 MeV, 15 kW x-ray linear accelerator. All x-ray irradiations were carried out at ambient temperature (ca. 25°C). Defined doses were targeted (ranging from 100 Gy to 1500 Gy, depending on the organism) and delivered by securing the samples to the opposite wall of the horizontally mounted x-ray linear accelerator.

The 100 keV x-ray irradiations were carried out at the NSC accelerator building using a Norelco MG300 industrial radiography machine consisting of one x-ray tube with a tungsten target. For voltages below 250 keV, the maximum current was 15 mA. All x-ray irradiations were carried out at ambient temperature (ca. 25°C). Defined doses were targeted (ranging from 50 Gy to 200 Gy, due to the low dose rate) and delivered by removing the filter and placing the samples directly underneath the x-ray tube.

Dosimetry

Alanine dosimetry was used for all the different radiation sources. This method is based on the irradiation of L-α-alanine followed by free radical detection with an Electron Paramagnetic Resonance (EPR) spectrometer (61). For a more detailed explanation see Appendix A. Dosimeters (L-α-alanine pellet dosimeters; Harwell Dosimeters, Oxfordshire, United Kingdom) were placed on the samples to measure the absorbed dose. The entrance and exit doses were measured and an average absorbed dose was calculated. Previous dose mapping for all the sources confirmed that the DUR was close to 1.0. The dosimeters were read using the Bruker e-scan EPR spectrometer (Bruker, Billerica, MA). The dosimetry system was traceable to international standards. The absorbed dose values were used for data plotting and analysis.

Bacterial enumeration

All samples were analyzed within 6 hours of irradiation. Samples were aseptically transferred from the Whirl Pak bags to sterile 2 ml microcentrifuge tubes. Tenfold serial dilutions were made in PBS as needed and 0.1 ml of either the original cell suspension or appropriate dilutions were plated onto Tryptic Soy Agar (TSA) plates and incubated at 35°C for up to 4 days. Colonies were enumerated after 24 hours and again on day 4 (to account for possible slow growers).

Data analysis

Each irradiation experiment was performed in triplicate, and whenever possible three independent irradiation experiments were performed. The surviving bacterial concentrations (CFU/ml) were plotted as a function of the absorbed dose (Gy). Preliminary experiments (data not shown) confirmed that bacterial inactivation was linear and therefore linear regression analyses were performed (63, 64). The negative reciprocal of the slope was calculated to be the D_{10} value (dose required to kill 90% (or 1 log) of the population). Student's t-test was performed to determine whether there was any statistically significant difference (P-value <0.05) between the organisms' D_{10} values for the different ionizing radiation sources.

Results

Electron beam radiation

10 MeV electron beam

The inactivation curves of *E. coli* (25922), *E. coli* (#5), *S.* Typhimurium, and *S.* 4,[5],12:i:- in PBS under 10 MeV eBeam irradiation are shown in Figures 1 and 2. The D_{10} values of *E. coli* (25922), *E. coli* #5, *S.* Typhimurium and *S.* 4,[5],12:i:- were calculated to be 68±4 Gy, 107±2 Gy, 170±16 Gy, and 147±15 Gy, respectively.

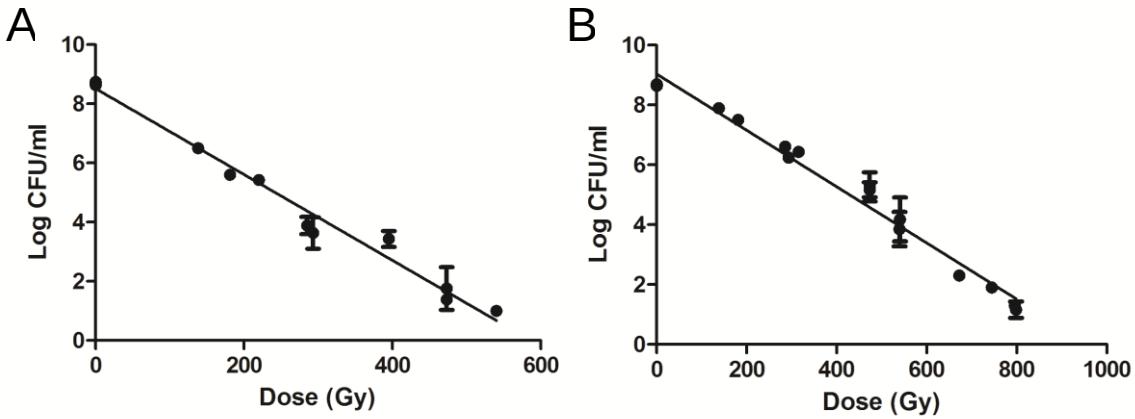

Figure 1. Inactivation of (A) *E. coli* (25922) and (B) *E. coli* (#5) in PBS under 10 MeV eBeam irradiation with D_{10} values of 68±4 Gy and 107±2 Gy, respectively. For each organism, three independent experiments were performed in triplicate, with standard deviations shown.

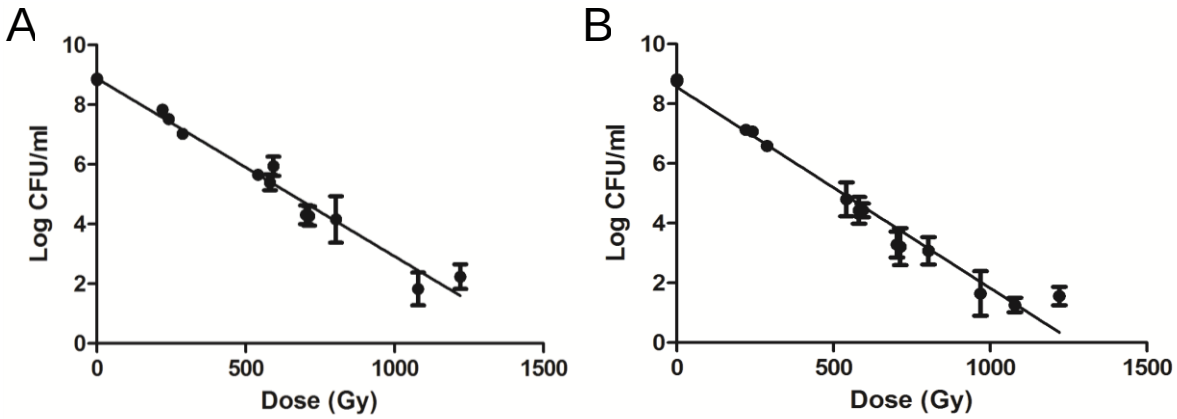

Figure 2. Inactivation of (A) *S.* Typhimurium and (B) *S.* 4,[5],12:i:- in PBS under 10 MeV eBeam irradiation with D_{10} values of 170±16 Gy and 147±15 Gy, respectively. For each organism, three independent experiments were performed in triplicate, with standard deviations shown.

8.5 MeV electron beam

The inactivation curves of *E. coli* (25922), *E. coli* (#5), *S.* Typhimurium, and *S.* 4,[5],12:i:- in PBS under 8.5 MeV eBeam irradiation are shown in Figures 3 and 4. The D_{10} values of *E. coli* (25922), *E. coli* (#5), *S.* Typhimurium and *S.* 4,[5],12:i:- were calculated to be 103 Gy, 129 Gy, 163 Gy, and 163 Gy, respectively. Due to the 8.5 MeV eBeam becoming available only towards the end of this study and scheduling conflicts, only one experiment for each organism was conducted.

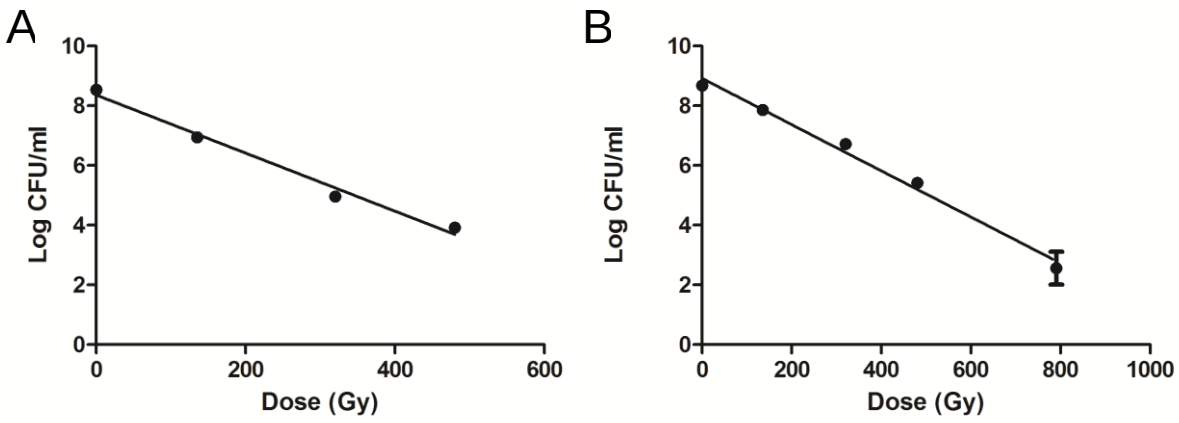

Figure 3. Inactivation of (A) *E. coli* (25922) and (B) *E. coli* (#5) in PBS under 8.5 MeV eBeam irradiation with D_{10} values of 103 Gy and 129 Gy, respectively. For each organism, one independent experiment was performed in triplicate, with standard deviations shown.

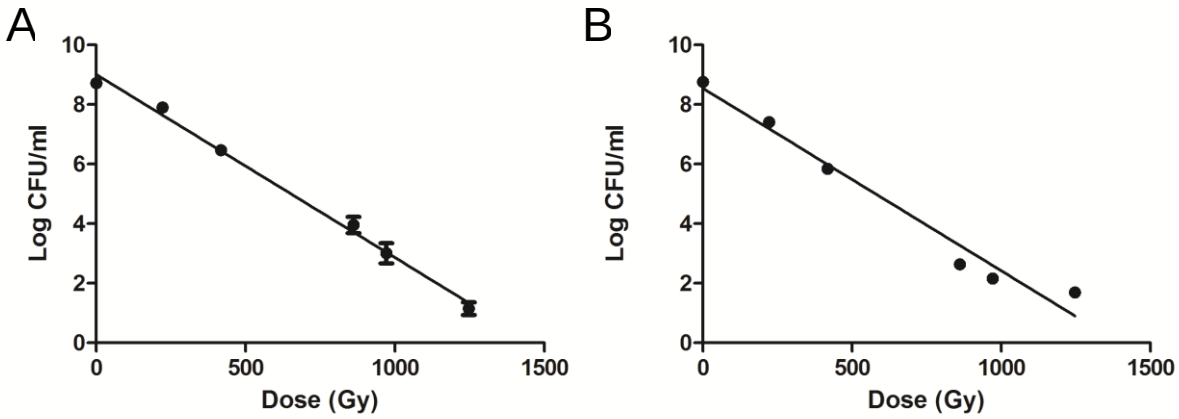

Figure 4. Inactivation of (A) *S.* Typhimurium and (B) *S.* 4,[5],12:i:- in PBS under 8.5 MeV eBeam irradiation with D_{10} values of 163 Gy and 163 Gy, respectively. For each organism, three independent experiments were performed in triplicate, with standard deviations shown.

Attenuated and non-attenuated 10 MeV electron beam

Three independent wedge tests were performed to determine the beam energy under the HDPE attenuation. The most probable (median) electron beam energy (Ep) was estimated to be 2.9 ± 0.22 MeV (data not shown). The Ep was calculated using the ISO/ASTM formula A3.4. Ep rather than Ea (average beam energy) was calculated since the wedge tests under attenuation permitted only two measurable dose points at the tail end of the depth-dose curve as opposed to a complete curve under non-attenuated conditions. Even though Ea is most appropriate for the kind of eBeam at the NCEBR, it requires the value of D50 (half of the maximum dose) for its calculation. Since the wedge tests under attenuation did not yield a complete depth-dose curve, D50 was unavailable. Hence it was decided that Ep was a more appropriate estimate of beam energy than Ea in this case because Ep does not require D50 for its calculation.

The inactivation curves of *S.* 4,[5],12:i:- in PBS under non-attenuated and attenuated 10 MeV eBeam irradiation are shown in Figure 5. The D_{10} values of *S.* 4,[5],12:i:- when exposed to non-attenuated and attenuated eBeam irradiation were calculated to be 220±45 Gy and 222±62 Gy, respectively.

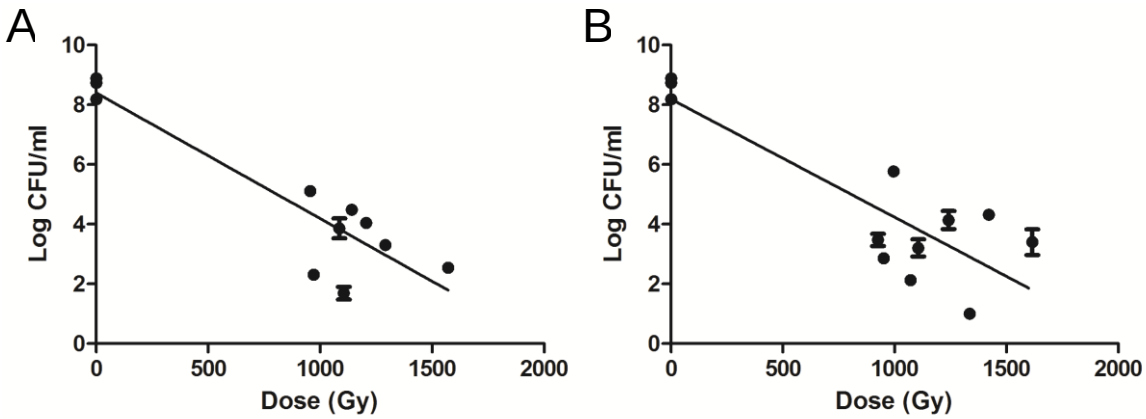

Figure 5. Inactivation of *S.* 4,[5],12:i:- in PBS under (A) non-attenuated and (B) attenuated 10 MeV eBeam irradiation with D_{10} values of 220±45 Gy and 222±62 Gy, respectively. For each condition, three independent experiments were performed in triplicate, with standard deviations shown.

The inactivation curves of a *Salmonella* cocktail (*S.* 4,[5],12:i:-, *S.* Heidelberg, *S.* Newport, *S.* Typhimurium, *S.* Enteritidis) in PBS when exposed to non-attenuated and attenuated 10 MeV eBeam irradiation are shown in Figure 6. The D_{10} values for the *Salmonella* cocktail were 270±46 Gy for non-attenuated eBeam irradiation and 289±20 Gy for attenuated eBeam irradiation.

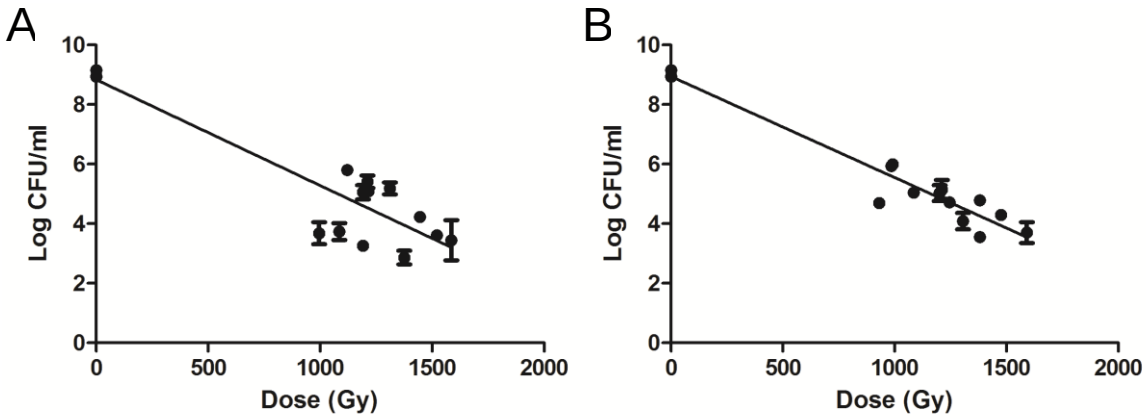

Figure 6. Inactivation of a *Salmonella* cocktail (*S.* 4,[5],12:i:-, *S.* Heidelberg, *S.* Newport, *S.* Typhimurium, *S.* Enteritidis) in PBS under (A) non-attenuated and (B) attenuated 10 MeV eBeam irradiation with D_{10} values of 270±46 Gy and 289±20 Gy, respectively. For each condition, three independent experiments were performed in triplicate, with standard deviations shown.

Gamma radiation

Lanthanum-140

Figures 7 and 8 show the inactivation curves of *E. coli* (25922) and *S.* Typhimurium in PBS under 1.59 MeV La-140 gamma irradiation. The D_{10} values of *E. coli* (25922) and *S.* Typhimurium were calculated to be 95±10 Gy and 178±9 Gy, respectively.

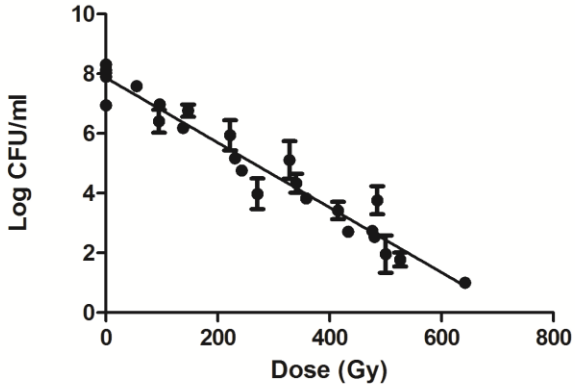

Figure 7. Inactivation of *E. coli* (25922) in PBS under 1.59 MeV La-140 gamma irradiation with a D_{10} value of 95±10 Gy. Five independent experiments were performed in triplicate, with standard deviations shown.

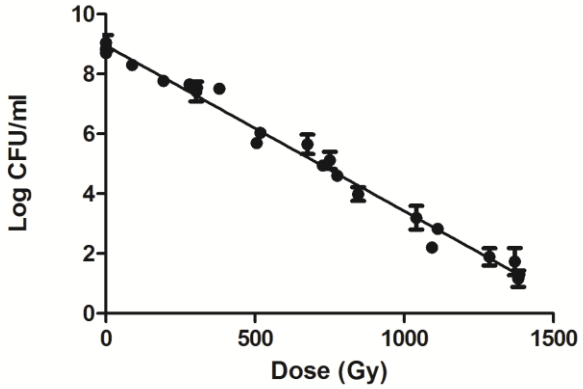

Figure 8. Inactivation of *S.* Typhimurium in PBS under 1.59 MeV La-140 gamma irradiation with a D_{10} value of 178±9 Gy. Five independent experiments were performed in triplicate, with standard deviations shown.

Nuclear reactor core

The inactivation curves of *E. coli* (25922), *E. coli* (#5), *S.* Typhimurium, and *S.* 4,[5],12:i:- in PBS under irradiation from the reactor core with an average gamma energy of 0.7-0.97 MeV are shown in Figures 9 and 10. The D_{10} values of *E. coli* (25922), *E. coli* (#5), *S.* Typhimurium and *S.* 4,[5],12:i:- were calculated to be 75±3 Gy, 138±15 Gy, 174±5 Gy, and 164±0.2 Gy, respectively.

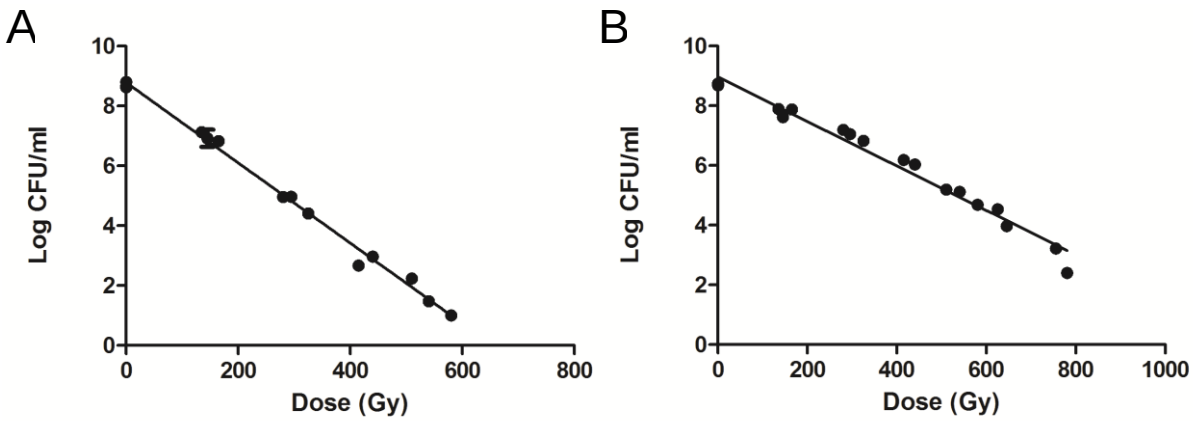

Figure 9. Inactivation of (A) *E. coli* (25922) and (B) *E. coli* (#5) in PBS under irradiation from the reactor core with an average gamma energy of 0.7-0.97 MeV with D_{10} values of 75±3 Gy and 138±15 Gy, respectively. For each organism, three independent experiments were performed in triplicate, with standard deviations shown.

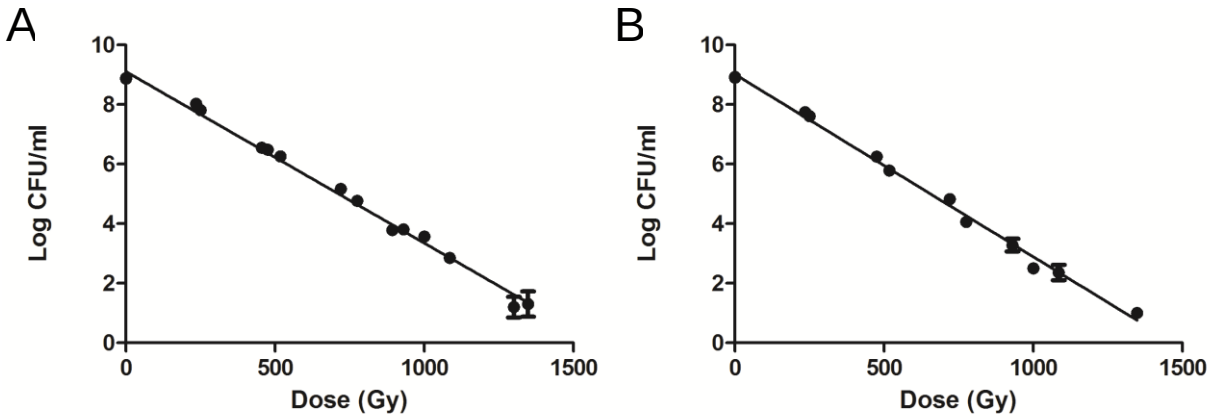

Figure 10. Inactivation of (A) *S.* Typhimurium and (B) *S.* 4,[5],12:i:- in PBS under irradiation from the reactor core with an average gamma energy of 0.7-0.97 MeV with D_{10} values of 174±5 Gy and 164±0.2 Gy, respectively. For *S.* Typhimurium three independent experiments were performed in triplicate, with standard deviations shown. For *S.* 4,[5],12:i:- two independent experiments were performed in triplicate, with standard deviations shown.

X-ray radiation

5 MeV x-ray

The inactivation curves of *E. coli* (25922) and *E. coli* (#5) in PBS under 5 MeV x-ray irradiation are shown in Figure 11. The D_{10} values of *E. coli* (25922) and *E. coli* (#5) were calculated to be 90±7 Gy and 151 Gy, respectively. Due to the 5 MeV x-ray system becoming non-functional during the research study, only one experiment was conducted for *E. coli* (#5).

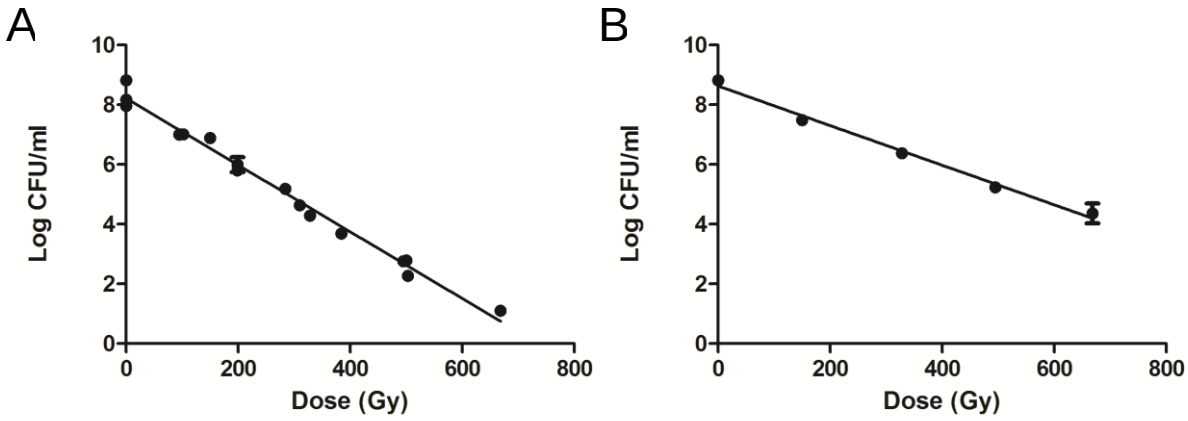

Figure 11. Inactivation of (A) *E. coli* (25922) and (B) *E. coli* (#5) in PBS under 5 MeV x-ray irradiation with D_{10} values of 174±5 Gy and 164±0.2 Gy, respectively. For *E. coli* (25922) three independent experiments were performed in triplicate, with standard deviations shown. For *E. coli* (#5) one independent experiment was performed in triplicate, with standard deviations shown.

100 keV x-ray

The inactivation curve of *E. coli* (25922) in PBS under 100 keV x-ray irradiation is shown in Figure 12. The inactivation curve follows a non-linear trend as determined by low R^2 values (data not shown); hence a linear regression analysis was not appropriate. A better fit for this curve was a quadratic model ($Y=B_0 + B_1X + B_2X^2$). For such a model, a single overall D_{10} value cannot be computed, since the slope of the line changes along the curve. The 100 keV x-ray source was the only ionizing radiation source that displayed such a trend, all other sources exhibited linear inactivation curves. It is also important to note that the slope seems to remain constant (if not slightly increasing) after ca. 150-200 Gy, indicating that the level of surviving bacteria is staying the same. Due to the extremely low dose rate (0.6 Gy/min) resulting in very long exposure times, only

experiments with the most radiosensitive organism (*E. coli* 25922) were performed to avoid overheating of the x-ray tube.

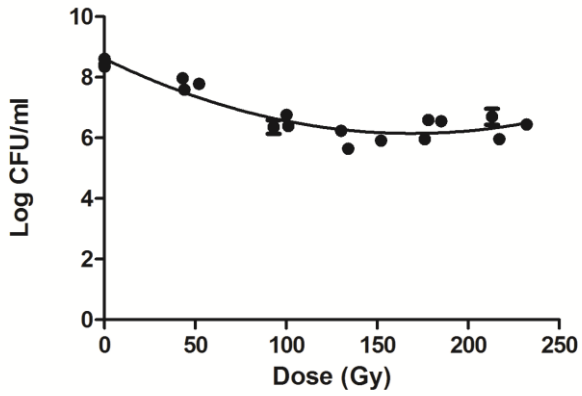

Figure 12. Quadratic model of *E. coli* (25922) inactivation in PBS under 100 keV x-ray irradiation. Three independent experiments were performed in triplicate, with standard deviations shown.

Table 2 is a summary of the D_{10} values for the different organisms and ionizing radiation sources used in this study. Since the 10 MeV eBeam had to be attenuated to obtain inactivation curves, a separate study was conducted to determine whether or not attenuation has an effect on the inactivation kinetics of bacteria. Those results are summarized in Table 3.

Table 2. Summary of all the D_{10} values for *E. coli* spp. and *Salmonella* spp. and the different ionizing radiation sources.

	D_{10} Value[a] (Gy)			
Radiation Source	***E. coli* (25922)**	***E. coli* (#5)**	***Salmonella* Typhimurium**	***Salmonella* 4,[5],12:i:-**
10 MeV eBeam	68 ± 4^{B}	107 ± 2^{D}	170 ± 16^{E}	147 ± 15^{F}
8.5 MeV eBeam	103^{A}	$129^{C,D}$	163^{E}	163^{F}
La-140 (gamma)	95 ± 10^{A}	ND	178 ± 9^{E}	ND
Reactor core (gamma)	75 ± 3^{B}	138 ± 15^{C}	174 ± 5^{E}	164 ± 0.2^{F}
5 MeV x-ray	90 ± 7^{A}	151^{C}	ND	ND
100 keV x-ray	NA	ND	ND	ND

[a] Values are means ± standard deviation. D_{10} values with different letters indicate statistically significant ($P \leq 0.05$) differences. Statistical analyses were performed for each organism against all the different radiation sources. ND, not determined. NA, not applicable.

Table 3. D_{10} values for *Salmonella* 4,[5],12:i:- and a *Salmonella* cocktail (*S.* 4,[5],12:i:-, *S.* Heidelberg, *S.* Newport, *S.* Typhimurium, *S.* Enteritidis) when exposed non-attenuated and attenuated 10 MeV eBeam irradiation.

	D_{10} Value[a,b] (Gy)	
Radiation Source	***Salmonella* 4,[5],12:i:-**	***Salmonella* cocktail**
Non-attenuated 10 MeV eBeam	220 ± 45^{A}	270 ± 46^{A}
Attenuated 10 MeV eBeam	222 ± 62^{A}	289 ± 20^{A}

[a] Values are means ± standard deviation.

[b] There was no statistically significant ($P \leq 0.05$) difference in D_{10} values between attenuated and non-attenuated conditions.

The results indicate that there is a statistically significant difference between the different ionizing radiation sources for the two *E. coli* strains but not for the two *Salmonella* serovars (Table 2). For *E. coli* (25922), the D_{10} values for 10 MeV eBeam and the reactor core were statistically different from the other three sources for which the organism exhibited a linear inactivation curve, namely 8.5 MeV eBeam, the La-140 source, and 5 MeV x-ray. For *E. coli* (#5), the D_{10} value for 10 MeV eBeam was

statistically different from the reactor core and 5 MeV x-ray. There was no statistically significant difference between the two eBeam energies. The 8.5 MeV eBeam was not statistically different from the reactor core or the 5 MeV x-ray. There was no statistically significant difference between the D_{10} values of the individual *Salmonella* serovar 4,[5],12:i:- (P=0.962) or the *Salmonella* cocktail (P=0.621) when exposed to eBeam irradiation with and without attenuation (Table 3).

Discussion

Determining inactivation kinetics is important to any industry that utilizes ionizing radiation to inactivate microorganisms. The commercial sterilization industry uses mainly three types of ionizing radiation, eBeam, gamma, and x-ray. Historically, the scientific literature has been unsettled with regards to the relative biological effectiveness (RBE) of different ionizing radiation sources (2, 8, 9, 11-18, 59, 60). This was mainly due to researchers using different dosimetry systems to measure the absorbed dose. Furthermore, maintaining the same experimental conditions across different ionizing radiation sources was often not possible due to the limited availability of different radiation sources on a single university campus. Researchers were forced to either ship their samples overnight or travel long distances to different radiation facilities, which inevitably changed their experimental conditions. To investigate the issue of RBE of different ionizing radiation sources, we employed the same alanine dosimetry system and the same experimental conditions for all the different ionizing radiation sources tested (Table 1).

The results of the inactivation kinetics indicate that *E. coli* (25922) is most susceptible to ionizing radiation out of all the organisms studied. In general, *E. coli* strains are more sensitive to ionizing radiation than *Salmonella* serovars (Table 2). These results are in agreement with a study by Lucht et. al. that looked at the inactivation of a number of microorganisms, including *E. coli* and *Salmonella*, exposed to gamma radiation (65). We also observed strain to strain variability, a phenomenon that has been previously documented in the literature (65).

All of the inactivation kinetics followed a linear trend, except for *E.coli* (25922) exposed to 100 keV x-ray. In this particular case, the response was fitted to a quadratic model (Fig. 12). The data indicate that after ca. 150-200 Gy, there is no further reduction of the organism. We hypothesize that this is due to the low dose rate (0.6 Gy/min) which seems to allow the bacteria enough time to repair any damage (DNA, protein or otherwise) caused by the irradiation. With a dose rate of 0.6 Gy/min, it took 5 hours and 30 minutes to reach a dose of 200 Gy. In comparison, it only took 50 minutes to reach a dose of 200 Gy with the La-140 gamma source (the second lowest dose rate used in this study). With a difference of almost 5 hours to reach the same adsorbed dose, it is not surprising that the organism exhibits a different response. The ability to grow under irradiation stress has been observed in the radioresistant bacteria, *Deinococcus radiodurans*, which is able to grow normally at 1 Gy/min (66). As for our study, it appears that for most of the dose rates tested (Table 1), the inactivation kinetics of *E. coli* and *Salmonella* were very similar. Only at the lowest dose rate (i.e. 0.6 Gy/min), did the response of *E. coli* change.

In order to determine the inactivation kinetics under a high energy 10 MeV eBeam, it was necessary to attenuate the beam with HDPE sheets. Through aluminum wedge tests, the energy underneath the attenuation was estimated to be 2.9 ± 0.22 MeV. Since this is an energy difference of over 7 MeV, a comparison study was performed to determine whether or not the attenuation has an effect on the inactivation kinetics of bacteria. Due to equipment limitations at the NCEBR, the lowest deliverable dose with the unattenuated 10 MeV eBeam is ca. 1000 Gy. Hence *Salmonella* was chosen for this portion of the study because it is more radioresistant than *E. coli*. At a dose of 1000 Gy, hardly any *E. coli* are expected to survive in PBS. Since the non-attenuated 10 MeV eBeam could not deliver a dose below 1 kGy, the dose points for the *Salmonella* inactivation curves are skewed toward the lower end (Fig. 5 and 6). This resulted in larger standard deviations compared to the ones observed for inactivation curves with a more even spread of data points (Table 2 and 3). Larger standard deviations as well as tails are often observed towards the lower end of inactivation curves, most likely due to the remaining survivors being more resistant (67, 68). The results indicate that attenuation of a high energy 10 MeV eBeam has no effect on the inactivation kinetics of *Salmonella* spp. There was no statistically significant difference between the D_{10} values of either *Salmonella* 4,[5],12:i:- or the *Salmonella* cocktail (*S.* 4,[5],12:i:-, *S.* Heidelberg, *S.* Newport, *S.* Typhimurium, *S.* Enteritidis) when irradiated with either the non-attenuated 10 MeV eBeam or the attenuated 10 MeV eBeam (Table 3). These results are in agreement with Tallentire et al., who compared the inactivation kinetics of *Bacillus*

pumilus under four different irradiations (10 MeV eBeam, Cobalt 60 gamma photons, and 80 and 100 keV eBeam) and found no difference in the survival response (68).

Overall, the results of our study indicate that the inactivation kinetics for *E. coli* and *Salmonella* are very similar for the different ionizing radiation sources (Table 2). A statistically significant difference was detected between the different ionizing radiation sources for the two *E. coli* strains but not for the two *Salmonella* serovars (Table 2). However, a dose difference of tens of Grays, as is the case for both *E. coli* strains (Table 2), will not be discernible under normal commercial processing conditions (for any source type). This is a result of both the radiation equipment as well as the dosimetry uncertainty (4-8%). Commercial processing facilities are typically set up to deliver doses within a 5% margin of error. In case of linear accelerators, radiation processing parameters, such as energy, current, scan, and processing table, are typically interlocked at a 5% margin of error (A. Hawkes, pers. comm.). In other words, in the 'real' world, the statistically significant differences found will be absorbed within the 5% margin of error for the radiation equipment and the 4-8% uncertainty in dosimetry. Furthermore, a D_{10} value is an estimate and not an absolute number. Sterilization doses based on D_{10} values should always be confirmed (at least three times) and a safety margin should be built into the sterilization dose to account for processing and dosimetry uncertainty, the margin of error associated with standard laboratory culture practices, and product variability.

CHAPTER IV

PHYSIOLOGICAL CHARACTERIZATION OF BACTERIA EXPOSED TO LETHAL DOSES OF IONIZING RADIATION

Overview

Experiments in our laboratory as well as reports in the literature suggest that bacteria exposed to sub lethal and lethal (no bacterial replication) doses remain metabolically active. To investigate this phenomenon further, we lethally irradiated *Salmonella* Typhimurium and *Escherichia coli* cells and measured their membrane integrity, DNA damage, metabolic activity, ATP levels, and overall cellular functionality post-irradiation. Non-irradiated and heat-killed cells were used as positive and negative controls, respectively. The results showed that the membrane integrity of *S.* Typhimurium and *E. coli* cells was maintained and that the cells remained metabolically active up to 9 days post-irradiation when stored at 4°C. The ATP levels in lethally irradiated cells were similar to non-irradiated control cells. Extensive DNA damage was also visualized and cellular functionality was confirmed based on the ability to propagate bacteriophage for up to 9 days post-irradiation. Overall, the results indicate that lethally irradiated *S.* Typhimurium and *E. coli* cells resemble live non-irradiated cells more closely than heat-killed (dead) cells.

Introduction

Studies have shown that bacteria exposed to a lethal dose of gamma radiation retain their metabolic and transcriptional activities (20, 21). Magnani et. al. demonstrated that lethally gamma irradiated *Brucella melitensis* cells had lost their ability to replicate but still possessed metabolic and transcriptional activity. The cells also persisted in macrophages, generated antigen-specific cytotoxic T cells, and protected mice against virulent bacterial challenge. The authors concluded that the pathogen's metabolic activity had a positive influence on shaping protective host immune responses (20). Secanella-Fandos et. al. observed that lethally gamma irradiated *Mycobacterium bovis* cells were metabolically active and exhibited similar tumor growth inhibition and induction of cytokines compared to live cells (21).

The overall objective of this study was to characterize *S.* Typhimurium and *E. coli* cells exposed to lethal doses of gamma and electron beam (eBeam) irradiation. For the purpose of this study, lethally irradiated cells are defined as cells that have lost their replication capabilities. The first objective was to characterize the membrane integrity of lethally irradiated cells. The assay used to accomplish this task consisted of a two-color fluorescent dye system. The SYTO® 9 green-fluorescent nucleic acid stain can penetrate cells with either intact or damaged membranes. On the other hand, the red-fluorescent nucleic acid stain, propidium iodide, penetrates only cells with damaged membranes. When used in combination, this dye system stains cells with intact membranes green and cells with damaged membranes red. The underlying hypothesis was that lethally

irradiated cells would have intact membranes. The second objective was to visualize the DNA Double-Strand Breaks (DSBs) in lethally irradiated cells. The neutral comet assay, adapted for bacteria, was used to visualize DSBs under a fluorescent microscope. This assay, also known as single-cell gel electrophoresis, offers direct visualization of DSBs through the appearance of DNA tails or comets. The cells of interest were immobilized in low melting agarose, lysed, and electrophoresed. This allowed the DNA to migrate out of the cell in a pattern determined by the extent of DNA damage (69, 70). The underlying hypothesis was that lethally irradiated cells would have extensive DNA damage compared to non-irradiated (control) cells. The third objective was to monitor the metabolic activity in lethally irradiated cells over time. The assay that was chosen used cellular reducing conditions to monitor metabolic activity/cell health. Resazurin, the active ingredient, is a non-fluorescent compound. Upon entering the cell, it is converted to resorufin, a highly fluorescent compound, via the cell's reducing environment. Alive and healthy cells have more reducing power than injured/dead cells and will produce a higher fluorescent signal (71-73). The underlying hypothesis was that electron transport processes would still be functional in lethally irradiated cells for extended periods of time. The fourth objective was to monitor the ATP levels in lethally irradiated cells over time. ATP is an indicator of metabolically active cells and can be detected via a bioluminescence assay (73). The underlying hypothesis was that lethally irradiated cells would have similar levels of ATP compared to non-irradiated (control) cells. The fifth objective was to study the overall cellular functionality of lethally irradiated cells via bacteriophage propagation. Well-studied bacteriophages, namely λ,

T4, and T7, were used in this study (74-79). These bacteriophages require the host cell's machinery to varying degrees to produce progeny phage particles. Phage λ relies completely on the host cell to reproduce, T4 requires certain cellular components of the host cell, and T7 only requires the host's machinery at the very beginning of infection (75, 76, 78, 79). The underlying hypothesis was that lethally irradiated cells could still function as hosts for bacteriophages.

Materials and Methods

Preparation and irradiation of bacterial cultures

Overnight cultures of *S*. Typhimurium (ATCC 14028) were grown in Tryptic Soy Broth (TSB) at 35°C in a shaking water bath. The cultures were centrifuged at 4000 x g for 10 minutes at Room Temperature (RT), the growth media removed and the cell pellets washed once in Phosphate Buffered Saline (PBS). After washing, the cell pellets were resuspended in PBS to an OD_{600} of ca. 1.0, resulting in approximately $1x10^8$ Colony Forming Units (CFU)/ml. Aliquots of the cell suspension in PBS were packaged for irradiation as previously described (Chapter IV). Samples were irradiated at a lethal target dose of 2.0 kGy as previously described in Chapter IV. Non-irradiated samples (0 kGy) were used as controls. The control samples were packaged the same way as experimental samples and were transported to the irradiation facility to eliminate possible differences in survival due to transport and handling.

Overnight cultures of the *E. coli* K-12 wild-type strain MG 1655 were grown in Luria-Bertani (LB) broth at 35°C in a shaking water bath. The day of the irradiation, log-phase cultures of *E. coli* were prepared by seeding LB broth with the fresh overnight culture at a ratio of 1:100. The culture was allowed to grow at 35°C to an $O.D._{600}$ of ca. 0.5 resulting in approximately $1x10^8$ CFU/ml. The log-phase culture was subsequently chilled on ice for 10 min to arrest cell growth. Aliquots of the log-phase culture in LB broth were packaged and eBeam irradiated to a lethal target dose of 7.0 kGy as previously described in Chapter IV. Non-irradiated samples (0 kGy) were used as a positive control and handled as previously described in the *Salmonella* section above. Heat-killed cells (70°C for 60 min) were used as a negative control.

Membrane integrity of lethally irradiated cells

Following eBeam and heat treatment, the *E. coli* samples were stored at 4°C in the LB broth they had been treated in and the membrane integrity was examined at the following time points: 0, 4, 24, and 216 hours. The LIVE/DEAD® *Bac*Light™ Bacterial Viability Kit (Molecular Probes®, Grand Island, NY) was used according to the manufacturer's instructions with minor modifications. Briefly, 0.5 ml of the sample was centrifuged for 1 minute at RT at maximum speed in a microcentrifuge. The pellet was resuspended in 0.5 ml 0.85% sodium chloride (NaCl) solution. 1.5 µl of the dye mixture (equal volume SYTO 9 and propidium iodide) were added protected from light. The sample was vortexed and incubated for 15 min at RT in the dark. Slides with 10 µl of sample were prepared for fluorescent microscopy. Images were taken immediately with

an Olympus BX50 fluorescent microscope with a FITC/TexasRed filter and a 200x magnification.

Visualization of DNA double-strand breaks in lethally irradiated cells

Following eBeam irradiation, the *S.* Typhimurium and *E. coli* samples were transported to the laboratory on ice and stored at 4°C for 1-2 hours until the comet assay could be performed. The neutral comet assay was performed using the Trevigen CometAssay® protocol (Reagent Kit for CometAssay®, Catalog # 4250-050-K) with modifications. Briefly, a 50 µl aliquot ($1x10^7$ cells/ml) of the appropriate bacterial cell suspension (eBeam irradiated, non-irradiated control, and heat-killed) was mixed with lysozyme (final conc. 0.5 mg/ml) and RNAse A (final conc. 5 µg.ml) prior to adding 500 µl of molten Comet LMAgarose (0.5% low-melting agarose) (Trevigen Inc., Gaithersburg, MD) kept at 37°C. After mixing the sample, a 50 µl aliquot was pipetted onto the CometSlide (Catalog # 4250-050-03, Trevigen Inc., Gaithersburg, MD), resulting in approximately 50,000 cells per sample area. The slides were incubated at 4°C for 10 minutes in the dark. Following gelling of the agarose disc, the slides were placed in plastic Coplin Jars containing lysis solution [2.5 M NaCl, 100 mM EDTA, 10 mM Tris pH 10, 1% sodium lauroyl sarcosine, 1% Triton X-100 (added fresh)] and incubated for 1 hour at RT. Following cell lysis, slides were placed in an enzyme digestion buffer [2.5 M NaCl, 10 mM EDTA, 10 mM Tris pH 7.4, 1 mg/ml Proteinase K] for 2 hours at 37°C. After draining the excess buffer, slides were immersed in pre-chilled 1X electrophoresis buffer [100 mM Tris pH=9, 300 mM sodium acetate] and incubated for at least 30

minutes at 4°C; slides may also be stored overnight at this point. Slides were placed in a horizontal electrophoresis unit (Owl; Model B-2) containing fresh 1X electrophoresis buffer and electrophoresed at 1 V/cm for 1 hour at RT. The slides were then placed in 1 M ammonium acetate in ethanol for 30 minutes at RT. DNA precipitation was followed by ethanol dehydration of the agarose. Slides were immersed in absolute ethanol for 1 hour at RT and air-dried, followed by 70% ethanol for 15 minutes at RT and then air-dried. Slides were then stained with 50 µl of freshly prepared SYTO 9 solution (1.25 µM in 0.04% DMSO) for 15 minutes in the dark. The excess SYTO 9 stain was removed by gently tapping the slide on a KimWipe. Slides were then air-dried for 30 minutes in the dark, followed by 5 minutes at 40°C in the dark. Observations were made using an Olympus BX50 fluorescent microscope with a FITC filter and a 1000x magnification. CFU counts were obtained by plating the *Salmonella* samples on TSA and the *E. coli* samples on LB agar and incubating them at 37°C for 4 days.

Metabolic activity in lethally irradiated cells

To measure the metabolic activity in lethally irradiated *S.* Typhimurium, cells either remained in the PBS they had been irradiated in or were placed in growth media (1:10 dilution in 1xTSB). Cells were subsequently incubated either at 37°C or at 4°C. Metabolic activity and bacterial CFU counts were monitored at the following time points: 0, 2, 4, 6, 8, 12, 24, 48, 120, and 168 hours. Metabolic activity was measured with the redox indicator alamarBlue® (Invitrogen, Grand Island, NY) according to the manufacturer's instructions. Briefly, 10 µl of the alamarBlue® reagent were added to 100

µl of cells (in a black 96-well plate), mixed, and incubated in the dark at 37°C for 1 hour. Following the 1 hour incubation, the fluorescence was measured with a Perkin Elmer Wallac 1420 VICTOR2™ microplate reader. The CFU counts were obtained by plating the samples on TSA and incubating them at 37°C for 4 days. Two independent experiments were performed for each ionizing radiation source (eBeam and gamma).

To measure the metabolic activity in lethally irradiated and heat-killed *E. coli* cells, the samples were stored at 4°C in the LB broth they had been treated in and the metabolic activity was monitored at the following time points: 0, 4, 24, and 216 hours, as previously described above. Two independent experiments were performed.

ATP levels in lethally irradiated *E. coli* cells

Following eBeam and heat treatment, the *E. coli* samples were stored at 4°C in the LB broth they had been treated in and the ATP levels were examined at the following time points: 0, 4, 24, and 216 hours. Cellular ATP levels were determined with the BacTiter-Glo™ Microbial Cell Viability Assay (Promega, Madison, WI) according to the manufacturer's instructions with minor modifications. Briefly, 10 µl of the BacTiter-Glo reagent were added to 10 µl of cells (in a white 384-well plate), mixed, and incubated for 5 minutes at RT. Following the incubation, the luminescence was measured with a Perkin Elmer Wallac 1420 VICTOR2™ microplate reader. The cellular ATP concentrations were interpolated from a standard curve.

Bacteriophage multiplication in lethally irradiated *E. coli* cells

Following eBeam and heat treatment, the *E. coli* samples were kept at 4°C in the LB broth they had been treated in and the overall cellular functionality was determined at the following time points: 0, 4, 24, and 216 hours. One milliliter of the sample was centrifuged for 1 minute at RT in a microcentrifuge at maximum speed. The cell pellet was resuspended in 50 µl amended LB broth (5 mM $CaCl_2$ and 5 mM $MgSO_4$) and 50 µl of the bacteriophage (lambda vir 101, T4D or T7), also in amended LB broth, were added at a Multiplicity of Infection (MOI) of 0.01 (10^8 CFU/ml to 10^6 PFU/ml). The mixture was vortexed and incubated in a 37°C shaking water bath for 24 hours. Following the incubation, samples were placed on ice, diluted in amended LB broth and spot plated on LB agar using the top agar overlay method (80). Ten microliters from each dilution (-0 to -8) were spotted to determine the dilutions that would yield countable numbers. LB plates were incubated at 37°C for 16-18 hours. Following spot plating, the samples were stored at 4°C overnight and full plate titrations, also using the top agar overlay method, of the appropriate dilutions were performed the next day. LB plates were incubated at 37°C for 16-18 hours and then counted for Plaque Forming Units (PFUs). The ability of the *E. coli* cells to replicate (or not) was confirmed by plating survivors on LB agar plates and incubating them at 37°C for 4 days. Two independent experiments were performed.

Statistical analysis

Statistical significance (P-value <0.05) was determined through pairwise Student's t-tests using the JMP statistical software (version 11).

Results

Membrane integrity of lethally irradiated cells

The results indicated that, as expected, the non-irradiated (control) *E. coli* cells had intact membranes at all the time points (Fig. 13). At both the 24 hour and day 9 time points, the control showed a few cells with damaged membranes. In contrast, the heat-killed cells had only damaged membranes for all the time points (Fig. 13). Overall, the irradiated cells had intact membranes similar to the non-irradiated (control) cells (Fig. 13). At 0 and 4 hours post-irradiation, the irradiated samples showed a few cells with damaged membranes. As the incubation continued, the number of cells with damaged membranes increased. At day 9 of incubation in LB broth at 4°C, approximately half of the cells showed signs of membrane damage (based on qualitative analysis) (Fig. 13).

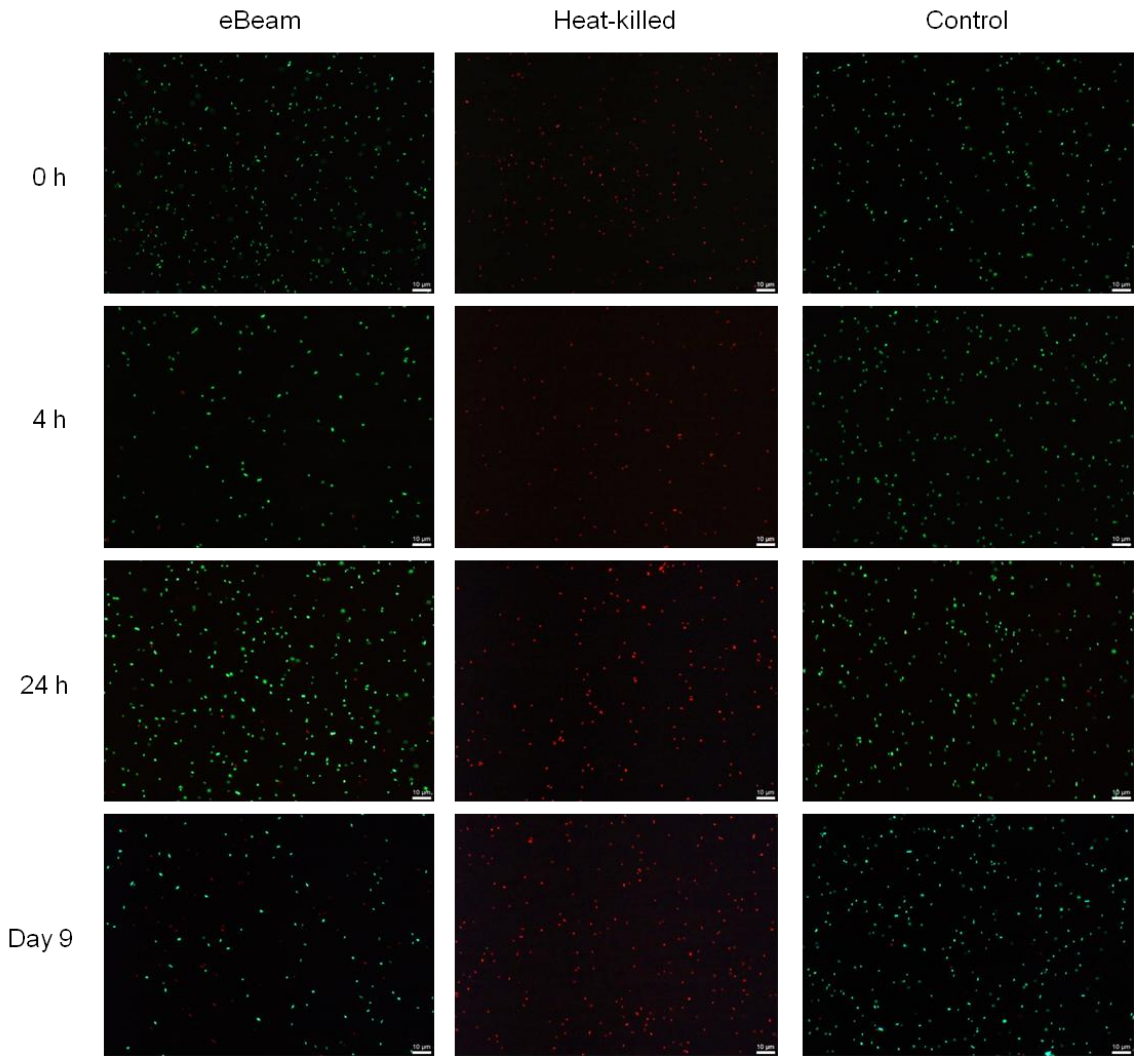

Figure 13. Representative images depicting membrane integrity in lethally eBeam irradiated, heat-killed, and non-irradiated *E. coli* cells. Cultures were incubated at 4°C in LB broth post-treatment and images were taken at 0, 4, 24 hours, and 9 days.

Visualization of DNA double-strand breaks in lethally irradiated cells

The neutral comet assay was performed to visualize the DNA double-strand breaks (DSBs) in *S.* Typhimurium cells (in PBS) and *E. coli* cells (in LB) exposed to lethal eBeam irradiation doses, a lethal heat treatment (70°C for 60 minutes) or no treatment (positive control). The measured eBeam doses for *S.* Typhimurium cells (irradiated in PBS) and *E. coli* cells (irradiated in LB) were 2.16 kGy and 7.04 kGy, respectively. Non-irradiated (control) cells showed only a few DSBs as seen by a few long DNA tails while irradiated cells showed extensive DSBs as seen by no distinct DNA tails (Figs. 14 and 15). The extent of DNA damage in heat-killed cells was not as extreme as for irradiated cells, as indicated by the DNA tails protruding from some cells, but the DNA damage was more pronounced than in the non-irradiated (control) cells, since not every cell had distinct DNA tails (Figs. 14 and 15).

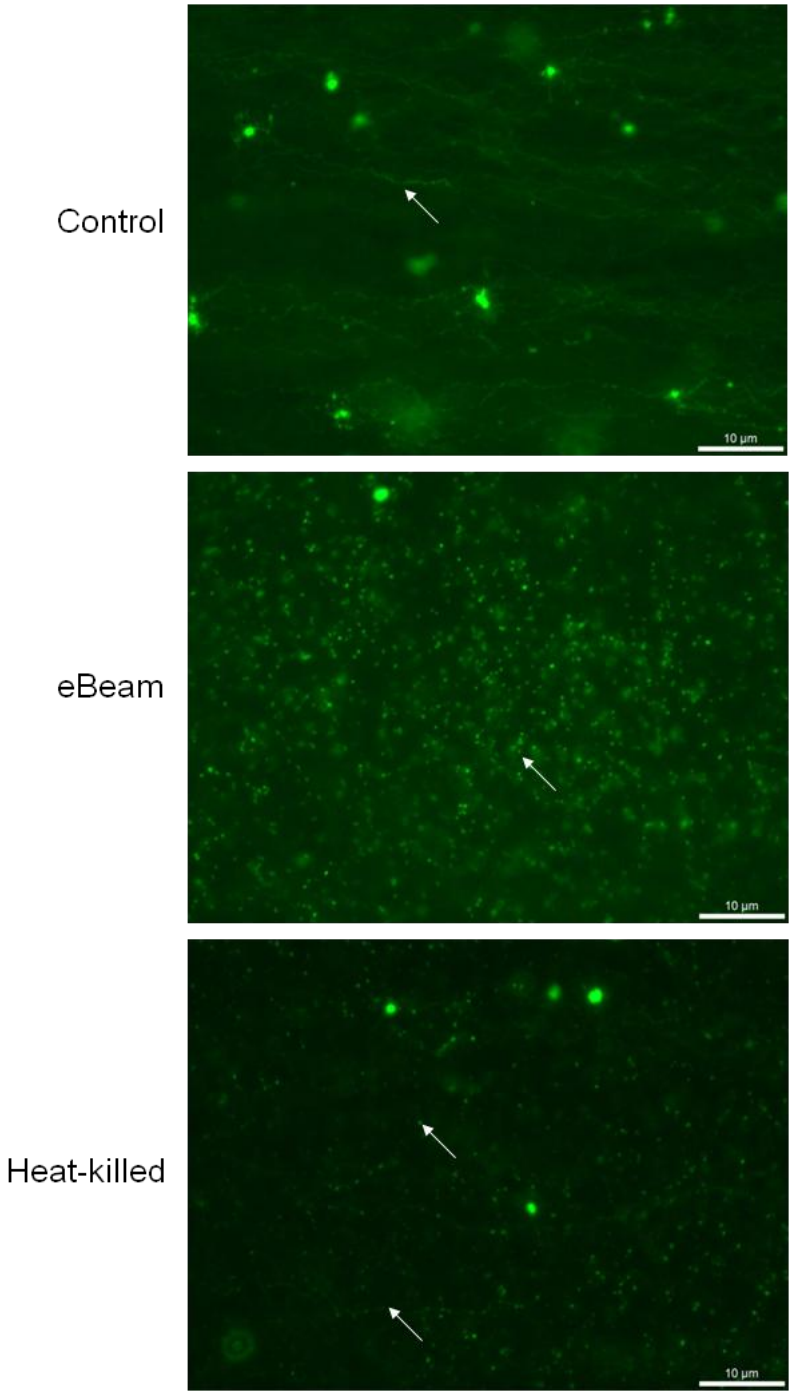

Figure 14. Representative images showing the detection of DNA double-strand breaks in *S*. Typhimurium cells using the neutral comet assay. Cells were exposed to either a lethal eBeam irradiation dose (absorbed dose: 2.16 kGy), a lethal heat treatment (70°C for 60 minutes) or no treatment (positive control). Arrows indicate DNA tails (control), putative DNA fragments (eBeam) or both (heat-killed).

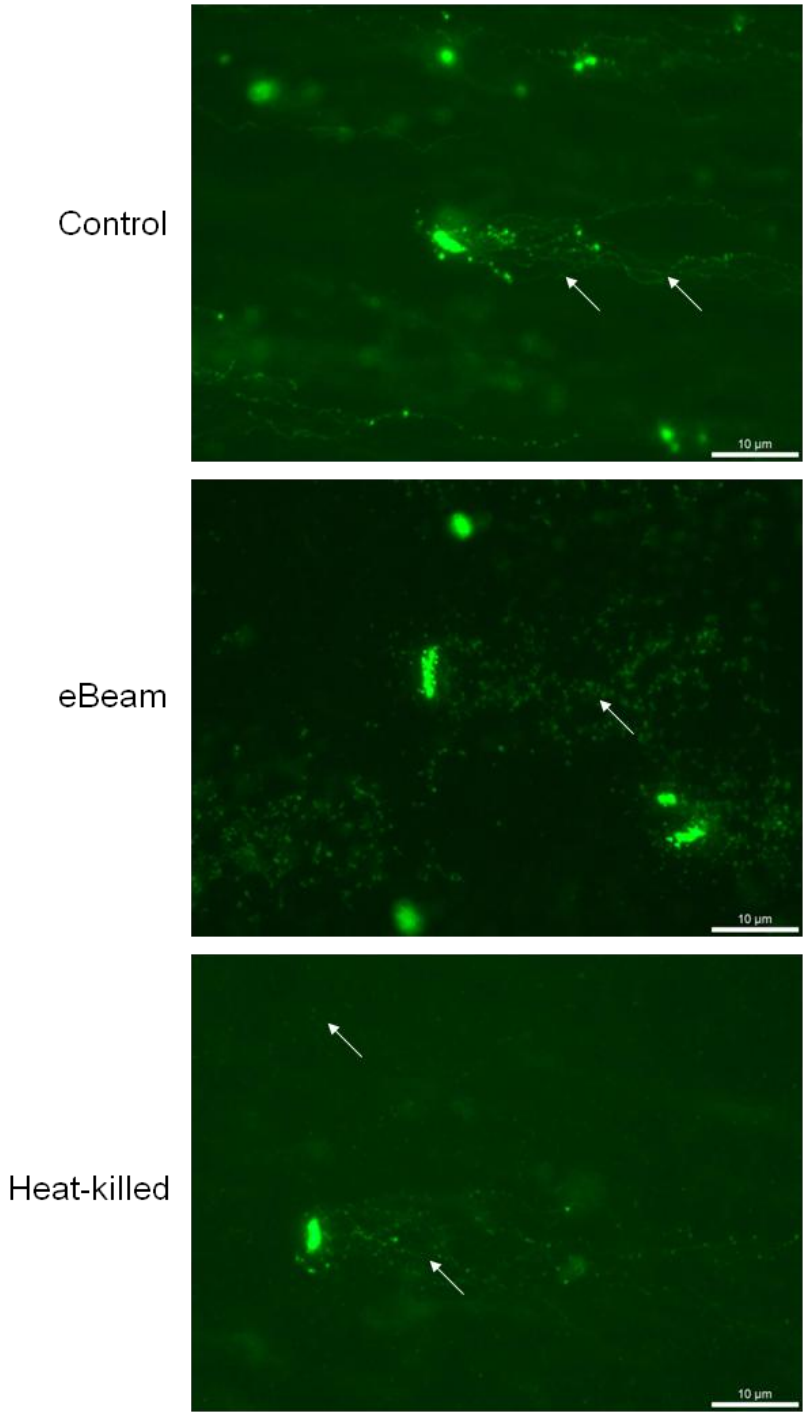

Figure 15. Representative images showing the detection of DNA double-strand breaks in *E. coli* cells using the neutral comet assay. Cells were exposed to either a lethal eBeam irradiation dose (absorbed dose: 7.04 kGy), a lethal heat treatment (70°C for 60 minutes) or no treatment. Arrows indicate DNA tails (control), putative DNA fragments (eBeam) or both (heat-killed).

Metabolic activity in lethally irradiated *S*. Typhimurium cells

When incubated in TSB at 4°C, *S*. Typhimurium cells that were eBeam irradiated maintained the lowest metabolic activity for 7 days compared to the positive controls and eBeam irradiated cells incubated in PBS (Fig. 16A). The non-irradiated control cells in TSB showed a slightly higher metabolic activity level than the eBeam irradiated cells in TSB (Fig. 16A). For cells that were eBeam irradiated and incubated in PBS, a metabolic activity level almost twice as high as for cells incubated in TSB was observed (Fig. 16A). Both, the eBeam irradiated and the controls cells maintained their metabolic activity for the entire study period of 7 days, regardless of the incubation medium (TSB or PBS) (Fig. 16A).

When incubated at 37°C in PBS, the metabolic activity of *S*. Typhimurium cells that were eBeam irradiated declined to almost zero over a 24 hour period. After 48 hours, the activity was almost non-existent and by day 5, all metabolic activity had ceased (Fig. 16B). The non-irradiated (control) cells in PBS maintained their metabolic activity for 48 hours. By day 5, it was almost non-existent and by day 7 there was no discernable metabolic activity left (Fig. 16B). When incubated at 37°C in TSB, the metabolic activity of *S*. Typhimurium cells that were eBeam irradiated more than doubled in the first 8 hours, followed by a more gradual increase up to 48 hours. By day 5, the metabolic activity was declining and by day 7, it was approaching zero (Fig. 16B). The non-irradiated (control) cells in TSB displayed a dramatic increase in metabolic activity within the first 12 hours. Between 12 to 48 hours, the activity was maintained. On days 5

and 7, and increase in metabolic activity was observed again (Fig. 16B). The non-irradiated (control) cells in TSB at 37°C had the highest metabolic activity out of all the different incubation combinations (as expected), since they were actively multiplying (Fig. 16B). The viable numbers for the non-irradiated (control) cells were between 8-9 log CFU/ml for all the different combinations, with cells in TSB at 37°C having the highest number of survivors (Fig. 17). Lethally eBeam irradiated *S*. Typhimurium cells yielded no survivors.

Overall, the trends in metabolic activity for lethally gamma irradiated *S*. Typhimurium cells were similar to the eBeam irradiated cells for all 4 post-irradiation incubation conditions. However, some differences were observed. When incubated at 4°C, gamma irradiated cells in both buffer (PBS) and growth media (TSB) had slightly higher metabolic activity levels for the first 48 hours than the non-irradiated (control) cells (Fig. 18A). This was different from the eBeam irradiated cells, which exhibited metabolic activity similar to the non-irradiated (control) cells (Fig. 16A).

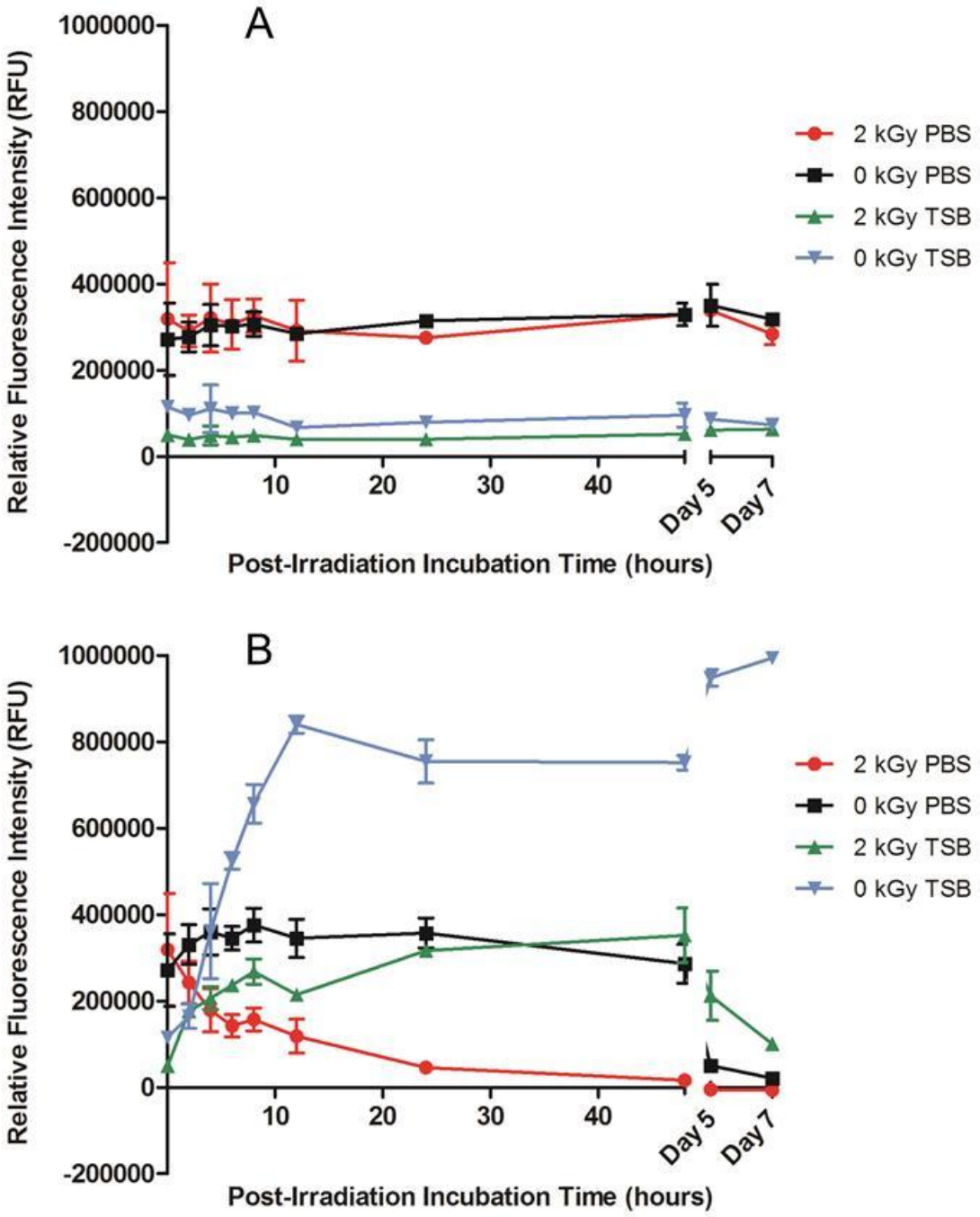

Figure 16. Metabolic activity of lethally eBeam irradiated (2 kGy) and non-irradiated (0 kGy) *S.* Typhimurium cells incubated at (A) 4°C and (B) 37°C in either buffer (PBS) or growth media (TSB). Two independent experiments were performed, with standard deviations shown. Lethal eBeam dose was 2.105±0.04 kGy.

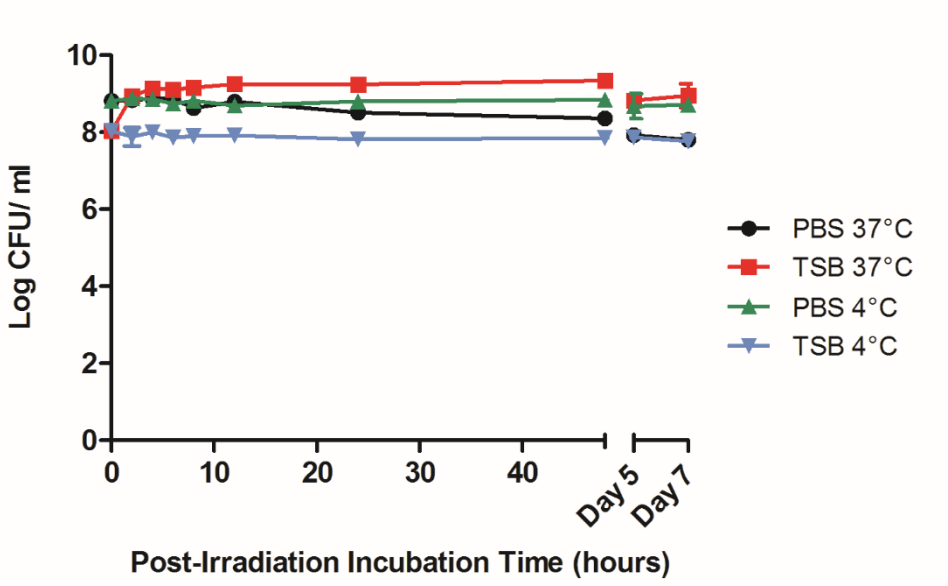

Figure 17. Viable cell counts of non-irradiated (control) *S.* Typhimurium cells incubated at 4°C and 37°C in either buffer (PBS) or growth media (TSB). Lethally eBeam irradiated *S.* Typhimurium cells yielded no survivors. Two independent experiments were performed, with standard deviations shown.

Both eBeam and gamma irradiated cells exhibited metabolic activity for up to 7 days when incubated at 4°C in either buffer (PBS) or growth media (TSB). However, the metabolic activity levels of gamma irradiated cells were higher than those of eBeam irradiated cells (Figs. 16A and 18A). When incubated at 37°C in PBS, the metabolic activity of gamma irradiated *S.* Typhimurium cells declined to almost zero over a 12 hour period. After 24 hours, the metabolic activity was virtually non-existent and by day 5 it had ceased completely (Fig. 18B). This rapid decline in activity over a 12 hour period was twice as fast as for eBeam irradiated cells, which declined to similar levels over a 24 hour period (Fig. 16B). By day 5, the metabolic activity had ceased in eBeam irradiated cells as well. The non-irradiated (control) cells at 37°C in PBS almost doubled

their metabolic activity within the first 24 hours. The metabolic activity was maintained until 48 hours and by day 5 it was almost non-existent. There was no discernable metabolic activity left on day 7 (Fig. 18B). For the gamma irradiated cells in TSB at 37°C, metabolic activity was maintained at a constant level over the first 48 hours. However, by day 5, no metabolic activity was detected. This was in contrast to eBeam irradiated cells, which still showed metabolic activity on days 5 and 7 (Fig. 16B). The non-irradiated (control) cells in TSB at 37°C displayed an increase in metabolic activity within the first 24 hours. The metabolic activity was maintained between 24-48 hours and increased again by days 5 and 7 (Fig. 18B). The viable numbers for the non-irradiated (control) cells, as confirmed through plate counts, were between 8-9 log CFU/ml for all the different combinations, with cells in TSB at 37°C having the highest number of survivors (Fig. 19). Lethally gamma irradiated *S*. Typhimurium cells yielded no survivors.

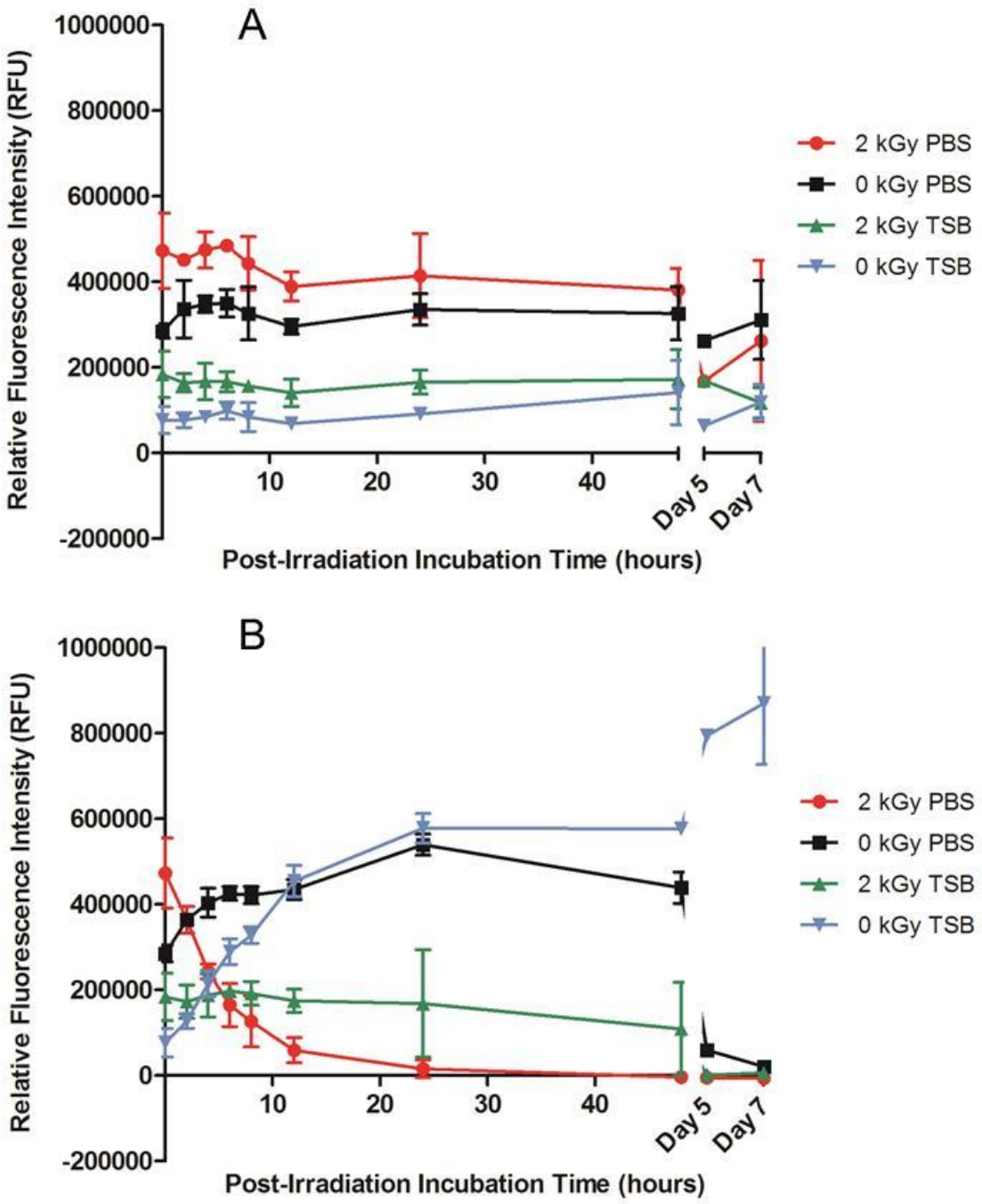

Figure 18. Metabolic activity of lethally gamma irradiated (2 kGy) and non-irradiated (0 kGy) *S*. Typhimurium cells incubated at (A) 4°C and (B) 37°C in either buffer (PBS) or growth media (TSB). Two independent experiments were performed, with standard deviations shown. Gamma dose was 2.171±0.46 kGy.

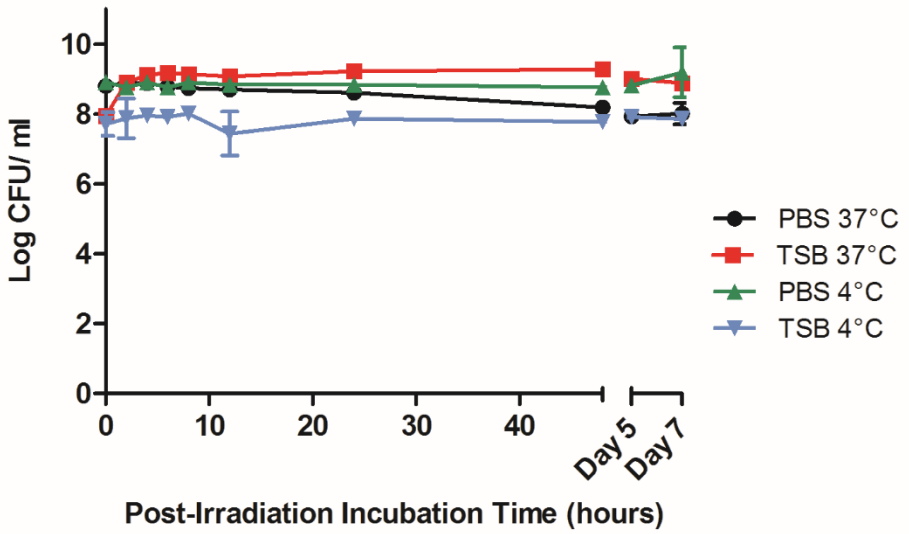

Figure 19. Viable cell counts of the non-irradiated (0 kGy) *S.* Typhimurium control cells incubated at 4°C and 37°C in either buffer (PBS) or growth media (TSB). Lethally gamma irradiated *S.* Typhimurium cells yielded no survivors. Two independent experiments were performed, with standard deviations shown.

Overall, eBeam and gamma irradiated S. Typhimurium cells showed similar patterns of metabolic activity. The greatest differences were observed with cells incubated at 37°C. Gamma irradiated cells in PBS lost their activity twice as fast as eBeam irradiated cells (24 vs. 48 hours). Gamma irradiated cells in TSB showed no metabolic activity on day 5, whereas eBeam irradiated cells still showed activity on day 7 (Figs. 16B and 18B). It appears that gamma irradiated cells lose their metabolic activity more rapidly than eBeam irradiated cells.

Metabolic activity in lethally irradiated E. coli cells

E. coli control samples maintained a high level of metabolic activity over the entire 9 day incubation period (LB broth at 4°C), whereas heat-killed samples exhibited no metabolic activity (Fig. 20). In fact, the heat-killed samples were significantly different ($p<0.0001$) from eBeam irradiated and control samples (Fig. 20). Metabolic activity in eBeam irradiated *E. coli* samples was maintained at levels comparable to the control over a period of 24 hours post-irradiation. By day 9, the metabolic activity in the irradiated samples had significantly ($p<0.0001$) declined compared to the control. (Fig. 20).

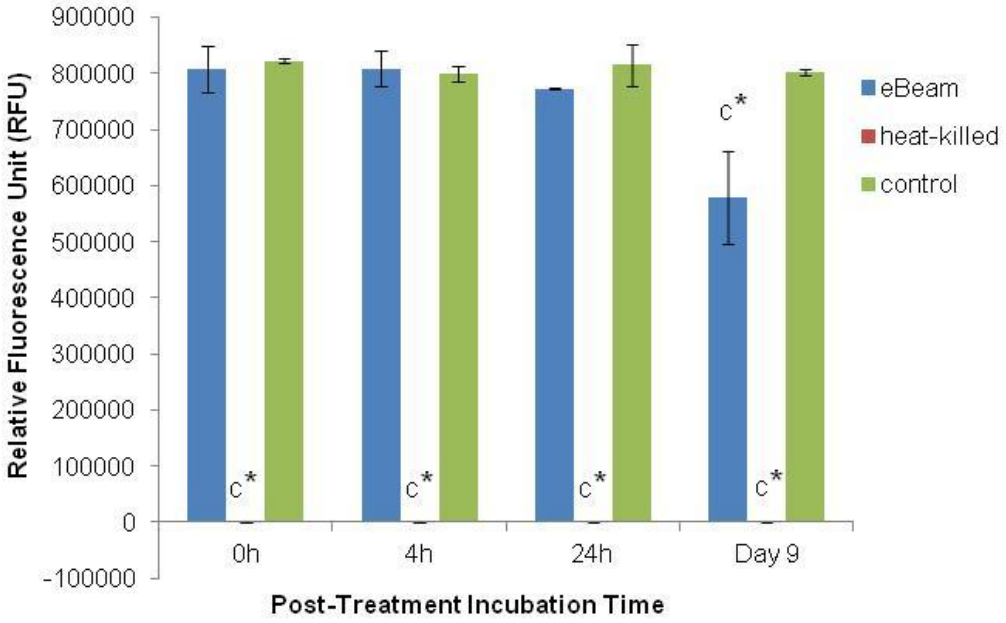

Figure 20. Metabolic activity of lethally eBeam irradiated, heat-killed and non-treated *E. coli* cells. Samples were incubated at 4°C in LB broth post-treatment and measurements were taken at 0, 4, 24 hours, and 9 days. Two independent experiments were performed, with standard deviations shown. C* denotes statistical significance ($p<0.0001$).

ATP levels in lethally irradiated *E. coli* cells

ATP levels for the *E. coli* control samples increased over the 9 day incubation period (0h: 1.06 µM; 4h: 0.94 µM; 24h: 1.19 µM; Day 9: 1.73 µM) (Fig. 21). In contrast, heat-killed cultures maintained constant ATP levels throughout the entire 9 day incubation period (0h: 0.67 µM; 4h: 0.63 µM; 24h: 0.63 µM; Day 9: 0.66 µM) (Fig. 21). ATP levels for eBeam irradiated *E. coli* samples were much more variable compared to heat-killed and control samples (0h: 1.4 µM; 4h: 0.92 µM; 24h: 1.56 µM; Day 9: 0.38 µM) (Fig. 21). At 0 hours, the eBeam irradiated samples had the highest ATP levels compared to control and heat-killed samples. In addition, the ATP levels were significantly different ($p<0.0062$) from the heat-killed samples. At 4 hours, all three treatment groups had very similar ATP levels. At 24 hours, irradiated samples had the highest ATP levels and heat-killed samples the lowest. The ATP levels in the irradiated samples were significantly different ($p<0.0011$) from the heat-killed samples. After 9 days of incubation at 4°C, irradiated samples had the lowest levels of ATP and the control samples the highest. Both, the irradiated and heat-killed samples had ATP levels that were significantly different ($p<0.0001$ and $p<0.0003$, respectively) from the control samples on day 9 (Fig. 21).

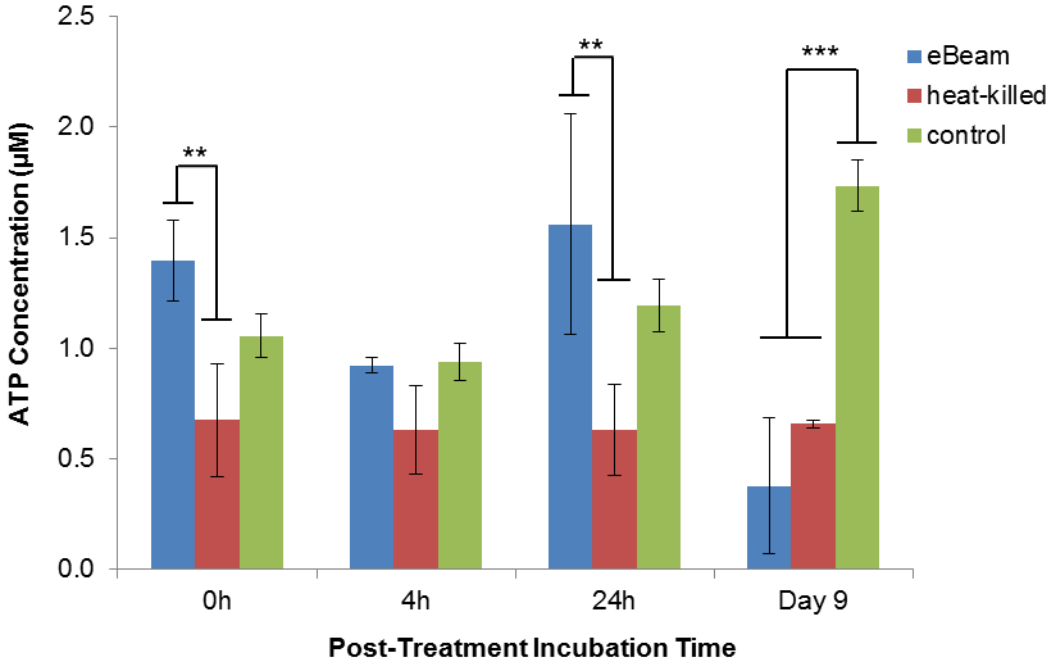

Figure 21. ATP levels of lethally eBeam irradiated, heat-killed and non-treated *E. coli* cells. Samples were incubated at 4°C in LB broth post-treatment and measurements were taken at 0, 4, 24 hours, and 9 days. Two independent experiments were performed, with standard deviations shown. ** denotes statistical significance ($p<0.01$) and *** denotes statistical significance ($p<0.001$).

Bacteriophage multiplication in lethally irradiated *E. coli* cells

Phage λ was able to reproduce in healthy *E. coli* host cells (PC) as indicated by the significant difference ($p<0.0001$) to the no host cell (NC) negative control at every time point. The average log PFU increase was 3.18 ± 0.02 across all the time points (Fig. 22). Phage λ was able to propagate in eBeam irradiated (EB) host cells that were incubated for 24 hours post-irradiation (in LB broth at 4°C) (Fig. 22). At this time point, a statistically significant difference ($p<0.05$) based on a log PFU increase of 0.61was observed between EB and NC. At the other 3 time points (0 hours, 4 hours, 9 days),

there was no statistically significant difference between the PFU counts for λ incubated with EB cells and no host cells (NC). However, a slight increase in log PFU numbers (ca. 0.3) was observed at these three time points (Fig. 22). Phage λ was not able to reproduce in heat-killed (HK) host cells. In fact, a 0.3 log reduction in PFU counts was observed at all four time points (Fig. 22). A significant difference ($p<0.05$) was observed between irradiated and heat-killed host cells at every time point (Fig.22).

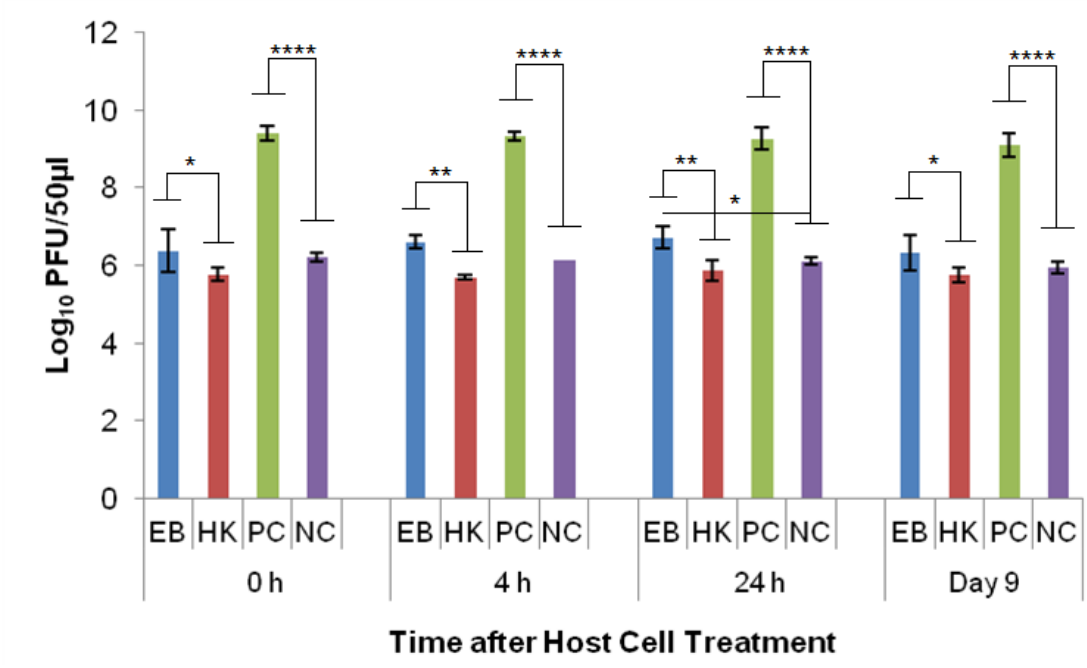

Figure 22. Bacteriophage λ numbers after incubation (at 37°C for 24 hours) with eBeam irradiated host cells (EB), heat-killed host cells (HK), non-treated host cells (PC – positive control) and no host cells (NC – negative control). The 0, 4, 24 hours, and day 9 time points represent the time after host cell treatment. Two independent experiments were performed, with standard deviations shown. * denotes statistical significance ($p<0.05$). ** denotes statistical significance ($p<0.01$) and **** denotes statistical significance ($p<0.0001$).

Phage T4D was able to reproduce in healthy *E. coli* host cells (PC) as indicated by the significant difference ($p<0.001$) to the no host cell control (NC) at every time point. The average log PFU increase was 2.04 ± 0.15 across all the time points (Fig. 23). Phage T4D numbers in lethally eBeam irradiated host cells (EB) remained at the same levels as the NC for all the time points, indicating that T4D was unable to propagate in EB cells (Fig. 23). Heat-killed host cells (HK) turned out to be a net sink for T4D phages, reducing its numbers by 2.88 logs on average, as indicated by the significant difference ($p<0.0001$) to the no host cell (NC) control (Fig. 23).

Phage T7 was able to reproduce in healthy *E. coli* host cells (PC) as indicated by the significant difference ($p<0.0001$) to the no host cell control (NC) at every time point. The average log PFU increase was 3.57 ± 0.15 across all the time points (Fig. 24).Phage T7 was able to produce progeny particles in eBeam irradiated host cells (EB) at every time point (0, 4, 24 hours, and 9 days post-irradiation) (Fig. 24). Phage T7 numbers in EB cells were significantly different ($p<0.0001$) from the no host cell control (NC), increasing by at least 2.6 logs at every time point (Fig. 24). There was no significant difference between the T7 phage numbers in heat-killed host cells (HK) compared to the NC, indicating that T7 phages were unable to propagate in HK host cells (Fig. 24). However, HK host cells were not a net sink for T7 phages as they had been for T4 phages.

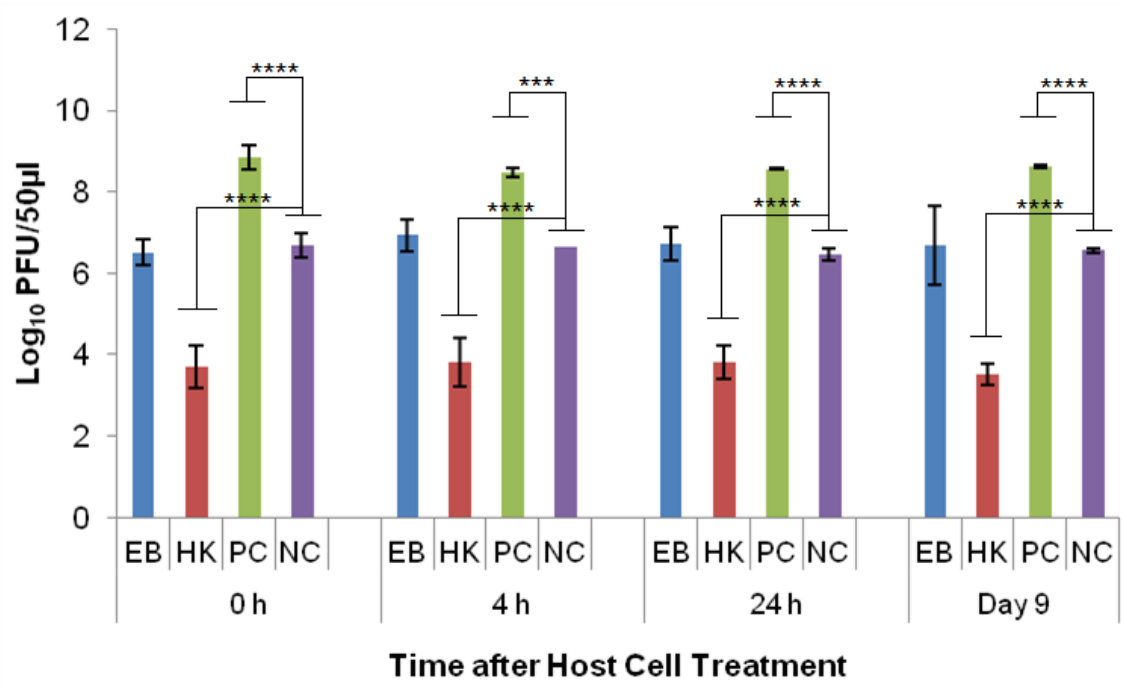

Figure 23. T4 bacteriophage numbers after incubation (at 37°C for 24h hours) with lethally eBeam irradiated host cells (EB), heat-killed host cells (HK), non-treated host cells (PC – positive control) and no host cells (NC – negative control). The 0, 4, 24 hours, and day 9 time points represent the time after host cell treatment. Two independent experiments were performed, with standard deviations shown. *** denotes statistical significance ($p<0.001$) and **** denotes statistical significance ($p<0.0001$).

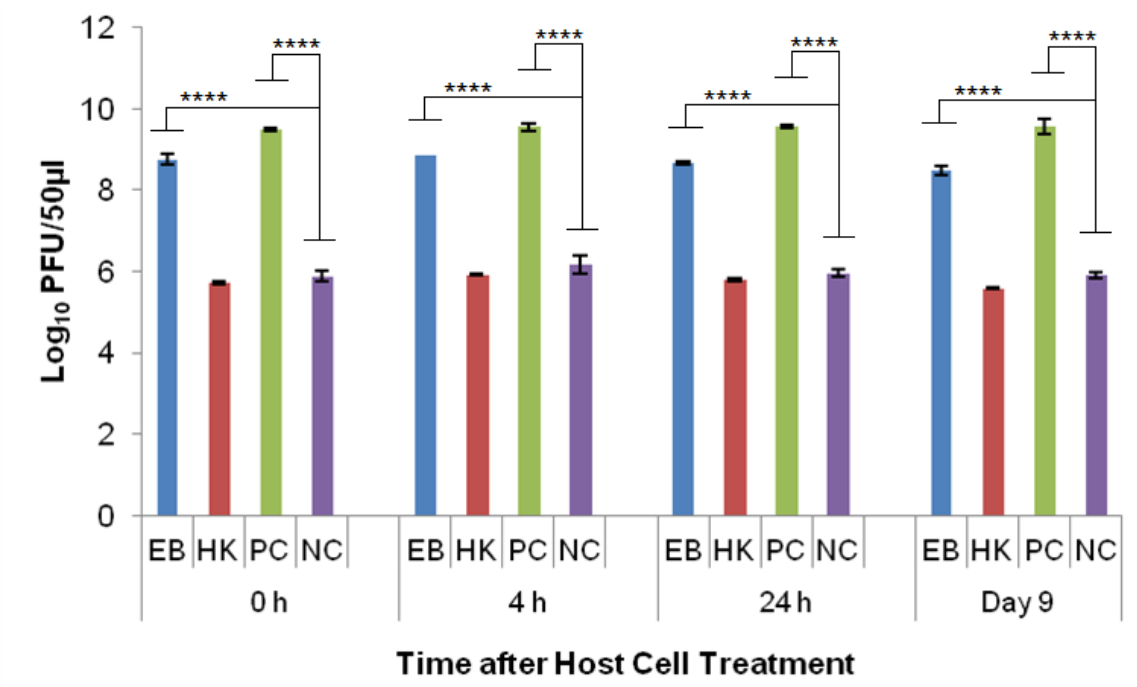

Figure 24. T7 bacteriophage numbers after incubation (at 37°C for 24 hours) with lethally eBeam irradiated host cells (EB), heat-killed host cells (HK), non-treated host cells (PC – positive control) and no host cells (NC – negative control). The 0, 4, 24 hours, and day 9 time points represent the time after host cell treatment. Two independent experiments were performed, with standard deviations shown. **** denotes statistical significance ($p<0.0001$).

Discussion

Membrane integrity of lethally irradiated cells

The vast majority of lethally eBeam irradiated *E. coli* cells maintained their membrane integrity up to 24 hours post-irradiation when kept in LB broth at 4°C. These results are congruent with a study by Jesudhasan et. al., which found that a large majority of *Salmonella* Enteritidis cells had intact membranes after exposure to a lethal 2.5 kGy eBeam dose (19). Only after 9 days of incubation did the membrane damage in the lethally irradiated *E. coli* cells become more prevalent (Fig. 13). This is in stark contrast to heat-killed cells, which showed membrane damage immediately following the heat treatment (Fig. 13). These results indicate that eBeam irradiation does not damage the cell membrane. In fact, eBeam irradiated cells resemble live cells more closely with respect to their membrane integrity.

Visualization of DNA double-strand breaks in lethally irradiated cells

Ionizing radiation is known to cause DNA double-strand breaks (DSBs) (46). DSBs are the most lethal form of DNA damage and most organisms can generally tolerate only a few of them (47). To confirm that a lethal eBeam dose results in extensive DNA damage, the neutral comet assay was performed on *S.* Typhimurium cells irradiated in PBS and *E. coli* cells irradiated in LB broth. The fluorescent images obtained from the comet assay showed extensive DSBs in both organisms after exposure to lethal eBeam irradiation. This is evident by the complete absence of distinct DNA tails/comets. The extensive damage to the nucleic acid made the quantification of DSBs impossible (Figs.

14 and 15). On the other hand, non-irradiated control cells showed only minor DNA damage as seen by a few long DNA tails, while heat-killed cells exhibited both patterns (Fig 14 and 15). The lack of distinct DNA tails in the eBeam irradiated cells is a result of the large number of DNA double-strand breaks. It has been estimated that 100 Gy of ionizing radiation cause approximately 1 DSB per one million base pairs (Mbp) (48). For the genomes of *S.* Typhimurium (4.8 Mbp) and *E. coli* strain K-12 (4.6 Mbp) this translates roughly to 3-5 DSBs per 100 Gy (81, 82). Therefore, a dose of 2 kGy would theoretically result in 60-100 DSBs per *Salmonella* genome and a dose of 7 kGy would result in 210-350 DSBs per *E. coli* genome. The paper by Singh et. al. (1999) is the only other published report that utilized the neutral comet assay to visualize DSBs in irradiated bacteria (83). They studied x-ray irradiated *E. coli* cells at 0.125 – 1 Gy and were able to quantify the DNA tails. However, considering the substantial difference in the dose, (1 Gy) they employed versus the 2000 Gy (employed in these studies), and the theoretical number of DSBs (0.03 vs 60 per cell), it is not surprising that distinct or countable DNA tails were not observed in these studies.

Metabolic activity of lethally irradiated *S*. Typhimurium cells

To determine if irradiated *S.* Typhimurium cells maintain their metabolic activity (i.e. maintain reducing conditions) post-irradiation, the cells were monitored over a period of 7 days using the redox indicator alamarBlue®. The results showed that eBeam and gamma irradiated *S.* Typhimurium cells were metabolically active for up to 7 days under certain post-irradiation incubation conditions. In general, eBeam and gamma irradiated

cells behaved similarly. When incubated at 4°C, both eBeam and gamma irradiated cells maintained their metabolic activity over the entire study period of 7 days, regardless of whether they were in buffer (PBS) or growth media (TSB). In prokaryotes, exposure to low temperatures, between 0-8°C, is typically associated with arrested cell growth and changes in cellular composition and function, such as a decrease in protein synthesis. (84-86). Since prokaryotic cells slow down large portions of their metabolism while mounting cold stress responses, it is not surprising that the metabolic activity levels of irradiated *S.* Typhimurium cells did not increase when incubated at 4°C (85). The difference in metabolic activity levels observed between cells in TSB and PBS may be due to the tenfold dilution in TSB, resulting in lower cell numbers. Irradiated cells were diluted in TSB rather than resuspended to avoid centrifugation. Although, the metabolic activity levels are different for cells in PBS and TSB, they are maintained in either medium at 4°C (Fig. 16A and 18A).

When incubated at 37°C in TSB, eBeam irradiated *S.* Typhimurium cells showed a slight and gradual increase in metabolic activity in the first 24-48 hours. By day 5, the metabolic activity declined. The initial increase in activity may be due to the up-regulation of DNA repair pathways due to the damage caused by the irradiation and the down-regulation of other non-essential activities (52, 59, 66, 87). The decline in activity by day 5 may be explained by the nature of batch cultures (closed system to which all nutrients are added at the beginning) and the fact that bacterial cells enter the death phase of their natural life cycle after 2-3 days (under batch culture growing conditions)

(Fig. 16B) (88, 89). On the other hand, gamma irradiated cells under the same incubation conditions did not exhibit an increase in metabolic activity within the first 48 hours. The reasons for this are unclear, since gamma irradiated cells also experienced DNA and other cellular damage caused by the irradiation. The difference in dose rate may play a role here because the gamma irradiation lasted 3 hours, whereas the eBeam irradiation was almost instantaneous. By day 5 of incubation, gamma irradiated cells exhibited no metabolic activity, most likely because the cells had entered their natural death phase (under growing conditions) (88, 89). Gamma irradiated cells incubated in PBS at 37°C showed no increase in metabolic activity (compared to TSB), but rather exhibited a sharp decline to almost zero within the first 12-24 hours of incubation. We hypothesize that the cells were attempting to repair the DNA damage caused by the irradiation (Fig. 18B) (52, 59, 66, 87), but since no nutrients were available in PBS, the cells exhausted all of their cellular resources more rapidly than the cells in TSB at the same temperature (90).

eBeam irradiated *E. coli* cells incubated in LB broth at 4°C maintained metabolic activity levels on par with the positive control cells for the first 24 hours (Fig. 20). This trend was also observed for lethally irradiated *S.* Typhimurium cells incubated in TSB at 4°C. We hypothesize that the lethally irradiated cells are adapting to the cold environment and are adjusting their metabolic needs to focus on DNA repair (52, 59, 66, 85, 87). By day 9 of incubation the metabolic activity in irradiated cells had decreased significantly compared to the control (Fig. 20). This trend could signify the beginning of

the cell death phase and is congruent with an observed decrease in membrane integrity (Fig. 13) (88, 89).

ATP levels in lethally irradiated *E. coli* cells

ATP levels for eBeam irradiated *E. coli* samples were more variable compared to heat-killed and control samples (Fig. 21). In general, irradiated samples resembled control samples more closely than heat-killed ones, except on day 9 of incubation, at which point the ATP levels in lethally irradiated cells had decreased significantly. The observed trend in ATP levels indicates that irradiated cells were metabolically active (to varying degrees) over the 9 day incubation period. These observations together with the results from the redox indicator (alamarBlue®) support our hypothesis that lethally irradiated cells remain metabolically active for extended periods of time after irradiation. Similar results were obtained by Magnani et. al. and Secanella-Fandos et. al. with lethally gamma irradiated *Brucella melitensis* and *Mycobacterium bovis* cells, respectively (20, 21).

Bacteriophage multiplication in lethally irradiated *E. coli* cells

All of the three bacteriophages tested, namely λ, T4 and T7, are tailed, double-stranded DNA phages belonging to the order *Caudovirales* (91). All three of them require their host cell's machinery to varying degrees for their propagation. Phage λ relies completely on the host cell to reproduce, T4 requires certain components of the host cell, and T7 only requires the host's machinery at the very beginning of infection (75, 78, 79).

Phage λ is most dependent on its host cell and it also has one of the best-understood complex regulatory systems. λ is a temperate phage, with an ability to choose between two alternative life styles: the lytic and the lysogenic growth cycles. The decision between the two cycles is made within the first 10-15 minutes of infection and depends both on the multiplicity of infection (MOI) and the physiological state of the host cell (76). λ uses the energy of the host cell's metabolism and its biosynthetic machinery to produce ca. 50-100 progeny virions (76). Cell lysis occurs after ca. 1 hour of infection in healthy host cells (76). The results of this study showed that at the 24 hour time point (post-irradiation), there was a statistically significant difference ($p<0.05$) between eBeam irradiated host cells and the no host cell control (Fig. 22), indicating that phage λ was able to propagate successfully in eBeam irradiated cells. A similar trend was observed for the remaining three time points (0 hours, 4 hours, day 9), but the increase in virus numbers was not statistically significant (Fig. 22). Since λ phages are able to propagate inside eBeam irradiated *E. coli* host cells, we hypothesize that all of the necessary cellular resources/machineries are still functioning within the irradiated cells. Phage λ requires the host's 1) RNA polymerase for all its transcription needs, 2) entire DNA replication apparatus for its phage DNA replication, and 3) translation machinery to make its proteins (75, 92). All of these cellular functions must still be in "good working order" in eBeam irradiated cells; otherwise phage λ would not be able to propagate. It is possible that λ used the host cell's pre-formed RNA polymerase as well as other macromolecules to carry out the transcription and translation of its DNA. Whether or not pre-formed molecules were used, these results prove that the host cell's

RNA polymerase is able to transcribe DNA and the ribosomes are able to translate and make proteins after a lethal eBeam irradiation dose.

The results for the T4 phage experiments revealed that they were unable to propagate in eBeam irradiated host cells. Interestingly, heat-killed host cells were a net sink for T4 phages, reducing phage numbers by approximately 3 logs (Fig. 23). T4 phages also depend on many vital host structures and functions, such as membranes, energy metabolism, transcriptional and translational machines, and some chaperones (79, 93, 94). T4 phages use and modify the core host RNA polymerase, through phage-induced proteins, to selectively transcribe the hydroxymethylcytosine (HMC) residue containing phage DNA rather than the cytosine residue containing host DNA (79, 95, 96). In fact, all host DNA and mRNA present at the time of infection, are rapidly degraded and the breakdown products are used to synthesize phage DNA and RNA. Furthermore, after infection, the translation of host messages ceases and ribosomes are re-programmed to translate T4 messages (97). Other than phage λ, T4 phage codes for all the components of its own DNA replication and recombination complexes (79, 98-100). It is unclear which structural or functional component(s) of the eBeam irradiated host cells were not functioning properly to prevent T4 propagation. It is possible that all of the host cell modifications (i.e. RNA polymerase) initiated by T4 phages increased the overall oxidative stress within the host cells, rendering them ineffective for phage propagation. Krisko and Radman found that the decline of what they called biosynthetic efficacy (measured by λ propagation) was correlated to radiation-induced oxidative damage

(101). Targeted studies are needed to address this issue as well as the sink phenomenon observed in heat-killed host cells (Fig. 23).

The results for the T7 phage experiments showed that they were the most successful in utilizing eBeam irradiated host cells for their propagation out of all the phages tested (Fig. 24). T7 growth is remarkably independent of host enzymes; it only requires the host's translational apparatus and biosynthetic machinery for precursor synthesis (78). The host cell's RNA polymerase is used to make early RNAs, but most of the transcription is catalyzed by the T7 RNA polymerase (once it has been synthesized by the host cell). T7 DNA replication and recombination are also independent of host proteins, except for thioredoxin (78, 102, 103). Just like T4 phages, T7 phages attach to the lipopolysaccharides of the outer membrane and translocate their DNA via a self-made channel into the host cell's cytoplasm. DNA translocation is highly-temperature dependent and requires membrane potential (78, 104). Since T7 phages require the least amount of host cell resources and functionalities, this may be the reason why they were able to propagate so efficiently in eBeam irradiated host cells (Fig. 24). Furthermore, the results indicate that all of the cellular components (i.e. RNA polymerase) needed by the phage to replicate are functioning properly in eBeam irradiated host cells. It would further appear that irradiated cells kept at 4°C post-irradiation are "frozen in time" (in terms of their cellular activities), since T7 phages were able to propagate in cells that had been stored for 9 days just as well as in freshly irradiated cells (Fig. 24). This is in contrast to post-irradiation incubation at 37°C. Marsden et. al. found that sub-lethally

irradiated *E. coli* cells rapidly lost their ability to support T4 phage growth after 2 hours of post-irradiation incubation at 37°C (105). Even though, T7 phages were able to propagate well in irradiated cells, the increase in numbers was still significantly different ($p<0.0001$) from the non-irradiated (control) cells (Fig. 24). This leads to the conclusion that some cellular components, apart from the DNA, were rendered less functional due to the irradiation with a lethal eBeam dose. These results are in line with earlier studies that examined phage growth in x-ray irradiated *E. coli* host cells (106, 107). The results presented here with eBeam irradiated *E. coli* host cells have raised many more interesting questions (i.e. do phages use pre-formed or newly synthesized RNA polymerase) and warrant further investigation. Using bacteriophages to investigate the functionality of lethally irradiated bacterial cells may prove to be a very elegant model system.

In conclusion, the results presented indicate that both lethally irradiated *S.* Typhimurium and *E. coli* cells resemble live (non-irradiated) cells more closely than heat-killed cells. Despite their extensive DNA damage, lethally irradiated cells have intact membranes, are metabolically active, and are able to support the propagation of bacteriophages.

CHAPTER V

TRANSCRIPTOMIC RESPONSES OF *SALMONELLA* TYPHIMURIUM AFTER EXPOSURE TO LETHAL DOSES OF ELECTRON BEAM AND GAMMA RADIATION

Overview

There is evidence bacteria retain their metabolic functions as well as their transcriptional activities after exposure to lethal doses of ionizing radiation. To the best of our knowledge, there have been no published reports that investigate the global transcriptomic response of lethally irradiated bacterial cells. The primary objective of this study was to determine if there is a difference in gene expression in lethally eBeam irradiated and lethally gamma irradiated *S.* Typhimurium cells and non-irradiated (control) cells. The method employed was RNA Sequencing (RNA-Seq), a technology that uses the capabilities of next-generation high-throughput sequencing to reveal a snapshot of RNA presence and quantity in a cell at a given point in time. The results of this study show that post-irradiation incubation in PBS buffer at 4°C results in minimal differential gene expression over a period of 24 hours in eBeam and gamma irradiated *S.* Typhimurium cells. When incubated in growth media (TSB) at 37°C, however, the transcriptomic responses in both eBeam and gamma irradiated cells have unique characteristics. In general, lethally irradiated cells focus on repairing DNA and membrane damage over a 24 hour period. Gamma irradiated cells exhibit more extensive DNA and membrane repair than eBeam irradiated cells. Both types of irradiated cells

down-regulate major metabolic pathways, such as the citric acid cycle, presumably to redirect the energy expenditure to focus on DNA and membrane repair. In essence, lethal ionizing radiation creates senescent bacterial cells that are no longer capable of dividing but are still alive and metabolically active for an extended period of time after irradiation.

Introduction

The results from our characterization studies (Chapter IV) as well as reports in the literature have shown that bacteria exposed to a lethal dose of ionizing radiation retain their metabolic and transcriptional activities (20, 21, 106, 107). Magnani et. al. demonstrated that lethally gamma irradiated *Brucella melitensis* cells had lost their ability to replicate but still possessed metabolic and transcriptional activity. The cells also persisted in macrophages, generated antigen-specific cytotoxic T cells, and protected mice against virulent bacterial challenge. The authors concluded that the pathogen's metabolic activity had a positive influence on shaping protective host immune responses (20). Secanella-Fandos et. al. observed that lethally gamma irradiated *Mycobacterium bovis* cells were metabolically active and exhibited similar tumor growth inhibition and induction of cytokines compared to live cells (21).

Most of the reports in the literature that investigate lethally irradiated bacteria do so in the context of vaccines and immunogenicity (19-22). All of these studies have shown that lethally irradiated bacteria impart an immune response similar to live vaccines,

indicating that the epitopes' structure and functionality are preserved. To the best of our knowledge, there have been no published reports that investigate the overall transcriptomic response of bacteria that have been exposed to lethal eBeam or gamma irradiation. We wanted to gain a better understanding of the global transcriptomic response of *S.* Typhimurium, a foodborne pathogen and causative agent of salmonellosis (108), to lethal ionizing radiation. The primary objective of this study was to determine if there is a difference in gene expression in lethally eBeam and gamma irradiated S. Typhimurium cells compared to each other as well as non-irradiated (control) cells.

This study was designed to elucidate 4 specific research questions, namely 1. Is there a difference in gene expression in irradiated cells immediately after irradiation compared to prolonged storage in PBS buffer at 4°C? 2. Is there a difference in gene expression patterns between eBeam and gamma irradiated cells when incubated for extended periods of time in TSB growth media? 3. What happens to cells immediately after lethal irradiation? 4. Are the gene expression patterns in irradiated cells different from non-irradiated (control) cells when incubated in TSB growth media at an optimum incubation temperature?

Materials and Methods

Preparation and irradiation of *Salmonella* Typhimurium cultures

Overnight cultures of *S*. Typhimurium (ATCC 14028) were grown in tryptic soy broth (TSB) at 35°C in a shaking water bath. The cultures were centrifuged at 4000 x g for 10 minutes at room temperature (RT), the growth media removed and the cell pellets washed once in phosphate buffered saline (PBS). After washing, the cell pellets were resuspended in PBS to an OD_{600} of ca. 1.0, resulting in approximately $1x10^8$ Colony Forming Units (CFU)/ml. Aliquots (2 ml) of the adjusted and well-mixed cell suspension were individually packaged for irradiation as previously described in Chapter IV to allow for discrete sampling post-irradiation. Samples were irradiated to a lethal dose of 2 kGy with either a 10 MeV eBeam at the NCEBR or with the reactor core at the NSC as previously described in Chapter IV. To reach a dose of 2 kGy with eBeam only took a few seconds. To reach the same dose with gamma took 180 minutes (3 hours). Dose measurements were obtained as previously described in Chapter IV. Non-irradiated samples (0 kGy) were used as controls. These samples were packaged the same way as the experimental samples and were transported to the irradiation facility to eliminate possible differences in survival due to transport and handling.

Experimental design

To investigate the transcriptomic response of *S.* Typhimurium following a 'lethal' radiation dose cells were irradiated in PBS at ambient temperature (ca. 25°C). Immediately after irradiation (0 hours), aliquots of the cell suspension were flash frozen

in a dry ice/isopropanol slurry at the radiation facility. For the remaining time points post-irradiation, the cells either remained in the PBS they were irradiated in or they were transferred to an equal volume of 2x TSB. The cells in PBS were incubated at 4°C and the cells in TSB were incubated at 37°C. RNA was collected after 4 and 24 hours of incubation (Fig. 25). In addition, OD_{600} readings (Eppendorf Spectrophotometer) along with viable cell counts (on TSA) were obtained at the 0, 4, and 24 hour time points. A discrete sampling scheme was chosen to prevent the chance of contamination. A total of 12 individual sample bags containing 2 ml of the cell suspension each were prepared: 10 (5 each for irradiation and control) for RNA collection and 2 (irradiated and control) for OD_{600} readings and viable cell counts. Four independent experiments were performed for each radiation source.

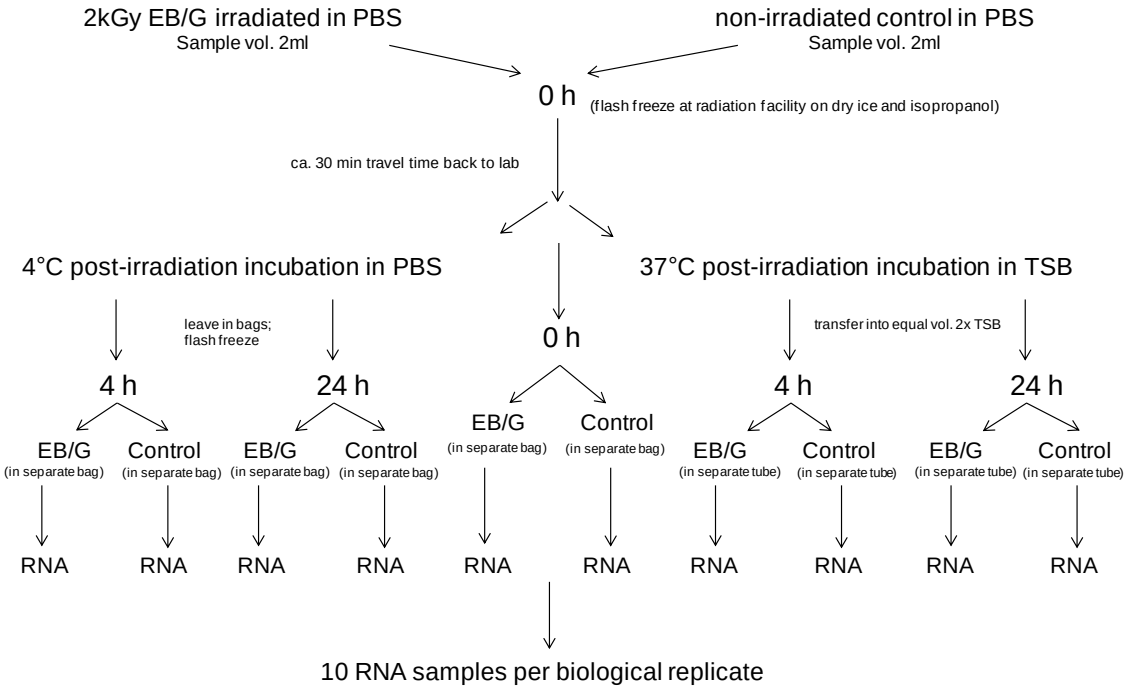

Figure 25. Experimental Design for the RNA-Seq Study. EB refers to lethal eBeam irradiation doses and G refers to lethal gamma irradiation doses.

RNA collection

RNA was collected at 0, 4, and 24 hours post-irradiation. For the 0 hour time point, two 50 ml conical tubes containing 4 ml (2x sample volume) of RNAprotect Bacteria Reagent (Qiagen, Valencia, CA) were prepared. The reagent offers immediate RNA stabilization in bacterial cultures. The sample bags were cut open aseptically and the frozen cell suspensions were slid into the tubes. The cell suspension was allowed to thaw completely while submerged in the reagent. The samples were then vortexed and incubated for 5 minutes at RT. Following the incubation, the samples were centrifuged at 4000 x g for 15 minutes at RT. The supernatant was removed and the cell pellets were

stored at -80°C for no more than two weeks before RNA extraction. For the 4 and 24 hour time points, the samples in PBS at 4°C were flash frozen on a dry ice/isopropanol slurry and processed the same way as the samples at the 0 hour time point. To the irradiated samples in TSB at 37°C, 8 ml of RNAprotect Bacteria Reagent were added directly to the 15 ml conical tube containing 4 ml of sample. Since the non-irradiated control cells were actively growing in TSB at 37°C, only 200 µl of the cell culture were mixed with 600 µl (3x sample volume) of RNAprotect Bacteria Reagent. Preliminary experiments revealed that at 4 and 24 hours, 4 ml of culture contained ca. $1.2x10^{10}$ cells. To keep the number of cells similar across all samples, and to not overload the downstream RNA extraction method, only 200 µl, resulting in ca. $6x10^{8}$ cells, were collected. Preliminary experiments also showed that adding 3x the sample volume of RNAprotect Bacteria Reagent to the control cells in TSB resulted in better RNA quality. Following the addition of the RNAprotect Bacteria Reagent, the samples were centrifuged at 4000 x g for 15 minutes at RT. The supernatant was removed and the cell pellets were stored at -80°C for no more than two weeks before RNA extraction.

RNA extraction

RNA was extracted using the RNeasy Mini Kit (Qiagen, Valencia, CA) according to the manufacturer's instructions with minor modifications. Briefly, the cells pellets were thawed at RT and 200 µl of TE buffer (10 mM Tris-Cl, 1 mM EDTA, pH 8.0) containing lysozyme (1mg/ml) was added. Samples were transferred to a RNase-free microcentrifuge tube, vortexed and incubated for 30 minutes at RT. During the

incubation, samples were vortexed every 2 minutes. Following the incubation, 700 µl of RLT buffer containing β-mercaptoethanol were added and the samples were vortexed vigorously. Then 500 µl of 100% ethanol were added and the samples were mixed again. 700 µl of the lysate was then transferred to a spin column and centrifuged in a microcentrifuge at RT for 1 minute at 10000 x g. The flow-through was discarded and the remaining lysate was transferred to the spin column and centrifuged as before. Then 350 µl of RW1 buffer were added to the spin column and centrifuged as before to wash the spin column membrane. This was followed by an on-column DNase digestion for 15 minutes with the Qiagen RNase-free DNase I kit (Catalog #: 79254). The digestion was followed by another wash step with 350 µl RW1 buffer. The RNeasy spin column was placed in a new 2 ml collection tube and washed twice with 500 µl RPE buffer via centrifugation as before. The flow-through was discarded after the first wash step. The spin column was then transferred to yet another new 2 ml collection tube and centrifuged for 1 minute at full speed to remove all of the ethanol. Next, the spin column was transferred to a 1.5 ml RNase-free microcentrifuge tube and the RNA was eluted with 50 µl RNase-free water via centrifugation for 1 minute at 10000 x g. RNA quantity was determined immediately following RNA extraction using a NanoDrop ND-1000 spectrophotometer (ThermoScientific, Wilmington, DE). Prior to freezing the RNA samples at -80°C, separate 5 µl aliquots of RNA (1-2 µl RNA diluted in RNase-free water) were made and also stored at -80°C for subsequent RNA quality analysis with the Agilent RNA 6000 Nano Kit on the Agilent 2100 Bioanalyzer System (Santa Clara,

CA). The RNA quality check was performed within one week of RNA extraction and according to the manufacturer's instructions.

RNA-Seq analysis

Total RNA samples were sent to the Genomics and Bioinformatics Services at Texas A&M AgriLife Research, Texas A&M University for RNA-Seq library preparation and analysis. Library preparation was performed using the ScriptSeq™ Complete (Bacteria) Kit (Epicentre, Madison, WI). The first step in this kit is the Ribo-Zero™ ribosomal RNA (rRNA) removal module (Fig. 26). It effectively depletes rRNA (23S, 16S, 5S) in bacteria. The second module in this kit is the ScriptSeq™ v2 RNA-Seq library preparation. This step creates a stranded Illumina sequencing library (Fig. 27). Following library preparation, 100-base-paired-end sequencing using the Illumina HiSeq-2500 platform was performed. Sequence cluster identification, quality pre-filtering, base calling and uncertainty assessment were done in real time using Illumina's HCS 2.2.38 and RTA 1.18.61 software with default parameter settings. Samples were demultiplexed during the conversion from BCL files to FASTQ format files. The quality of the paired-end reads was checked using FastQC software (109). The quality plots of the sequencing runs were provided by the Genomics and Bioinformatics Center, and all the runs passed the quality control (QC). One of the important quality measurements are the overall quality scores for each sample. All the samples had satisfactory Q30 scores. In the next step, the reads from each sample were independently mapped to the NCBI reference genome for *S*. Typhimurium (accession number

GCA_000022165.1_ASM2216v1) using the CLC Genomics Workbench software (version 6.0.1) (CLC bio, Boston, MA). Mapping parameters were as follows: mismatches allowed (applies to short reads): 2; minimum length fraction: 0.9; minimum similarity fraction: 0.85 (90% of the length of the read had to map to a gene sequence with at least 85% similarity); unspecific match limit: 10; minimum exon coverage fraction: 0.2; minimum number of reads: 10; minimum and maximum paired distance: 180 – 250.

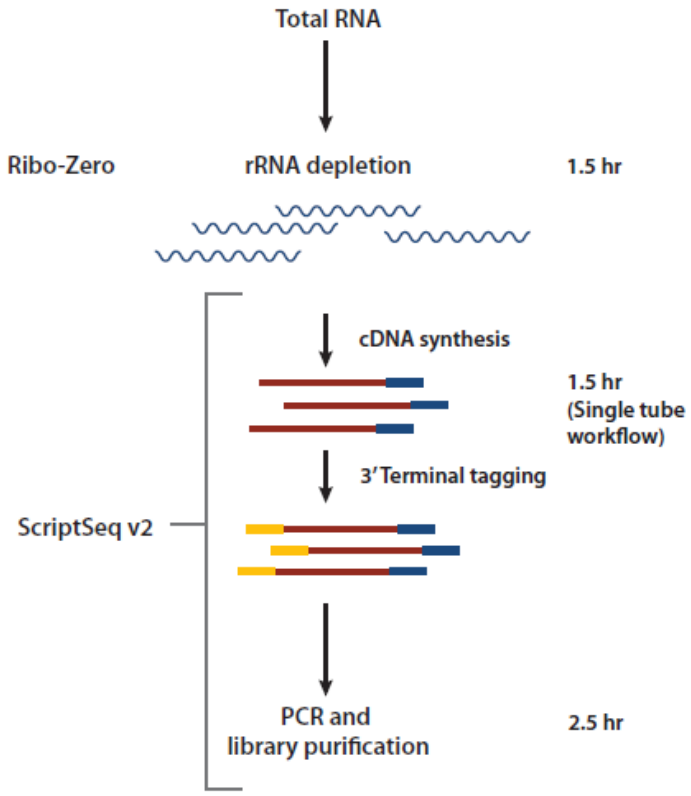

Figure 26. An overview of the ScriptSeq Complete Kit (Bacteria) procedure. rRNA is first removed from the sample using the Ribo-Zero Magnetic Kit (Bacteria). The ScriptSeq v2 RNA-Seq Library Preparation Kit is then used to make the RNA-Seq library from the Ribo-Zero treated RNA (110).

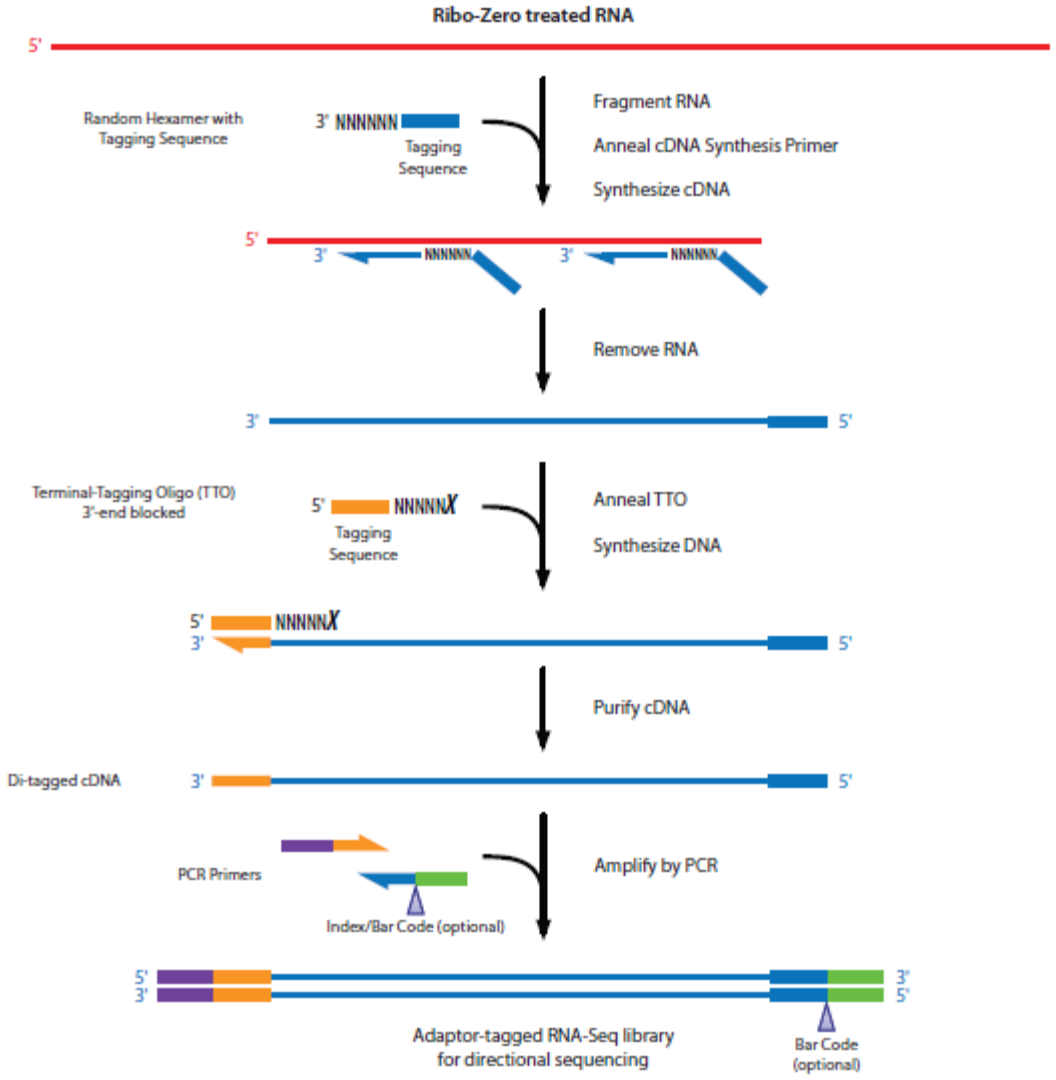

Figure 27. An overview of the procedure for the ScriptSeq v2 RNA-Seq library preparation kit (110).

Statistical analyses were performed using the statistical language R, in particular the edgeR package from Bioconductor (111-113) via the iPlant Collaborative online platform (114). Total read counts were exported from CLC RNA-Seq mappings and normalized using the edgeR trimmed mean of M-values (TMM) normalization. Dispersions were estimated using the quantile-adjusted conditional maximum likelihood (qCML) method. The edgeR CPM (counts per million) filter was used to eliminate the genes with low coverage (Table 4). Differential gene expression was determined using the Fisher's exact test (pairwise comparisons). In order to determine the most appropriate multiple testing correction factor, the performance of the False Discovery Rate (FDR), the Benjamini-Hochberg algorithm (BH) as well as several other algorithms were compared (Table 5). Following the test comparisons, it was determined that the Benjamini-Hochberg (BH) correction factor ($BH \leq 0.05$) (edgeR default) and a CPM filter of 16 (due to 8 replicates) together were most appropriate. All analyses were performed with these parameters. Table 6 lists all of the pairwise comparisons that were performed.

Table 4. Overview of the output from three pairwise comparisons with the Fisher's exact test in edgeR performed with different numbers for the CPM filter to remove genes that are expressed at very low levels or not at all.

CPM[a] filter	**10[b]**	**16**	**24**	**52**
Multiple Testing Correction Factor	BH[c]	BH	BH	BH
Significance Level	0.05	0.05	0.05	0.05
DE[d] genes for Comparison 1[e]	465	465	465	466
DE genes for Comparison2 [f]	1853	1854	1854	1856
DE genes for Comparison 3[g]	3253	3253	3253	3253

[a] counts per million; [b] minimum sum count across data columns; [c] Benjamini-Hochberg; [d] differentially expressed; [e] eBeam PBS at 4°C 0 vs. 4 hours; [f] eBeam vs. gamma at 0 hours; [g] control vs. gamma 4 hours TSB at 37°C

Table 5. Overview of the output from three pairwise comparisons with the Fisher's exact test in edgeR performed with different multiple testing correction factors to control the false discovery rate (FDR).

Multiple Testing Correction Factor	**BH[a]**	**FDR**	**Hommel**	**Holm**	**Hochberg**	**BY[b]**	**Bonferroni**
CPM[c] filter	5[h]	5	5	5	5	5	5
Significance Level	0.05	0.05	0.05	0.05	0.05	0.05	0.05
DE[d] genes for Comparison 1[e]	465	465	16	16	16	22	16
DE genes for Comparison 2[f]	1853	1853	490	474	474	1105	467
DE genes for Comparison 3[g]	3253	3253	1924	1900	1900	2705	1847

[a] Benjamini-Hochberg; [b] Benjamini-Yekutieli; [c] counts per million; [d] differentially expressed; [e] eBeam PBS at 4°C 0 vs. 4 hours; [f] eBeam vs. gamma at 0 hours; [g] control vs. gamma 4 hours TSB at 37°C [h] edgeR default

Table 6. Pairwise Comparisons performed in edgeR using the Fisher's Exact Test.

Description	Abbreviation
1. Is there a difference in gene expression in irradiated cells immediately after irradiation compared to prolonged storage in buffer (PBS) at 4°C?	
eBeam irradiated cells immediately after irradiation compared to cells stored in PBS at 4°C for 4 hours	EB-PBS-4°C 0h vs 4h
eBeam irradiated cells immediately after irradiation compared to cells stored in PBS at 4°C for 24 hours	EB-PBS-4°C 0h vs 24h
eBeam irradiated cells stored in PBS at 4°C for 4 hours compared to cells stored in PBS at 4°C for 24 hours	EB-PBS-4°C 4h vs 24h
gamma irradiated cells immediately after irradiation compared to cells stored in PBS at 4°C for 4 hours	G-PBS-4°C 0h vs 4h
gamma irradiated cells immediately after irradiation compared to cells stored in PBS at 4°C for 24 hours	G-PBS-4°C 0h vs 24h
eBeam irradiated cells stored in PBS at 4°C for 4 hours compared to cells stored in PBS at 4°C for 24 hours	G-PBS-4°C 4h vs 24h
2. Is there a difference in gene expression patterns between eBeam and gamma irradiated cells when incubated for extended periods of time in TSB growth media?	
eBeam irradiated cells immediately after irradiation compared to gamma irradiated cells immediately after irradiation	0h EB vs G
eBeam irradiated cells stored in PBS at 4°C for 4 hours compared to gamma irradiated cells stored in PBS at 4°C for 4 hours	4h-PBS-4°C EB vs G
eBeam irradiated cells stored in PBS at 4°C for 24 hours compared to gamma irradiated cells stored in PBS at 4°C for 24 hours	24h-PBS-4°C EB vs G
eBeam irradiated cells incubated in TSB at 37°C for 4 hours compared to gamma irradiated cells incubated in TSB at 37°C for 4 hours	4h-TSB-37°C EB vs G
eBeam irradiated cells incubated in TSB at 37°C for 24 hours compared to gamma irradiated cells incubated in TSB at 37°C for 24 hours	24h-TSB-37°C EB vs G
3. What happens to cells immediately after lethal irradiation?	
eBeam irradiated cells immediately after irradiation compared to non-irradiated (control) cells	0h C vs EB
gamma irradiated cells immediately after irradiation compared to non-irradiated (control) cells	0h C vs G
4. Are the gene expression patterns in irradiated cells incubated in TSB at an optimum growth temperature different from non-irradiated (control) cells?	
eBeam irradiated cells incubated in TSB at 37°C for 4 hours compared to non-irradiated (control) cells incubated in TSB at 37°C for 4 hours	4h-TSB-37°C C vs EB
eBeam irradiated cells incubated in TSB at 37°C for 24 hours compared to non-irradiated (control) cells incubated in TSB at 37°C for 24 hours	24h-TSB-37°C C vs EB
gamma irradiated cells incubated in TSB at 37°C for 4 hours compared to non-irradiated (control) cells incubated in TSB at 37°C for 4 hours	4h-TSB-37°C C vs G
gamma irradiated cells incubated in TSB at 37°C for 24 hours compared to non-irradiated (control) cells incubated in TSB at 37°C for 24 hours	24h-TSB-37°C C vs G

Following the statistical analysis in edgeR, the resulting lists of differentially expressed genes (DE genes) from each pairwise comparison were further analyzed for up- and down-regulation. DE genes (BH ≤ 0.05) with a log fold change ≥ 2 were considered up-regulated and DE genes with a log fold change ≤ -2 were considered down-regulated. These lists of up- and down-regulated DE genes were analyzed for their functions.

Functional gene annotation

Functional annotation clustering was performed with the Database for Annotation, Visualization and Integrated Discovery (DAVID) (version 6.7) (115, 116). The lists of both up- and down-regulated DE genes were uploaded and analyzed separately. Annotations were limited to *Salmonella enterica* and the classification stringency was set to "medium". In the DAVID annotation system, the Fisher's exact test was adopted to measure the gene-enrichment (specific gene association) in annotation terms, resulting in a p-value for every annotation cluster. Since DAVID runs the gene list of interest through many databases (i.e. SP_PIR_KEYWORDS, KEGG PATHWAY, GOTERM, UP_SEQ_FEATURE, and INTERPRO), each annotation cluster has more than one p-value. The group enrichment score associated with each cluster is the geometric mean (in – log scale) of all the p-values in that cluster. It is used to rank the clusters in terms of their biological significance. A cutoff value of 1.3 for the enrichment score was used to filter out non-significant annotation clusters ($-\log(0.05) = 1.3$).

Data presentation

RNA-Seq experiments are known to generate massive amounts of data. Organizing this data in a meaningful way can be quite challenging. First, the total numbers of DE genes for each pairwise comparison were grouped according to their biological question. This gave an overview of total gene expression across treatments and time points. Next, the lists of DE genes were subjected to functional annotation analysis and tables showing the functional clusters for both up- and down-regulated genes were generated for each pairwise comparison. Through this analysis, it was also determined that quite a large portion of the DE genes had no known "function". To illustrate this point, a table was generated showing the number of DE genes with known/unknown function.

Results

An overview of the total number of DE genes for each pairwise comparison is presented in Table 6. The total number of DE genes for irradiated *S.* Typhimurium cells incubated in PBS at 4°C was low. For eBeam irradiated cells, it ranged from 0.6 to 5.6% of total genes over a 24 hour period. Gamma irradiated cells exhibited no differential gene expression over the same time period. Immediately after irradiation (0 hours), 9.7% of the total number of genes were differentially expressed between eBeam and gamma irradiated cells. After a 4 hour incubation in PBS at 4°C only 1.4% were differentially expressed between eBeam and gamma irradiated cells. After a 24 hour incubation period, this number had increased to 12.5%. When eBeam and gamma irradiated cells were incubated in TSB (growth media) at 37°C, 7.8% of the total genes were

differentially expressed between them after 4 hours and only 1.2% after 24 hours. When eBeam irradiated cells were compared to non-irradiated (control) cells immediately after irradiation, no difference in gene expression was observed. In contrast, gamma irradiated cells showed that 15.1% of the total genes were differentially expressed when compared to the non-irradiated (control) cells immediately after irradiation. Out of all the pairwise comparisons, differential gene expression was greatest, ranging from 12.5 to 27.6%, between irradiated cells and non-irradiated (control) cells when incubated in TSB at 37°C (Table 7). A large proportion, sometimes more than half, of these DE genes had no known function (Table 8). Tables 9 through 16 show the functional clusters obtained for each pairwise comparison examined. For two of the comparisons there were too few DE genes with a known function, hence no functional clusters were obtained. In these instances, the list of up- or down-regulated DE genes was included (Tables 10 and 11).

Table 7. Overview of the number of differentially expressed (DE) genes in *S.* Typhimurium for each pairwise comparison.

Comparison		Total DE genes	% of total genes	Upregulated DE genes (log FC[a] ≥ 2)	% of total genes	Downregulated DE genes (log FC ≤ -2)	% of total genes	Total # DE genes with log FC ≥ 2, ≤ -2	% of total genes
EB[b]-PBS-4°C	0h vs 4h	465	8.3	313	5.6	2	0.04	**315**	**5.6**
EB-PBS-4°C	0h vs 24h	260	4.6	12	0.21	22	0.39	**34**	**0.6**
EB-PBS-4°C	4h vs 24h	98	1.7	0	0	87	1.5	**87**	**1.5**
G[c]-PBS-4°C	0h vs 4h	1	0.02	1	0.02	0	0	**1**	**0.02**
G-PBS-4°C	0h vs 24h	0	0	0	0	0	0	**0**	**0**
G-PBS-4°C	4h vs 24h	0	0	0	0	0	0	**0**	**0**
0h	EB vs G	1854	33.0	288	5.1	255	4.5	**543**	**9.7**
4h-PBS-4°C	EB vs G	288	5.1	44	0.78	32	0.57	**76**	**1.4**
24h-PBS-4°C	EB vs G	1601	28.5	634	11.3	71	1.3	**705**	**12.5**
4h-TSB-37°C	EB vs G	2091	37.2	419	7.5	20	0.36	**439**	**7.8**
24h-TSB-37°C	EB vs G	356	6.3	28	0.50	39	0.69	**67**	**1.2**
0h	C[d] vs EB	0	0	0	0	0	0	**0**	**0**
0h	C vs G	1673	29.7	620	11.0	229	4.1	**849**	**15.1**
4h-TSB-37°C	C vs EB	3525	62.7	717	12.7	548	9.7	**1265**	**22.5**
24h-TSB-37°C	C vs EB	1502	26.7	603	10.7	98	1.7	**701**	**12.5**
4h-TSB-37°C	C vs G	3253	57.8	1232	21.9	319	5.7	**1551**	**27.6**
24h-TSB-37°C	C vs G	2055	36.5	705	12.5	179	3.2	**884**	**15.7**

[a] Fold change; [b] eBeam; [c] Gamma; [d] Control

Table 8. Overview of the number of differentially expressed (DE) genes in *S.* Typhimurium with known and unknown function.

Comparison		Upregulated DE genes (log FC[a] ≥ 2)	Gene Function		Downregulated DE genes (log FC[a] ≤ -2)	Gene Function	
			Known (%)	Unknown (%)		Known (%)	Unknown (%)
0h	**EB[b] vs G[c]**	288	142 (49.3)	146 (50.7)	255	224 (87.8)	31 (12.2)
4h-TSB-37°C	**EB vs G**	419	176 (42.0)	243 (58.0)	20	4 (20)	16 (80)
24h-TSB-37°C	**EB vs G**	28	17 (60.7)	11 (39.3)	39	38 (97.4)	1 (2.6)
0h	**C[d] vs EB**	0			0		
0h	**C vs G**	620	307 (49.5)	313 (50.5)	229	204 (89.1)	25 (10.9)
4h-TSB-37°C	**C vs EB**	717	443 (61.8)	274 (38.2)	548	402 (73.4)	146 (26.6)
24h-TSB-37°C	**C vs EB**	603	410 (68.0)	193 (32.0)	98	79 (80.6)	19 (19.4)
4h-TSB-37°C	**C vs G**	1232	682 (55.4)	550 (44.6)	319	251 (78.7)	68 (21.3)
24h-TSB-37°C	**C vs G**	705	448 (63.5)	257 (36.5)	179	155 (86.6)	24 (13.4)

[a] Fold change; [b] eBeam; [c] Gamma; [d] Control

Table 9. Differentially expressed functional gene clusters for gamma irradiated and eBeam irradiated *S.* Typhimurium cells in PBS immediately after irradiation.

Cluster	Upregulated Functional Clusters	# Genes	ES[a]	Downregulated Functional Clusters	# Genes	ES
1	bacterial secretion / virulence	5-14	3.7	propanoate metabolism	6-10	8.6
2	phenylalanine, tyrosine and tryptophan biosynthesis	3-6	2.1	ABC transporters	13-19	8
3	cell redox homeostasis	3-6	1.9	butanoate metabolism	4-17	5.7
4	fructose and mannose metabolism	3-4	1.9	tricarboxylic acid cycle	4-7	4.2
5	cell envelope	6-11	1.4	valine, leucine and isoleucine degradation	3-6	4.1
6	isomerase	3-6	1.4	valine, leucine and isoleucine degradation	3-6	3.9
7	pili assembly chaperone	3-7	1.3	organic acid catabolic process	4-13	3.8
8				lipid catabolic process	3-8	3.2
9				periplasm / amino acid transport	5-8	3.1
10				arginine and proline metabolism	3-8	3
11				C5-branched dibasic acid metabolism	3	2.3
12				ligase activity	3-8	2.1
13				glutathione metabolism	3-4	2.1
14				metal binding	18-34	2.1
15				pyruvate metabolism	3-6	2.1
16				alanine racemase	3-6	2
17				ABC transporters	3-14	1.9
18				oxidoreductase	12-25	1.8
19				amino-acid transport	3-8	1.3

[a] Enrichment Score: geometric mean (in – log scale) of all the p-values in a cluster

Table 10. Differentially expressed functional gene clusters for gamma irradiated and eBeam irradiated *S*. Typhimurium cells in TSB after incubation for 4 hours at 37°C post-irradiation.

Cluster	Upregulated Functional Clusters	# Genes	ES[a]	Gene ID[b]	Downregulated Gene Function and / or Product
1	ABC transporters	5-12	6.9	STM14_5065	putative phage tail core protein
2	Bacterial secretion system	4-13	4.5	STM14_5067	putative cytoplasmic protein
3	transmembrane transport	13-34	3.6	STM14_5064	
4	pili assembly chaperone	6-15	3.5	STM14_5068	putative cytoplasmic protein
5	pentose and glucuronate interconversions	3-4	3.4	STM14_5066	putative phage tail sheath protein
6	two-component system	3-5	2	STM14_5052	putative phage baseplate protein
				STM14_5051	putative phage baseplate protein
				STM14_5050	putative phage tail protein
				STM14_5047	putative cytoplasmic protein
				STM14_5049	putative phage tail fiber protein H
				STM14_5048	putative cytoplasmic protein
				STM14_5069	putative inner membrane protein
				STM14_5071	putative inner membrane protein
				pflB	pyruvate formate lyase I
				STM14_5070	putative soluble lytic murein transglycosylase
				STM14_5062	putative phage tail protein
				STM14_5061	putative methyl-accepting chemotaxis protein
				yfiD	autonomous glycyl radical cofactor for GrcA stress-induced glycyl radical protein that can replace an oxidatively damaged pyruvate formate-lyase subunit
				adhE	bifunctional acetaldehyde-CoA/alcohol dehydrogenase
				nmpC	putative outer membrane porin protein

[a] Enrichment Score: geometric mean (in – log scale) of all the p-values in a cluster

[b] only 4 of the 20 downregulated (log Fold Change ≤ -2) genes had a known function; no clusters were obtained, so genes are listed individually

Table 11. Differentially expressed functional gene clusters for gamma irradiated and eBeam irradiated *S*. Typhimurium cells in TSB after incubation for 24 hours at 37°C post-irradiation.

Gene ID[a]	Upregulated Gene Function and / or Product	Cluster	Downregulated Functional Clusters	# Genes	ES[b]
trxC	thioredoxin 2 protein	1	fructose and mannose metabolism	3-6	4.5
STM14_3379	hypothetical protein	2	glycolysis / gluconeogenesis	3-7	4.3
STM14_4400	hypothetical protein	3	fructose and mannose metabolism (Phosphotransferase system (PTS))	3-7	3.6
ddg	lipid A biosynthesis palmitoleoyl acyltransferase	4	pyruvate metabolism	3	2.2
zraP	zinc resistance protein	5	signal (outer membrane)	3-9	1.6
yncJ	hypothetical protein				
STM14_1454	hypothetical protein				
STM14_2185	putative cytoplasmic protein				
STM14_1509	putative molecular chaperone protein				
cpxP	repressor of the Cpx envelope stress response pathway				
ytfE	cell morphogenesis/cell wall metabolism regulator				
ybiJ	hypothetical protein				
ibpB	heat shock chaperone				
acpD	azoreductase FMN-dependent; requires NADH;				
STM14_3074	putative transposase				
STM14_1982	putative SAM-dependent methyltransferase				
ybeD	hypothetical protein				
STM14_2250	hypothetical protein				
STM14_3374	putative regulatory protein ArsR family				
ybhM	putative integral membrane protein				
hmpA	nitric oxide dioxygenase flavohemoprotein				
STM14_0402	putative inner membrane protein				
pspA	phage shock protein PspA involved in maintaining membrane potential under membrane stress conditions				
yhcR	hypothetical protein membrane protein AaeX				
STM14_0191	putative restriction endonuclease				
yhcQ	p-hydroxybenzoic acid efflux subunit AaeA				
yehE	putative outer membrane protein				
ypeC	hypothetical protein				

[a] only 17 of the 28 upregulated (log Fold Change ≥ 2) genes had a known function; no clusters were obtained, so genes are listed individually

[b] Enrichment Score: geometric mean (in – log scale) of all the p-values in a cluster

Table 12. Differentially expressed functional gene clusters between eBeam irradiated and non-irradiated (control) *S.* Typhimurium cells in TSB after incubation for 4 hours at 37°C post-irradiation.

Cluster	Upregulated Functional Clusters	# Genes	ES[a]	Downregulated Functional Clusters	# Genes	ES
1	ribosome / RNA binding	33-65	52.8	citrate cycle	7-32	10.4
2	purine and pyrimidine metabolism	4-18	8.5	oxidative phosphorylation	11-12	9
3	cell membrane	17-71	6	cobalamin biosynthesis	4-33	6.2
4	(ribo)nucleotide binding	54-81	5.9	glyoxylate and dicarboxylate metabolism	7-8	5.9
5	DNA repair / SOS response	10-32	5.9	bacterial microcompartments protein	5-9	5.1
6	RNA processing	7-30	5.8	pyruvate metabolism	5-10	4.6
7	ABC transporters	7-24	5.7	glycerolipid metabolism	3-6	4.3
8	biosynthesis of siderophore group nonribosomal peptides	4-5	4.6	ABC transporters	8-19	4.3
9	GTP-binding	5-10	4.2	heme binding	6-8	3.9
10	DNA replication	13-32	4	glycerol, alditol, polyol metabolic process	5	3.7
11	magnesium binding	15-32	3.5	glycolysis / gluconeogenesis	4-8	3.7
12	phosphate transmembrane transport	3-14	3.5	porphyrin and chlorophyll metabolism	3-11	3.5
13	fatty acid biosynthesis	4-12	3.1	starch and sucrose metabolism	3-11	3.5
14	thiamine metabolism	5-13	3	methane metabolism	3-5	3.3
15	alkali metal ion binding	5-8	2.6	fructose and mannose metabolism	6-7	3.2
16	ATPase activity, coupled to transmembrane movement of ions	7-33	2.5	glycerophospholipid metabolism	4-5	2.8
17	sulfur metabolism	3-16	2.5	oxidative phosphorylation	3-11	2.7
18	DNA-directed RNA polymerase	3-8	2.5	two-component system	9-12	2.6
19	ATP synthesis	3-41	2.4	metal binding	3-42	2.6
20	phosphonate and phosphinate metabolism	3	2.4	FAD	5-11	2.4
21	homologous recombination	3-8	2.4	pentose phosphate pathway	3-6	2.3
22	methylation	4-5	2.4	flagellar assembly	3-12	2.2
23	translation regulation	3-7	2.3	oligosaccharide transport	3	2.1
24	protein complex disassembly	3-8	2.2	membrane transport	11-48	2
25	translation factor activity	4-7	2.2	nitrogen metabolism	4-5	2
26	protein secretion / export	3-11	2	flavoprotein	3-11	2
27	rRNA methyltransferase activity	3-7	1.9	flagellar assembly	3-12	1.8
28	amino acid biosynthesis	8-23	1.9	ascorbate and aldarate metabolism	3-4	1.8
29	biotin metabolism	3-8	1.9	alanine racemase	3-5	1.6

Table 12. Continued

Cluster	Upregulated Functional Clusters	# Genes	ES[a]	Downregulated Functional Clusters	# Genes	ES
30	flagellar assembly	3-16	1.9	glycogen biosynthesis	3-14	1.6
31	helicase activity	3-10	1.8	organic acid catabolic process	3-9	1.6
32	nucleotide excision repair	3	1.8	bacterial chemotaxis	3-4	1.5
33	cell division (chromosome organization)	3-8	1.7	fructose and mannose metabolism / phosphotransferase system	5-6	1.4
34	DNA unwinding	3-7	1.5	glutathione metabolism	3	1.3
35	DNA-repair protein	3-6	1.5	glycogen biosynthesis	3-14	1.6
36	glutamine amidotransferase	3-6	1.5	organic acid catabolic process	3-9	1.6
37	amino sugar and nucleotide sugar metabolism	3-7	1.4	bacterial chemotaxis	3-4	1.5
38	peptidoglycan biosynthesis	3-4	1.4			
39	alanine, aspartate and glutamate metabolism	3-6	1.3			
40	pentose and glucuronate interconversions	3-5	1.3			
41	nitrogen metabolism	3-4	1.3			
42	DNA topoisomerase	3-7	1.3			
43	ion transmembrane transport	3-22	1.3			
44	alkali metal ion binding	3-8	1.3			

[a] Enrichment Score: geometric mean (in – log scale) of all the p-values in a cluster

Table 13. Differentially expressed functional gene clusters between eBeam irradiated and non-irradiated (control) *S.* Typhimurium cells in TSB after incubation for 24 hours at 37°C post-irradiation.

Cluster	Upregulated Functional Clusters	# Genes	ES[a]	Downregulated Functional Clusters	# Genes	ES
1	ABC transporters	7-29	10.6	citrate cycle	3-11	4.7
2	SOS response (DNA repair)	10-25	6	arginine biosynthesis	4-10	3.5
3	two-component system	10-18	5.9	pyruvate metabolism	3	1.8
4	nucleotide binding / ATP binding	20-74	5.7			
5	cell membrane (transport)	12-62	5			
6	biosynthesis of siderophore group nonribosomal peptides	4-5	5			
7	fructose and mannose metabolism	5-10	4			
8	flagellar assembly	4-16	3.9			
9	metal-binding (magnesium)	10-34	3.9			
10	phosphate transmembrane transporter activity	4-28	3.5			
11	ATP / nucleotide binding / P-loop	4	3.3			
12	anion transmembrane transporter activity	3-11	2.9			
13	glycerolipid metabolism	3-5	2.9			
14	thiamine metabolism	4-25	2.8			
15	glycerophospholipid metabolism	4-5	2.7			
16	sulfur metabolism	3-15	2.7			
17	DNA replication / repair	3-25	2.3			
18	flagellar assembly	3-7	2.2			
19	bacterial microcompartments protein (CcmK/EutK/PduA short type)	3-6	2.1			
20	alkali metal ion binding / transport (potassium)	4-31	2.1			
21	pentose and glucuronate interconversions	3-6	2			
22	nucleotide excision repair	3	2			
23	metal-binding (iron)	5-54	1.9			
24	ferredoxin reductase-type FAD-binding	3-5	1.8			
25	iron transport	3-6	1.7			
26	glyoxylate and dicarboxylate metabolism	4	1.7			
27	small GTP-binding protein	3-5	1.6			
28	peptide biosynthetic process	3-5	1.6			
29	nitrogen metabolism	3-4	1.5			
30	tRNA-specific ribonuclease activity	3-14	1.5			

Table 13. Continued

Cluster	Upregulated Functional Clusters	# Genes	ES[a]	Downregulated Functional Clusters	# Genes	ES
31	protein phosphatase	3-6	1.4			
32	flavoprotein	3-8	1.4			
33	glycine, serine and threonine metabolism	3-4	1.4			
34	helicase	3-8	1.3			

[a] Enrichment Score: geometric mean (in – log scale) of all the p-values in a cluster

Table 14. Differentially expressed functional gene clusters between gamma irradiated and non-irradiated (control) *S.* Typhimurium cells in PBS immediately after irradiation.

Cluster	Upregulated Functional Clusters	# Genes	ES[a]	Downregulated Functional Clusters	# Genes	ES
1	secretion system	11-25	9.2	ABC transporters	3-20	5.8
2	two-component system	10-18	7.8	propanoate metabolism	3-10	4.1
3	flagellar assembly	3-25	4.5	pyruvate metabolism	4-6	3.2
4	cell membrane	18-46	3.8	arginine and proline metabolism	3-9	3.2
5	pili assembly / cell envelope	6-26	3.6	glutathione metabolism	3-4	2.9
6	glycerolipid metaboism	3-6	3	starch and sucrose metabolism	3-8	2.3
7	amino sugar and nucleotide sugar metabolism	3-8	2.9	glyoxylate cycle	3	2.2
8	pentose and glucuronate interconversions	3-6	2.4	non-membrane bound organelle	4-9	2.1
9	amino acid biosynthesis	4-13	2.4	zinc ion binding	9-30	2.1
10	fimbrial protein	5-14	2.3	histidine metabolism	3	2
11	intramolecular oxidoreductase activity	3-11	2.1	RNA degradation	3	1.9
12	glyoxylate and dicarboxylate metabolism	3-4	1.9	metal-binding	3-15	1.4
13	disulfide bond / redox-active center	3-5	1.9	lysine-arginine-ornithine-binding protein	3-10	1.3
14	ascorbate and aldarate metabolism	3	1.7			
15	outer membrane usher protein	3-6	1.5			
16	iron binding	3-10	1.5			
17	inner cell membrane	8-18	1.3			
18	citrate cycle	3-6	1.3			
19	pyruvate metabolism	3-6	1.3			

[a] Enrichment Score: geometric mean (in – log scale) of all the p-values in a cluster

Table 15. Differentially expressed functional gene clusters between gamma irradiated and non-irradiated (control) *S.* Typhimurium cells in TSB after incubation for 4 hours at 37°C post-irradiation.

Cluster	Upregulated Functional Clusters	# Genes	ES[a]	Downregulated Functional Clusters	# Genes	ES
1	ribosome / RNA binding	27-62	34.7	citrate cycle (oxidative phosphorylation)	4-26	9.1
2	ABC transporters	10-44	13.9	glycerolipid metabolism	3-6	4.8
3	membrane transport	31-144	13	metal binding (oxidation reduction)	7-42	4.7
4	two-component system	13-28	7.9	bacterial microcompartments protein (CcmK/EutK/PduA type)	4-6	3.7
5	flagellar assembly	3-39	7.1	glyoxylate and dicarboxylate metabolism	3-7	3.5
6	nucleotide binding	64-101	5.3	pyruvate metabolism	3-6	2.9
7	protein transport / bacterial secretion system	3-28	4.4	two-component system	5-10	2.7
8	SOS response / DNA repair	10-33	4.2	ascorbate and aldarate metabolism	3-7	2.2
9	biosynthesis of siderophore group nonribosomal peptides	4-5	4.2	carbohydrate (i.e. glycogen, starch, sucrose) biosynthesis	3-11	2.1
10	tRNA / ncRNA / rRNA processing	7-29	3.8	alanine racemase	3-5	2
11	cell motility and secretion (chaperone)	10-29	3.8	glycerol, alditol, polyol metabolic process	3	1.9
12	purine and pyrimidine metabolism	3-17	3.6	organic acid catabolic process	3-7	1.7
13	nucleotide binding / P-loop / ATP	4-5	3.6	ABC transporters (chemotaxis)	3-10	1.7
14	cell motility and secretion (outer membrane)	6-17	3.5	glycine, serine and threonine metabolism	3-4	1.7
15	pentose and glucuronate interconversions	3-13	3.5	nitrogen metabolism	3-4	1.7
16	DNA binding (H-T-H motif)	7-10	3.4	iron-sulfur (molybdopterin oxidoreductase)	4-11	1.6
17	arginine and proline metabolism	3-12	2.9	cold shock protein, CspA type	3	1.5
18	thiamine metabolism	5-14	2.6	flagellar assembly	3-4	1.5
19	small GTP-binding protein	3-8	2.5	amino sugar and nucleotide sugar metabolism	3-6	1.5
20	lipopolysaccharide biosynthesis	10-26	2.2	CoA-ligase activity (Propanoate metabolism)	3-4	1.4
21	methylation	4-6	2.1	monosaccharide metabolic process	4-11	1.4
22	sulfur metabolism	3-17	2.1	NADH dehydrogenase (ubiquinone) activity	4	1.4
23	magnesium ion binding	12-18	2.1	alanine, aspartate and glutamate metabolism	3	1.3
24	ATPase activity, coupled to transmembrane movement of substances	8-32	2.1	cysteine and methionine metabolism	3	1.3
25	DNA replication	12-33	2.1			
26	translation factor activity (elongation)	4-8	2			
27	homologous recombination	4-7	2			
28	fatty acid biosynthesis	3-5	2			
29	pyrimidine metabolism	3-9	2			

Table 15. Continued

Cluster	Upregulated Functional Clusters	# Genes	ES[a]	Downregulated Functional Clusters	# Genes	ES
30	post-transcriptional regulation of gene expression	3-6	1.8			
31	translation factor activity, nucleic acid binding / protein complex disassembly	3-8	1.8			
32	biotin metabolism	3-5	1.8			
33	ncRNA / rRNA processing	3-24	1.7			
34	Fructose and mannose metabolism	3-12	1.7			
35	cell projection (flagellum) organization	3-7	1.6			
36	nitrogen metabolism	4-5	1.6			
37	isomerase	3-20	1.5			
38	fimbrial protein	5-20	1.5			
39	amino sugar and nucleotide sugar metabolism	3-9	1.5			
40	purine metabolism	4-12	1.4			
41	alkali metal ion binding / transport	3-34	1.4			
42	metal binding	40-66	1.4			
43	potassium ion binding	3-8	1.3			
44	translation factor activity, nucleic acid binding / protein complex disassembly	3-8	1.8			

[a] Enrichment Score: geometric mean (in – log scale) of all the p-values in a cluster

Table 16. Differentially expressed functional gene clusters between gamma irradiated and non-irradiated (control) *S.* Typhimurium cells in TSB after incubation for 24 hours at 37°C post-irradiation.

Cluster	Upregulated Functional Clusters	# Genes	ES[a]	Downregulated Functional Clusters	# Genes	ES
1	ABC transporters	9-39	18.3	oxidative phosphorylation (citrate cycle)	3-32	9.9
2	two-component system	11-23	9	pyruvate metabolism	6-7	4.7
3	inner cell membrane transport	22-85	8.3	iron ion - sulfur binding	6-25	4.2
4	DNA repair / SOS response	11-30	7.3	glycolysis / gluconeogenesis	4-7	3.2
5	nucleotide binding / ATP binding	20-75	5.8	glycolysis / gluconeogenesis	4-10	3
6	phosphate transmembrane transporter activity	4-12	4.7	arginine biosynthesis	4-7	2.8
7	ATPase activity, coupled to movement of substances	10-54	4.6	alanine, aspartate and glutamate metabolism	4	2.7
8	flagellar assembly	3-15	3.7	NAD or NADH binding	7-16	2.4
9	disulfide bond	3-9	3.6	pentose phosphate pathway	4	2.3
10	thiamine metabolism	5-14	3.5	glycine, serine and threonine metabolism	3-4	1.7
11	biosynthesis of siderophore group nonribosomal peptides	3-4	3.4	glyoxylate and dicarboxylate metabolism	3	1.5
12	metal binding (magnesium)	10-33	3.4	lipoprotein	3-8	1.5
13	inorganic anion transmembrane transporter activity	3-11	2.9	nitrogen metabolism	3	1.5
14	Acyl carrier protein activity (phosphopantetheine-binding)	4	2.6	outer membrane	3-18	1.3
15	metal ion transmembrane transporter activity	4-31	2.5			
16	sulfur metabolism	3-14	2.5			
17	DNA replication	3-30	2.5			
18	metal ion binding	21-55	2.3			
19	mismatch repair	4-5	2.2			
20	homologous recombination / single-stranded DNA binding	3-5	2.1			
21	nucleotide excision repair	3	2.1			
22	flagellum organization	3-9	1.8			
23	branched-chain amino acid transport	4-11	1.7			
24	alkali metal ion binding	3-9	1.7			
25	flavoprotein / FAD / NADP / NAD	4-9	1.6			
26	homologous recombination	3-5	1.5			
27	cell envelope	11-27	1.4			
28	ncRNA / rRNA / tRNA processing	3-16	1.4			
29	phosphatase activity	3-5	1.3			
30	helicase	3-9	1.3			

[a] Enrichment Score: geometric mean (in – log scale) of all the p-values in a cluster

Discussion

As expected, lethally irradiated *S.* Typhimurium cells retained their transcriptional activity but not their ability to replicate. These findings are in congruence with Magnani et. al. who demonstrated that lethally gamma irradiated *Brucella melitensis* cells had lost their ability to replicate but still possessed metabolic and transcriptional activity (20). In essence, lethal ionizing radiation creates senescent bacterial cells that are no longer capable of dividing but are still intact and metabolically active for an extended period of time after irradiation. Ionizing radiation is known to cause DNA double-strand breaks (DSBs) (46). DSBs are the most lethal form of DNA damage and most organisms can generally tolerate only a few of them (47). It has been estimated that 100 Gy of ionizing radiation cause approximately 1 DSB per one million base pairs (Mbp) (48). For the genome of *S.* Typhimurium (4.8 Mbp) (82) this translates roughly to 3-5 DSBs per 100 Gy or 60-100 DSBs per 2 kGy. Theoretically, 60-100 DSBs result in DNA fragments that are ca. 48,000-80,000 base pairs long. When considering the average gene size for *S.* Typhimurium (947 base pairs) (82) and the fact that the bombardment with electrons results in random events that do not result in evenly spaced DSBs across the genome, the resulting DNA fragments are probably still intact enough to allow transcription. However, the sheer number of DSBs is probably preventing *S.* Typhimurium to reassemble its genome and achieve cellular multiplication. Our results indicate that *S.* Typhimurium cells are still actively transcribing genes for at least 24 hours post-irradiation. How these cells are incubated following lethal irradiation with either eBeam or gamma has a significant effect on the organism's gene expression (Tables 13-16).

To answer the first of our four biological questions, namely is there a difference in gene expression in lethally irradiated cells immediately after irradiation compared to prolonged storage in PBS buffer at 4°C, irradiated cells were compared to each other at 0, 4, and 24 hours of storage. For eBeam irradiated *S.* Typhimurium cells the analysis revealed that between the 0 and 4 hour time point, 315 genes or 5.6% of the total genes were differentially expressed. The number of DE genes between the 4 and 24 hour time point was only 87 or 1.5% of the total genes. The fewest number of DE genes were found between 0 and 24 hours, namely 34 genes or 0.6% of the total genes (Table 7). In prokaryotes, exposure to low temperatures, between 0-8°C, is typically associated with arrested cell growth and changes in cellular composition and function, such as a decrease in protein synthesis. (84-86). In addition, the cells are starved of nutrients due to their incubation in PBS (90). Since bacterial cells slow down major portions of their metabolism at low temperatures and PBS buffer does not supply any nutrients, it is not surprising that the overall percentage of DE genes in eBeam irradiated *S.* Typhimurium cells decreased over the 24 hour incubation period (Table 7). For gamma irradiated cells, the RNA-Seq analysis revealed that there was no difference in overall gene expression between any of the time points (Table 7). This could be related to the fact that the gamma irradiation lasted 3 hours, rather than only a few seconds as was the case for the eBeam irradiation, hence allowing the gamma irradiated cells time to alter their gene expression while being irradiated. Overall, these results indicate that the overall gene expression for irradiated *S.* Typhimurium cells changes only slightly when the cells are stored in PBS at 4°C. Since such a small percentage of genes was differentially

expressed when irradiated cells were stored at 4°C in PBS, we chose to focus our attention on the incubations in growth media at 37°C.

To answer the second biological question, is there a difference in gene expression patterns between eBeam and gamma irradiated cells when incubated for extended periods of time in growth media (TSB), the gene expression profiles of eBeam and gamma irradiated cells at 0, 4, and 24 hours were compared. Immediately after irradiation (0 hours), there were 288 up-regulated and 255 genes down-regulated genes (Table 7). Functional clustering revealed that the 142 up-regulated genes with known function in gamma irradiated cells were related to bacterial secretion/virulence, redox homeostasis, and membrane functions (Table 9). The 224 down-regulated genes with known function clustered in 19 groups. Most prominent was the overall trend in down-regulation of major metabolic pathways, such as the citric acid cycle in gamma irradiated cells compared to eBeam irradiated cells (Table 9).

When comparing gamma irradiated and eBeam irradiated cells incubated for 4 hours in TSB at 37°C, 419 genes were up-regulated, whereas only 20 genes were down-regulated. Almost all the functional clusters for the up-regulated genes were related to bacterial secretion and membrane function (Table 10). The same trend was also observed immediately after irradiation (Table 9). This suggests that the membrane damage during gamma irradiation is probably more severe than under eBeam irradiation conditions. A study by Ayari et. al. found that a sub lethal gamma irradiation dose of 1 kGy caused

significant changes in the membrane fatty acid content of *S*. Typhi. They observed an increase in the percentage of unsaturated fatty acids. Such an increase will render the membrane less rigid and more permeable to its environment (117). This may be the reason why *S*. Typhimurium cells in our study appeared to be focused on cellular redox homeostasis immediately after gamma irradiation and most likely during the 3 hour irradiation period (Table 9). Based on these differences in gene expression patterns between gamma and eBeam irradiated *S*. Typhimurium cells, it may be worthwhile to investigate the effect of eBeam irradiation on the membrane fatty acid content of bacterial cells. There were only 20 down-regulated genes at the 4 hour time point and 16 of them had no known function, indicating that there is only a minimal difference in the gene expression of gamma and eBeam irradiated cells in terms of down-regulation (Table 10).

After 24 hours in TSB at 37°C, there were only 28 up-regulated and 39 down-regulated genes, comprising 1.5% of the total genes, in lethally gamma irradiated cells compared to eBeam ones (Table 7). The up-regulated genes did not cluster, since only 17 had a known function (Table 11). Of those, thioredoxin was up-regulated 4.5 fold (log FC). Thioredoxin plays an important role in redox signaling and acts as an antioxidant by facilitating the reduction of other proteins (118, 119). The fact that this gene is most highly up-regulated, leads us to hypothesize that gamma irradiated cells are still struggling with redox homeostasis (i.e. maintaining reducing conditions in the cytoplasm) 24 hours after irradiation. The overall trend in down-regulating major, long-

term metabolic pathways, such as glycolysis and the citric acid cycle, was also observed 24 hours after irradiation (Table 11).

To answer the third question, what happens to lethally irradiated cells immediately after irradiation, the gene expression profiles of eBeam and gamma irradiated cells were compared to non-irradiated (control) cells. There was no difference in the gene expression patterns between eBeam irradiated *S.* Typhimurium cells and non-irradiated (control) cells. High energy (10MeV) eBeam irradiation has an extremely high dose rate (ca. 3000 Gy/sec), leaving the irradiated cells no time to adapt to the irradiation stress. Since the eBeam irradiated cells were flash frozen on a dry ice/isopropanol slurry immediately after exiting the irradiation chamber, it is not surprising that no difference in gene expression was observed. On the other hand, reaching a lethal irradiation dose of 2 kGy with gamma radiation using the reactor core took 3 hours. As a result of enduring ionizing radiation stress for 3 hours, the gene expression patterns of gamma irradiated *S.* Typhimurium cells are markedly different from non-irradiated (control) cells. A total of 849 genes (15.1%) were differentially expressed. 620 genes were up-regulated and 229 were down-regulated (Table 7). The 307 up-regulated genes with known function clustered in 19 groups. The first 6 clusters were all related to bacterial secretion, virulence and cell membrane (Table 14). Two clusters were associated with proper protein folding (oxidoreductase activity and disulfide bonds). The formation of disulfide bonds, catalyzed by oxidoreductase enzymes, is a critical step in the folding and stability of many secreted proteins, such as toxins and surface proteins (120). For example,

DsbA, the dithiol-disulfide oxidoreductase enzyme, is required by *S.* Typhimurium for the formation of a functional type III secretion system (121). It appears that immediately after lethal gamma irradiation, secretion, virulence and membrane-related genes are highly up-regulated. Whether or not this up-regulation is due to a change in membrane fatty acid content rendering the membranes more fluid/permeable is unclear at this point. The fact that DNA repair genes were not significantly up-regulated immediately after irradiation was surprising. We hypothesize that while the *S.* Typhimurium cells were being gamma irradiated, they were most likely focused on maintaining the reducing environment in the cell along with membrane functionality rather than DNA repair (Table 9 and 14). What good does it do for a cell to have intact DNA, but no environment to keep it in? This hypothesis is supported by the fact that genes involved in cell redox homeostasis were up-regulated in gamma irradiated cells compared to eBeam irradiated ones immediately after irradiation (Table 9). The 204 down-regulated genes with known function clustered in 13 groups. The first cluster was related to ABC transporters (Table 14). ABC transporters shuttle proteins, peptides, polysaccharides, and many other proteins across the bacterial membrane (122). Since clusters from both up- and down-regulated genes were related to membrane transport, it is possible that depending on the membrane damage, the regulation of the transport systems is site-specific. In other words, the cell may down-regulate membrane transport in an area with significant membrane damage and up-regulate it in another, less damaged section. The overall trend to down-regulate major metabolic pathways, such as pyruvate metabolism, was also observed (Table 14).

To answer the fourth biological question, are the gene expression patterns in lethally irradiated cells incubated in growth media at an optimum growth temperature different from non-irradiated (control) cells, the gene expression profiles of eBeam and gamma irradiated cells incubated in TSB at 37°C for 4 and 24 hours were compared to non-irradiated (control) cells. Overall, the results revealed that when eBeam and gamma irradiated *S.* Typhimurium cells are placed in growth media after irradiation, they exhibit a vastly different transcriptomic response compared to non-irradiated (control) cells (Table 7). After a 4 hour incubation in TSB at 37°C, eBeam irradiated cells had 1265 DE genes, comprising 22.5% of the total genes. Of those genes, 717 were up-regulated and 548 were down-regulated (Table 7). The 443 up-regulated genes with a known function clustered in 44 groups. Most notably in clusters related to RNA binding (ribosome), purine and pyrimidine metabolism, (ribo)nucleotide binding, DNA repair/SOS response, and RNA processing (Table 12). 101-196 genes clustered among these 5 groups alone. In general, clusters were either related to RNA and DNA activities as mentioned above or cell membrane activities, i.e. ABC transporters, fatty acid biosynthesis, protein secretion, flagellar assembly (Table 12). As far as the 548 down-regulated genes were concerned, the overall trend to down-regulate major metabolic pathways, such as the citric acid cycle and oxidative phosphorylation, was again observed (Table 12).

After 24 hours of incubation in growth media at 37°C, a significant decrease in the number of down-regulated genes in eBeam irradiated cells was observed (4 hours: 548 and 24 hours: 98). This resulted in only 3 functional clusters at the 24 hour time point,

compared to 34 clusters at the 4 hour time point. It was observed that at least 14 clusters moved from down-regulation to up-regulation, i.e. ABC transporters, two-component system, fructose and mannose metabolism, glycero(phospho)lipid metabolism (Tables 12 and 13). All of these 14 clusters were either related to membrane functions or cellular metabolism. This shift in gene regulation indicates that the organism is shifting back to normal metabolic functions. A more detailed analysis of the DE genes is needed to elucidate this general trend. Apart from the up-regulation in cellular metabolism functions, the eBeam irradiated cells' SOS response was still in full swing along with membrane (transport) activities after 24 hours of incubation in TSB at 37°C (Table 13).

Gamma irradiated *S*. Typhimurium cells behaved similarly to their eBeam irradiated counterparts when incubated in growth media at 37°C. Out of the 43 up-regulated clusters, 30 were also up-regulated in eBeam irradiated cells after 4h of incubation (Tables 12 and 15). All of these functional clusters were related to RNA/DNA activities as well as membrane functions. As for the 319 down-regulated genes, the overall trend to down-regulate major metabolic pathways, such as the citric acid cycle and oxidative phosphorylation, was also observed in gamma irradiated cells (Table 15). 15 of the 24 down-regulated clusters were the same between gamma and eBeam irradiated cells.

After 24 hours of incubation, the up-regulated functional clusters for gamma irradiated cells were also very similar to the eBeam irradiated cells. 18 of the clusters were shared between gamma and eBeam irradiated cells (Tables 13 and 16). As for eBeam irradiated

cells, the vast majority of the clusters were either related to RNA and DNA activities or cell membrane activities. In contrast to eBeam irradiated cells, gamma irradiated cells still had a significant number of down-regulated genes (EB: 98; G: 179). Functional clustering revealed that major metabolic pathways remained down-regulated after 24 hours compared to the non-irradiated (control) cells (Table 16). Even though this trend was also seen in eBeam irradiated cells, it was more pronounced in gamma irradiated cells. Overall, eBeam and gamma irradiated cells seemed to behave quite similarly during their incubation in growth media after lethal irradiation. It does appear, however, that gamma irradiated cells sustained a higher degree of membrane damage as well as DNA damage, as evidenced by the functional clusters still up-regulated after 24 hours, and required more time to repair the damage. We hypothesize that this difference in transcriptomic response is related to the differences in dose rate for the two ionizing radiation sources. Extended radiation exposure (gamma), over a 3 hour period, seems to wreak more havoc in bacterial cells compared to the exposure of only a few seconds (eBeam).

Since there are no published reports in the literature about the global transcriptomic response of lethally irradiated bacteria, the only comparison that can be made is with sub-lethally irradiated *Deinococcus radiodurans*, an extremely radioresistant gram-positive bacteria. It is important to note that this is not a true comparison because the *S.* Typhimurium cells in this study were lethally irradiated and had lost their ability to replicate, whereas the *D. radiodurans* cells were only sub-lethally irradiated and able to

grow post-irradiation (66). The gene expression patterns observed in this study with *S.* Typhimurium cells are similar to results obtained with sub-lethally gamma irradiated *D. radiodurans* (66). The researchers found that *D. radiodurans* recovery (in growth media at 32°C) progressed through three stages: early phase (0-3 hours) in which cell growth was inhibited and there was little DNA repair; mid phase (3-9 hours) in which growth was still inhibited, but DNA repair was occurring; and late phase (9-24 hours) in which cell growth was restored and DNA repair, specifically *recA*, was repressed (66). The lethally irradiated *S.* Typhimurium cells in this study also followed this general pattern. The only major difference observed between the two transcriptomic responses was the significant up-regulation in membrane related activities in *S.* Typhimurium cells, which was not observed in *D. radiodurans*. This may be due to the fact that *S.* Typhimurium is a gram-negative bacterium whereas *D. radiodurans* is gram-positive. Gram-positive cell walls consist of one lipid bilayer and a thick peptidoglycan layer, whereas gram-negative bacteria have an inner and outer lipid bilayer and a thin peptidoglycan layer (123). In addition, gram-negative bacteria have a higher membrane lipid content (117). Since peptidoglycan is responsible for the bacterial shape and mechanical stability of the cell and the fact that gamma irradiation shifts the fatty acid content towards more unsaturated fatty acids, rendering the cell membrane more permeable (117), it is not surprising that gram-positive bacteria can withstand membrane damage caused by irradiation better than gram-negative bacteria.

The results presented here provide an overview of the global transcriptomic response of lethally irradiated *S.* Typhimurium cells. More detailed analyses need to be performed within this RNA-Seq data set to better understand the intricacies of the transcriptomic response. In conclusion, post-irradiation incubation in PBS buffer at 4°C results in minimal differential gene expression over a period of 24 hours for both eBeam and gamma irradiated *S.* Typhimurium cells. When incubated in growth media (TSB) at 37°C, the transcriptomic response for both eBeam and gamma irradiated cells is markedly different from non-irradiated (control) cells and somewhat similar to each other. In general, irradiated cells focus on repairing DNA and membrane damage over a 24 hour period, gamma irradiated cells more extensively than eBeam irradiated cells. Both types of irradiated cells down-regulate major, long-term metabolic pathways, such as the citric acid cycle, presumably to redirect the energy expenditure to focus on DNA and membrane repair. In essence, lethal ionizing radiation creates senescent bacterial cells that are no longer capable of dividing but are still alive and metabolically active for an extended period of time after irradiation.

CHAPTER VI

SUMMARY

Summary

Ionizing radiation is used for many different applications that require a reduction in bioburden. Even though commercial irradiation services to reduce (or eliminate) bioburden are relatively common place, and the effectiveness of ionizing radiation to inactivate organisms has been studied for many decades, the scientific literature is still unsettled with regards to the Relative Biological Effectiveness (RBE) or kill efficiency of the different ionizing radiation sources, namely electron beam (eBeam), gamma, and x-ray. This is in large part due to the fact that researchers used many different dosimetry systems over the years. With the advances that have been made to date, mainly in dosimetry but also in microbiological and molecular technologies, we wanted to re-examine the RBE or kill efficiency of different ionizing radiation sources on microorganisms. Furthermore, we wanted to elucidate both the physiological characteristics as well as the transcriptomic responses of lethally irradiated bacteria.

Inactivation Kinetics of Bacteria Exposed to Ionizing Radiation

Inactivation kinetics of microbial cells exposed to ionizing radiation have been the key benchmark in comparing the effectiveness of the different ionizing radiation technologies as well as comparing the radiation sensitivity of different organisms. The objective of this study was to determine if the inactivation kinetics and D_{10} values (dose

required to kill 90% of the population) of bacteria are different for six different ionizing radiation sources under the same experimental conditions and using the same dosimetry system. The bacteria studied were *Escherichia coli*, a prototypical experimental organism, and *Salmonella*, a prototypical foodborne pathogen. Overall, the results indicate that the inactivation kinetics for *E. coli* and *Salmonella* are very similar for the different ionizing radiation sources. A statistically significant difference was detected between the different ionizing radiation sources for *E. coli* but not for *Salmonella*. This statistical difference is based on a rather small difference in absorbed dose (tens of Grays). Such a small difference in dose is not discernible under normal commercial radiation processing conditions (for any source type). In other words, in the 'real' world, the statistically significant differences found will be absorbed within the 5% margin of error for the radiation equipment and the 4-8% uncertainty in dosimetry. The results imply that microbial inactivation curves obtained with one source type are translatable to another. In other words, there is no difference in the relative biological effectiveness (RBE) of different ionizing radiation sources.

Physiological Characterization of Bacteria Exposed to Lethal Doses of Ionizing Radiation

To investigate the phenomenon of prolonged metabolic activity in bacterial cells exposed to lethal (no bacterial replication) ionizing radiation doses, *Salmonella* Typhimurium and *E. coli* cells were irradiated and the following physiological characteristics were examined: membrane integrity, DNA damage, metabolic activity,

ATP levels, and overall cellular functionality. The results showed that the membrane integrity of *S.* Typhimurium and *E. coli* cells was maintained and that the cells remained metabolically active up to 9 days post-irradiation when stored at 4°C. The ATP levels in lethally irradiated cells were similar to non-irradiated (control) cells. Extensive DNA damage was also visualized and overall cellular functionality was confirmed via bacteriophage propagation for up to 9 days post-irradiation. Overall, the results indicate that lethally irradiated *S.* Typhimurium and *E. coli* cells resemble live non-treated cells more closely than heat-killed dead cells.

Transcriptomic Responses of *Salmonella* Typhimurium after Exposure to Lethal Doses of Electron Beam and Gamma Radiation

To investigate the transcriptomic response of *S.* Typhimurium following a lethal ionizing radiation dose, cells were irradiated in PBS buffer. Immediately after irradiation (0 hours), aliquots of the cell suspension were flash frozen in a dry ice/isopropanol slurry at the radiation facility. For the remaining time points post-irradiation, the cells either remained in the PBS buffer they were irradiated in or they were transferred to growth media (TSB). The cells in PBS were incubated at 4°C and the cells in TSB were incubated at 37°C. RNA was collected after 4 and 24 hours of incubation. Total RNA was extracted and RNA-Seq analysis was performed. The results of this study show that post-irradiation incubation in PBS buffer at 4°C results in minimal differential gene expression over a period of 24 hours for both eBeam and gamma irradiated *S.* Typhimurium cells. When incubated in growth media (TSB) at 37°C, the transcriptomic

response for both eBeam and gamma irradiated cells is markedly different from non-irradiated (control) cells and more similar to each other. In general, lethally irradiated cells focus on repairing DNA and membrane damage over a 24 hour period with gamma irradiated cells doing so more extensively than eBeam irradiated cells. Both types of lethally irradiated cells down-regulate major, long-term metabolic pathways, such as the citric acid cycle, presumably to redirect the energy expenditure to focus on DNA and membrane repair. In essence, lethal ionizing radiation creates senescent bacterial cells that are no longer capable of dividing but are still alive and metabolically active for an extended period of time after irradiation.

CHAPTER VII

CONCLUSIONS AND FUTURE RESEARCH NEEDS

Conclusions

1. The relative biological effectiveness of different ionizing radiation sources, namely gamma, electron beam, and x-ray, is very similar

2. The membrane integrity is maintained in lethally irradiated *S.* Typhimurium and *E. coli* cells up to 9 days after irradiation

3. Lethally irradiated *S.* Typhimurium and *E. coli* cells remain metabolically active up to 9 days after irradiation when stored in PBS at 4°C

4. Lethally eBeam irradiated *E. coli* cells are able to support bacteriophage multiplication

5. There are minimal differences in gene expression between eBeam and gamma irradiated *S.* Typhimurium cells over a period of 24 hours when stored in PBS buffer at 4°C

6. The transcriptomic response of eBeam irradiated *S.* Typhimurium cells differs from that of gamma irradiated cells when incubated in growth media at 37°C as described in Chapter V

7. The transcriptomic response for both eBeam and gamma irradiated cells is markedly different from non-irradiated (control) cells when incubated in growth media (TSB) at 37°C as described in Chapter V

8. Gamma irradiated cells focus on repairing DNA and membrane damage over a 24 hour period much more extensively than eBeam irradiated cells

9. Both gamma and eBeam irradiated cells down-regulate major, long-term metabolic pathways, such as the citric acid cycle, presumably to redirect the energy expenditure to focus on DNA and membrane repair

10. Lethal ionizing radiation creates senescent bacterial cells that are no longer capable of dividing but are still alive and metabolically active for an extended period of time after irradiation

Future Research Needs

1. Lethally irradiated *S.* Typhimurium and *E. coli* cells maintain their membrane integrity for at least 24 hours post-irradiation. However, 9 days after irradiation the number of cells with damaged membranes increases. The transcriptomic analysis revealed that the cells are expending energy on membrane related activities. Further studies should be conducted to examine this phenomenon in greater detail, for example by investigating the lipopolysaccharides (LPS) of the outer membrane or the fatty acid content, especially in eBeam irradiated cells. Understanding the membrane changes/damages caused by lethal ionizing radiation could be useful in optimizing gamma and eBeam vaccine development.

2. Additional phage experiments should be performed to examine as to what exactly happens within an irradiated host cell. The following questions should be answered: How long do the phages take to lyse lethally irradiated host cells (longer, shorter, or the same as healthy cells)? Is the burst size in lethally irradiated cells the same as in healthy cells? Can phage λ sense that the physiological state of lethally irradiated cells is not optimal and hence enters into the lytic rather than the lysogenic state? Does the transcription of phage genes and phage DNA replication take longer in lethally irradiated host cells compared to healthy cells? Through the creation of phage mutants one could query what component is / is not functional in lethally irradiated host cells. Such studies would contribute to the fundamental understanding of the effects of lethal ionizing radiation on a prokaryote's cellular and molecular function.

3. The transcriptomic analysis revealed that there are a number of differences between gamma and eBeam irradiated *S.* Typhimurium cells. In these experiments, cells were irradiated in PBS buffer. It would be interesting to examine the gene expression of *S.* Typhimurium during / after exposure to a lethal gamma dose in growth media (i.e. TSB). Since the dose rate is so slow, it will take many hours to reach a lethal dose in growth media, during which time the organism may try to adapt to the irradiation stress. Understanding the organism's transcriptomic response during low dose rate irradiations will be advantageous when choosing an irradiation source for such applications as vaccine development.

4. The transcriptomic studies revealed an up-regulation in bacterial secretion, part of which was related to virulence. This warrants virulence studies with lethally irradiated *S.* Typhimurium. For example, irradiated cells are mixed with healthy cells and the production of virulence signals is monitored over time. Whether or not the gene expression of healthy cells changes should also be examined.

5. The research to date indicates that lethal irradiation creates senescent bacterial cells. But what if these cells are dividing into non-viable offspring (in one or more growth cycles). Or are they simply elongating but not-dividing? The unexplained increase in O.D. (0.24) between 0-4 hours in lethally eBeam irradiated cultures incubated in TSB at 37°C could be explained by such a phenomenon (Appendix A). This could be investigated in single-cell chemostat experiments (124).

REFERENCES

1. **Follett PA.** 2002. Mango seed weevil (Coleoptera : Curculionidae) and premature fruit drop in mangoes. J Econ Entomol **95:**336-339.

2. **Catcheside DG, Lea DE, Thoday JM.** 1946. The production of chromosome structural changes in *Tradescantia* microspores in relation to dosage, intensity and temperature. J Genet **47:**137-149.

3. **Goldblith SA, Proctor BE, Davison S, Kan B, Bates CJ, Oberle EM, Karel M, Lang DA.** 1953. Relative bactericidal efficiencies of 3 types of high-energy ionizing radiations. Food Res **18:**659-677.

4. **Hollaender A, Baker WK, Anderson EH.** 1951. Effect of oxygen tension and certain chemicals on the x-ray sensitivity of mutation production and survival. Cold Spring Harb Symp Quant Biol **16:**315-326.

5. **Hollaender A, Stapleton GE, Martin FL.** 1951. X-ray sensitivity of *E. coli* as modified by oxygen tension. Nature **167:**103-104.

6. **Howard-Flanders P.** 1958. Physical and chemical mechanisms in the injury of cells of ionizing radiations. Adv Biol Med Phys **6:**553-603.

7. **Stapleton GE, Billen D, Hollaender A.** 1953. Recovery of x-irradiated bacteria at suboptimal incubation temperatures. J Cell Compar Physl **41:**345-357.

8. **Tarpley W, Ilavsky J, Manowitz B, Horrigan RV.** 1953. Radiation sterilization. I. The effect of high energy gamma radiation from kilocurie radioactive sources on bacteria. J Bacteriol **65:**305-309.

9. **Dewey DL, Boag JW.** 1959. Modification of the oxygen effect when bacteria are given large pulses of radiation. Nature **183:**1450-1451.

10. **Dorpema JW.** 1990. Review and state-of-the-art on radiation sterilization of medical devices. Radiat Phys Chem **35:**357-360.

11. **Powers EL, Boag JW.** 1959. The role of dose rate and oxygen tension in the oxygen effect in dry bacterial spores. Radiat Res **11:**461.

12. **Purdie JW, Ebert M, Tallentire A.** 1974. Increased response of anoxic *Bacillus megaterium* spores to radiation at high dose rates. Int J Radiat Biol **26:**435-443.

13. **Tallentire A.** 1970. Radiation resistance of spores. J Appl Bacteriol **33:**141-146.

14. **Tallentire A.** 1980. Spectrum of microbial radiation sensitivity. Radiat Phys Chem **15:**83-89.

15. **Tallentire A, Powers EL.** 1963. Modification of sensitivity to x-irradiation by water in *Bacillus megaterium*. Radiat Res **20:**270-287.

16. **Thayer DW, Boyd G.** 1993. Elimination of *Escherichia coli* O157:H7 in meats by gamma irradiation. Appl Environ Microbiol **59:**1030-1034.

17. **Titani TM, Kondo M, Suguro H, Takahashi T.** 1958. Lethal effect of Co60 gamma rays upon parasite eggs and bacteria. Proceedings of the Second United Nations International Conference on the Peaceful Uses of Atomic Energy **27:**430-433.

18. **Zeitz L, Kim SH, Kim JH, Detko JF.** 1977. Determination of relative biological effectiveness (RBE) of soft x-rays. Radiat Res **70:**552-563.

19. **Jesudhasan PR, McReynolds JL, Byrd AJ, He HQ, Genovese KJ, Droleskey R, Swaggerty CL, Kogut MH, Duke S, Nisbet DJ, Praveen C, Pillai SD.** 2015. Electron-beam-inactivated vaccine against *Salmonella* Enteritidis colonization in molting hens. Avian Dis **59:**165-170.

20. **Magnani DM, Harms JS, Durward MA, Splitter GA.** 2009. Nondividing but metabolically active gamma-irradiated *Brucella melitensis* is protective against virulent *B. melitensis* challenge in mice. Infect Immun **77:**5181-5189.

21. **Secanella-Fandos S, Noguera-Ortega E, Olivares F, Luquin M, Julian E.** 2014. Killed but metabolically active *Mycobacterium bovis* bacillus Calmette-Guerin retains the antitumor ability of live bacillus Calmette-Guerin. J Urology **191:**1422-1428.

22. **Gaidamakova EK, Myles IA, McDaniel DP, Fowler CJ, Valdez PA, Naik S, Gayen M, Gupta P, Sharma A, Glass PJ, Maheshwari RK, Datta SK, Daly MJ.** 2012. Preserving immunogenicity of lethally irradiated viral and bacterial vaccine epitopes using a radio-protective Mn2+-peptide complex from *Deinococcus*. Cell Host Microbe **12:**117-124.

23. **Attix FH.** 2004. Introduction to radiological physics and radiation dosimetry. WILEY-VCH, Weinheim, Germany.

24. **FAO/IAEA.** 2004. Irradiation as a phytosanitary treatment of food and agricultural commodities. IAEA, Vienna, Austria.

25. **FAO/IAEA.** 2006. Use of irradiation to ensure the hygienic quality of fresh, pre-cut fruits and vegetables and other minimally processed food of plant origin. IAEA, Vienna, Austria.

26. **FAO/IAEA.** 2009. Irradiation to ensure the safety and quality of prepared meals. IAEA, Vienna, Austria.

27. **FAO/IAEA.** 2015. Radiation curing of composites for enhancing their features and utility in health care and industry. IAEA, Vienna, Austria.

28. **FAO/IAEA/WHO.** 2000. Irradiation of fish, shellfish and frog legs. IAEA, Vienna, Austria.

29. **IAEA.** 2007. Radiation processing: environmental applications. IAEA, Vienna, Austria.

30. **IAEA.** 2014. Radiation processed materials in products from polymers for agricultural applications. IAEA, Vienna, Austria.

31. **Farkas J, Mohacsi-Farkas C.** 2011. History and future of food irradiation. Trends Food Sci Tech **22:**121-126.

32. **Pillai SD, Shayanfar S.** 2015. Introduction to electron beam pasteurization in food processing, p 3-10. *In* Pillai SD, Shayanfar S (ed), Electron beam pasteurization and complementary food processing technologies. Woodhead Publishing, Cambridge, UK.

33. **Pillai SD, McElhany K.** 2011. Status of food irradiation in the USA. Safe Food **6:**1-10.

34. **Jeffers L.** 2014. Commodity approval & irradiation as a phytosanitary treatment, 2014 Annual Hands-On Workshop in eBeam and X-ray Irradiation Technologies, Texas A&M University, College Station, TX.

35. **Edwards RB, Peterson LJ, Cummings DG.** 1954. The effect of cathode rays on bacteria. Food Technol **8:**284-290.

36. **Epp ER, Weiss H, Santomasso A.** 1968. The oxygen effect in bacterial cells irradiated with high-intensity pulsed electrons. Radiat Res **34:**320-325.

37. **Weiss H, Epp ER, Ling CC, Heslin JM, Santomas.A.** 1974. Oxygen depletion in cells irradiated at ultra high dose rates and at conventional dose rates. Radiat Res **59:**247-248.

38. **Powers EL, Webb RB, Ehret CF.** 1958. Modification of sensitivity to radiation in single cells by physical means. Second United Nations International Conference on the Peaceful Uses of Atomic Energy **22:**404-408.

39. **Stratford IJ, Maughan RL, Michael BD, Tallentire A.** 1977. Decay of potentially lethal oxygen-dependent damage in fully hydrated *Bacillus megaterium* spores exposed to pulsed electron irradiation. Int J Radiat Biol **32:**447-455.

40. **Saleh FM.** 1977. PhD dissertation. University of Manchester, Manchester, UK.

41. **Bellamy WD, Lawton EJ.** 1954. Problems in using high-voltage electrons for sterilization. Nucleonics **12:**54-57.

42. **Lea DE.** 1955. Actions of radiations on living cells. Cambridge University Press, London, UK.

43. **von Sonntag C.** 1987. The chemical basis of radiation biology. Taylor & Francis, London, UK.

44. **Daly MJ.** 2009. A new perspective on radiation resistance based on *Deinococcus radiodurans*. Nat Rev Microbiol **7:**237-245.

45. **Hutchinson F.** 1966. Molecular basis for radiation effects on cells. Cancer Res **26:**2045-2052.

46. **Hutchinson F.** 1985. Chemical changes induced in DNA by ionizing radiation. Prog Nucleic Acid Re **32:**115-154.

47. **Krasin F, Hutchinson F.** 1977. Repair of DNA double-strand breaks in *Escherichia coli*, which requires RecA function and presence of a duplicate genome. J Mol Biol **116:**81-98.

48. **Daly MJ, Gaidamakova EK, Matrosova VY, Kiang JG, Fukumoto R, Lee DY, Wehr NB, Viteri GA, Berlett BS, Levine RL.** 2010. Small-molecule antioxidant proteome shields in *Deinococcus radiodurans*. Plos One **5**.

49. **Cox MM, Battista JR.** 2005. *Deinococcus radiodurans* - the consummate survivor. Nat Rev Microbiol **3:**882-892.

50. **Daly MJ, Minton KW.** 1995. Interchromosomal recombination in the extremely radioresistant bacterium *Deinococcus radiodurans*. J Bacteriol **177:**5495-5505.

51. **Holliday R.** 2004. Early studies on recombination and DNA repair in *Ustilago maydis*. DNA Repair **3:**671-682.

52. **Daly MJ, Minton KW.** 1996. An alternative pathway of recombination of chromosomal fragments precedes recA-dependent recombination in the radioresistant bacterium *Deinococcus radiodurans*. J Bacteriol **178:**4461-4471.

53. **Daly MJ, Minton KW.** 1997. Recombination between a resident plasmid and the chromosome following irradiation of the radioresistant bacterium *Deinococcus radiodurans*. Gene **187:**225-229.

54. **Holloman WK, Schirawski J, Holliday R.** 2007. Towards understanding the extreme radiation resistance of *Ustilago maydis*. Trends in Microbiol **15:**525-529.

55. **Daly MJ, Minton KW.** 1995. Resistance to radiation. Science **270:**1318-1318.

56. **Makarova KS, Omelchenko MV, Gaidamakova EK, Matrosova VY, Vasilenko A, Zhai M, Lapidus A, Copeland A, Kim E, Land M, Mavromatis K, Pitluck S, Richardson PM, Detter C, Brettin T, Saunders E, Lai B, Ravel B, Kemner KM, Wolf YI, Sorokin A, Gerasimova AV, Gelfand MS, Fredrickson JK, Koonin EV, Daly MJ.** 2007. *Deinococcus geothermalis*: the pool of extreme radiation resistance genes shrinks. Plos One **2**.

57. **Daly MJ, Gaidamakova EK, Matrosova VY, Vasilenko A, Zhai M, Leapman RD, Lai B, Ravel B, Li SMW, Kemner KM, Fredrickson JK.** 2007. Protein oxidation implicated as the primary determinant of bacterial radioresistance. Plos Biol **5:**769-779.

58. **Reesink HW, Panzer S, McQuilten ZK, Wood EM, Marks C, Wendel S, Trigo F, Biagini S, Olyntho S, Devine DV, Mumford I, Cazenave JP, Rasongles P, Garraud O, Richard P, Schooneman F, Vezon G, Al Radwan R, Brand A, Hervig T, Castro E, Lozano M, Navarro L, Puig L, Almazan C, MacLennan S, Cardigan R, Franklin IM, Prowse C.** 2010. Pathogen inactivation of platelet concentrates. Vox Sang **99:**85-95.

59. **Kimura S, Ishidou E, Kurita S, Suzuki Y, Shibato J, Rakwal R, Iwahashi H.** 2006. DNA microarray analyses reveal a post-irradiation differential time-dependent gene expression profile in yeast cells exposed to x-rays and gamma-rays. Biochem Biophys Res Commun **346:**51-60.

60. **Miyahara M, Miyahara M.** 2002. Effects of gamma ray and electron beam irradiations on survival of anaerobic and facultatively anaerobic bacteria. Kokuritsu Iyakuhin Shokuhin Eisei Kenkyusho Hokoku **120:**75-80.

61. **ISO/ASTM 51607.** 2004. Practice for use of analanine/EPR dosimetry system. ASTM International, West Conshohocken, PA 19428, USA.

62. **ISO/ASTM 51649.** 2005. Standard practice for dosimetry in an electron beam facility for radiation processing at energies between 300 keV and 25 MeV. ASTM International, West Conshohocken, PA 19428, USA.

63. **Miller RB.** 2005. Introduction to food irradiation. *In* Miller RB (ed), Electronic irradiation of foods: an introduction to the technology. Springer, New York.

64. **Praveen C, Jesudhasan PR, Reimers RS, Pillai SD.** 2013. Electron beam inactivation of selected microbial pathogens and indicator organisms in aerobically and anaerobically digested sewage sludge. Bioresour Technol **144:**652-657.

65. **Lucht L, Blank G, Borsa J.** 1998. Recovery of foodborne microorganisms from potentially lethal radiation damage. J Food Protect **61:**586-590.

66. **Liu YQ, Zhou JZ, Omelchenko MV, Beliaev AS, Venkateswaran A, Stair J, Wu LY, Thompson DK, Xu D, Rogozin IB, Gaidamakova EK, Zhai M, Makarova KS, Koonin EV, Daly MJ.** 2003. Transcriptome dynamics of *Deinococcus radiodurans* recovering from ionizing radiation. P Natl Acad Sci USA **100:**4191-4196.

67. **Ic E, Kottapalli B, Maxim J, Pillai SD.** 2007. Electron beam radiation of dried fruits and nuts to reduce yeast and mold bioburden. J Food Protect **70:**981-985.

68. **Tallentire A, Miller A, Helt-Hansen J.** 2010. A comparison of the microbicidal effectiveness of gamma rays and high and low energy electron radiations. Radiat Phys Chem **79:**701-704.

69. **Lemay M, Wood KA.** 1999. Detection of DNA damage and identification of UV-induced photoproducts using the CometAssay kit. Biotechniques **27:**846-851.

70. **Ostling O, Johanson KJ.** 1984. Microelectrophoretic study of radiation-induced DNA damages in individual mammalian cells. Biochem Biophys Res Commun **123:**291-298.

71. **Nakayama GR, Caton MC, Nova MP, Parandoosh Z.** 1997. Assessment of the alamar blue assay for cellular growth and viability *in vitro*. J Immunol Methods **204:**205-208.

72. **Rampersad SN.** 2012. Multiple applications of alamar blue as an indicator of metabolic function and cellular health in cell viability bioassays. Sensors **12:**12347-12360.

73. **Squatrito RC, Connor JP, Buller RE.** 1995. Comparison of a novel redox dye cell growth assay to the ATP bioluminescence assay. Gynecol Oncol **58:**101-105.

74. **Friedman DI, Court DL.** 2001. Bacteriophage lambda: alive and well and still doing its thing. Curr Opin Microbiol **4:**201-207.

75. **Hendrix RW, Casjens S.** 2006. Bacteriophage λ and its genetic neighborhood, p 409-447. *In* Calendar R (ed), The Bacteriophages, 2 ed. Oxford University Press, New York, NY.

76. **Little JW.** 2006. Gene regulatory circuitry of phage λ, p 74-82. *In* Calendar R (ed), The Bacteriophages, 2 ed. Oxford University Press, New York, NY.

77. **Los M, Golec P, Los JM, Weglewska-Jurkiewicz A, Czyz A, Wegrzyn A, Wegrzyn G, Neubauer P.** 2007. Effective inhibition of lytic development of bacteriophages lambda, P1 and T4 by starvation of their host, *Escherichia coli*. BMC Biotechnol **7**

78. **Molineux IJ.** 2006. The T7 group, p 277-301. *In* Calendar R (ed), The Bacteriophages, 2 ed. Oxford University Press, New York, NY.

79. **Mosig G, Eiserling F.** 2006. T4 and related phages: structure and development, p 225-267. *In* Calendar R (ed), The Bacteriophages, 2 ed. Oxford University Press, New York, NY.

80. **Adams MH.** 1959. Bacteriophages. Interscience Publishers, Inc., New York, N.Y.

81. **Blattner FR, Plunkett G, Bloch CA, Perna NT, Burland V, Riley M, ColladoVides J, Glasner JD, Rode CK, Mayhew GF, Gregor J, Davis NW, Kirkpatrick HA, Goeden MA, Rose DJ, Mau B, Shao Y.** 1997. The complete genome sequence of *Escherichia coli* K-12. Science **277:**1453-1462.

82. **Thomson NR, Clayton DJ, Windhorst D, Vernikos G, Davidson S, Churcher C, Quail MA, Stevens M, Jones MA, Watson M, Barron A, Layton A, Pickard D, Kingsley RA, Bignell A, Clark L, Harris B, Ormond D, Abdellah Z, Brooks K, Cherevach I, Chillingworth T, Woodward J, Norberczak H, Lord A, Arrowsmith C, Jagels K, Moule S, Mungall K, Sanders M, Whitehead S, Chabalgoity JA, Maskell D, Humphrey T, Roberts M, Barrow PA, Dougan G, Parkhill J.** 2008. Comparative genome analysis of *Salmonella* Enteritidis PT4 and *Salmonella* Gallinarum 287/91 provides insights into evolutionary and host adaptation pathways. Genome Res **18:**1624-1637.

83. **Singh NP, Stephens RE, Singh H, Lai H.** 1999. Visual quantification of DNA double-strand breaks in bacteria. Mutat Res-Fund Mol M **429:**159-168.

84. **Lim B, Gross CA.** 2011. Cellular response to heat shock and cold shock, p 93-114. *In* Storz G, Hengge R (ed), Bacterial Stress Responses, 2 ed. ASM Press, Washington, D.C.

85. **Panoff JM, Thammavongs B, Gueguen M, Boutibonnes P.** 1998. Cold stress responses in mesophilic bacteria. Cryobiology **36:**75-83.

86. **Phadtare S.** 2004. Recent developments in bacterial cold shock response. Curr Issues Mol Biol **6:**125-136.

87. **Dillingham MS, Kowalczykowski SC.** 2008. RecBCD enzyme and the repair of double-stranded DNA breaks. Microbiol Mol Biol R **72:**642-671.

88. **Finkel SE.** 2006. Long-term survival during stationary phase: evolution and the GASP phenotype. Nat Rev Microbiol **4:**113-120.

89. **Wanner U, Egli T.** 1990. Dynamics of microbial growth and cell composition in batch culture. Fems Microbiol Lett **75:**19-44.

90. **Postgate JR, Hunter JR.** 1962. Survival of starved bacteria. J Gen Microbiol **29:**233-263.

91. **Ackermann H-W.** 2006. Classification of bacteriophages, p 8-16. *In* Calendar R (ed), The Bacteriophages. Oxford University Press, New York, NY.

92. **Baranska S, Gabig M, Wegrzyn A, Konopa G, Herman-Antosiewicz A, Hernandez P, Schvartzman JB, Helinski DR, Wegrzyn G.** 2001. Regulation of the switch from early to late bacteriophage lambda DNA replication. Microbiol-UK **147:**535-547.

93. **Adelman K, Orsini G, Kolb A, Graziani L, Brody EN.** 1997. The interaction between the AsiA protein of bacteriophage T4 and the sigma(70) subunit of *Escherichia coli* RNA polymerase. J Biol Chem **272:**27435-27443.

94. **Bhagwat M, Nossal NG.** 2001. Bacteriophage T4 RNase H removes both RNA primers and adjacent DNA from the 5 ' end of lagging strand fragments. J Biol Chem **276:**28516-28524.

95. **Drivdahl RH, Kutter EM.** 1990. Inhibition of transcription of cytosine-containing DNA *in vitro* by the *alc* gene product of bacteriophage T4. J Bacteriol **172:**2716-2727.

96. **Kashlev M, Nudler E, Goldfarb A, White T, Kutter E.** 1993. Bacteriophage T4 Alc protein - a transcription termination factor sensing local modification of DNA. Cell **75:**147-154.

97. **Duckworth DH.** 1970. Biological activity of bacteriophage ghosts and take-over of host functions by bacteriophage. Bacteriol Rev **34:**344-363.

98. **Kolesky S, Ouhammouch M, Brody EN, Geiduschek EP.** 1999. Sigma competition: the contest between bacteriophage T4 middle and late transcription. J Mol Biol **291:**267-281.

99. **Mosig G.** 1998. Recombination and recombination-dependent DNA replication in bacteriophage T4. Annu Rev Genet **32:**379-413.

100. **Mosig G, Colowick NE, Pietz BC.** 1998. Several new bacteriophage T4 genes, mapped by sequencing deletion endpoints between genes 56 (dCTPase) and dda (a DNA-dependent ATPase-helicase) modulate transcription. Gene **223:**143-155.

101. **Krisko A, Radman M.** 2010. Protein damage and death by radiation in *Escherichia coli* and *Deinococcus radiodurans*. P Natl Acad Sci USA **107:**14373-14377.

102. **Imburgio D, Rong MQ, Ma KY, McAllister WT.** 2000. Studies of promoter recognition and start site selection by T7 RNA polymerase using a comprehensive collection of promoter variants. Biochemistry **39:**10419-10430.

103. **Martin CT, Muller DK, Coleman JE.** 1988. Processivity in early stages of transcription by T7 RNA polymerase. Biochemistry **27:**3966-3974.

104. **Molineux LJ.** 2001. No syringes please, ejection of phage T7 DNA from the virion is enzyme driven. Mol Microbiol **40:**1-8.

105. **Marsden H, Ginoza W, Pollard EC.** 1972. Effects of ionizing radiation on capacity of *Escherichia coli* to support bacteriophage T4 growth. J Virol **9:**1004-1016.

106. **Labaw LW, Mosley VM, Wyckoff RWG.** 1953. Development of bacteriophage in x-ray inactivated bacteria. J Bacteriol **65:**330-336.

107. **Pollard E, Setlow J, Watts E.** 1958. The effect of ionizing radiation on the capacity of bacteria to sustain phage growth. Radiat Res **8:**77-91.

108. **Scallan E, Hoekstra RM, Angulo FJ, Tauxe RV, Widdowson MA, Roy SL, Jones JL, Griffin PM.** 2011. Foodborne illness acquired in the United States-major pathogens. Emerg Infect Dis **17:**7-15.

109. **Andrews S.** 2010. FastQC: a quality control tool for high throughput sequence data, http://www.bioinformatics.babraham.ac.uk/projects/fastqc/.

110. **Epicentre.** 2013. ScriptSeq complete kit (bacteria) library preparation guide. http://support.illumina.com/content/dam/illumina-support/documents/documentation/chemistry_documentation/samplepreps_truseq/scriptseq-complete/scriptseq-complete-kit-bacteria-library-prep-guide.pdf. Accessed 06/10/15.

111. **Huber W, Carey VJ, Gentleman R, Anders S, Carlson M, Carvalho BS, Bravo HC, Davis S, Gatto L, Girke T, Gottardo R, Hahne F, Hansen KD, Irizarry RA, Lawrence M, Love MI, MacDonald J, Obenchain V, Oles AK, Pages H, Reyes A, Shannon P, Smyth GK, Tenenbaum D, Waldron L, Morgan M.** 2015. Orchestrating high-throughput genomic analysis with bioconductor. Nat Methods **12:**115-121.

112. **R Core Team.** 2015. R: A language and environment for statistical computing. R Foundation for Statistical Computing, Vienna, Austria. http://www.R-project.org/.

113. **Robinson MD, Smyth GK.** 2008. Small sample estimation of negative binomial dispersion, with applications to SAGE data. Biostatistics **9:**321-332.

114. **Goff SA, Vaughn M, McKay S, Lyons E, Stapleton AE, Gessler D, Matasci N, Wang LY, Hanlon M, Lenards A, Muir A, Merchant N, Lowry S, Mock S, Helmke M, Kubach A, Narro M, Hopkins N, Micklos D, Hilgert U, Gonzales M, Jordan C, Skidmore E, Dooley R, Cazes J, McLay R, Lu ZY, Pasternak S, Koesterke L, Piel WH, Grene R, Noutsos C, Gendler K, Feng X, Tang CL, Lent M, Kim SJ, Kvilekval K, Manjunath BS, Tannen V, Stamatakis A, Sanderson M, Welch SM, Cranston KA, Soltis P, Soltis D, O'Meara B, Ane C, Brutnell T, Kleibenstein DJ, et al.** 2011. The iPlant collaborative: cyberinfrastructure for plant biology. Front Plant Sci **2**.

115. **Huang DW, Sherman BT, Lempicki RA.** 2009. Systematic and integrative analysis of large gene lists using DAVID bioinformatics resources. Nature Protoc **4:**44-57.

116. **Huang DW, Sherman BT, Lempicki RA.** 2009. Bioinformatics enrichment tools: paths toward the comprehensive functional analysis of large gene lists. Nucleic Acids Res **37:**1-13.

117. **Ayari S, Dussault D, Millette M, Hamdi M, Lacroix M.** 2009. Changes in membrane fatty acids and murein composition of *Bacillus cereus* and *Salmonella* Typhi induced by gamma irradiation treatment. Int J Food Microbiol **135:**1-6.

118. **Holmgren A.** 1989. Thioredoxin and glutaredoxin systems. J Biol Chem **264:**13963-13966.

119. **Nordberg J, Arner ESJ.** 2001. Reactive oxygen species, antioxidants, and the mammalian thioredoxin system. Free Radical Bio Med **31:**1287-1312.

120. **Paxman JJ, Borg NA, Horne J, Thompson PE, Chin Y, Sharma P, Simpson JS, Wielens J, Piek S, Kahler CM, Sakellaris H, Pearce M, Bottomley SP, Rossjohn J, Scanlon MJ.** 2009. The structure of the bacterial oxidoreductase enzyme DsbA in complex with a peptide reveals a basis for substrate specificity in the catalytic cycle of DsbA enzymes. J Biol Chem **284:**17835-17845.

121. **Miki T, Okada N, Danbara H.** 2004. Two periplasmic disulfide oxidoreductases, DsbA and SrgA, target outer membrane protein SpiA, a component of the *Salmonella* pathogenicity island 2 type III secretion system. J Biol Chem **279:**34631-34642.

122. **Fath MJ, Kolter R.** 1993. ABC transporters - bacterial exporters. Microbiol Rev **57:**995-1017.

123. **Buttner FM, Renner-Schneck M, Stehle T.** 2015. X-ray crystallography and its impact on understanding bacterial cell wall remodeling processes. Int J Med Microbiol **305:**209-216.

124. **Moffitt JR, Lee JB, Cluzel P.** 2012. The single-cell chemostat: an agarose-based, microfluidic device for high-throughput, single-cell studies of bacteria and bacterial communities. Lab Chip **12:**1487-1494.

125. **Bruns MA, Maxcy RB.** 1979. Effect of irradiation temperature and drying on survival of highly radiation-resistant bacteria in complex menstrua. J Food Sci **44:**1743-1746.

126. **Cook AM, Widdowson JP.** 1967. Factors affecting recovery of gamma irradiated *Escherichia coli*. J Appl Bacteriol **30:**206-218.

127. **Ray B.** 1979. Methods to detect stressed microorganisms. J Food Protect **42:**346-355.

128. **Ray B.** 1989. Enumeration of injured indicator bacteria from foods, p 9-54. *In* Ray B (ed), Injured index and pathogenic bacteria: occurrence and detection in foods, water and feed. CRC Press, Boca Raton, FL.

129. **U.S. EPA.** 2006. Method 1682: Salmonella in sewage sludge (biosolids) by modified semisolid rappaport-vassiliadis (MSRV) medium. Washington, DC.

APPENDIX A

SUPPORTING EXPERIMENTS

Neutron Flux from the Nuclear Reactor Core

Even though the boron plate is supposed to shield the neutrons created by the fission reactions in the nuclear reactor core, an experiment was performed to verify that the bacterial cell suspensions received a dose consisting only of gamma rays and not neutrons. A piece of gold foil was placed in the same position as the samples and irradiated under the same conditions with the reactor core to estimate the neutron flux. The gold foil received 6051 Becquerel (Bq)/g (SI unit of radioactivity). This translates to 635,001 neutrons/cm^2/sec. Since the absorbed dose per neutron depends on the neutron energy, the atomic composition of the target, the size and shape of the target, and the room the target is located in converting the number of neutrons to absorbed dose is complicated. A detailed evaluation would involve a major computer simulation project. However, there are data tables specifically for the irradiation of humans with neutrons of different energies. The bacterial samples and humans have roughly the same atomic composition, which is the most important factor in determining the absorbed dose. The neutron spectrum is another factor. There are a wide variety of neutron energies emitted from a nuclear reactor, and most of them will have lost some energy between the reactor and the bacterial samples. For our calculations, we assumed an average neutron energy of 1 MeV. This value is likely an overestimation of the neutron energy. Assuming a higher neutron energy will ensure that the calculated absorbed dose is an overestimation

rather than an underestimation. The walls of the irradiation room were relatively far away from the samples, so room scattered neutrons did probably not contribute much to the absorbed dose. The size of the samples vs. the size of a human was the biggest source of error in this estimation. Since the samples were small, scattered neutrons may have leaked out of them, resulting in little neutron buildup or attenuation in the samples. Due to these reasons, it seemed reasonable to use neutron fluence factors to estimate the absorbed dose. According to the 1984 Health Physics and Radiological Health Handbook, $26x10^6$ neutrons/cm^2 (1 MeV) produce 1 rem. This table is based on Q=10, so $26x10^6$ neutrons produce 0.1 rad or 0.001 Gray (Gy) or 1 milliGray (mGy). The measured neutron flux/fluence from the gold foil was $0.635x10^6$ neutrons/cm^2/sec, so it was producing ca. 0.024 mGy/sec or ca. 88 mGy (0.088 Gy) per hour. This is such a small fraction of the total gamma ray dose that even an error of a factor of 10 in the conversion of neutron fluence to dose would be insignificant. This experiment verified that the neutrons contributed a fraction of one percent to the total gamma dose received by the bacterial cell suspensions. For example, to receive a gamma dose of 2000 Gy (the highest dose used in this research), samples were exposed for 3 hours. Over a period of 3 hours, neutrons contributed 0.26 Gy to the overall gamma dose of 2000 Gy, truly an insignificant amount.

Determination of Lethal Irradiation Dose for *Salmonella* Typhimurium

Overnight cultures of *S*. Typhimurium (ATCC 14028) were grown in Tryptic Soy Broth (TSB) at 35°C in a shaking water bath. The cultures were centrifuged at 4000 x g for 10 minutes at Room Temperature (RT), the growth media removed and the cell pellets washed once in Phosphate Buffered Saline (PBS). After washing, the cell pellets were resuspended in PBS to an OD_{600} of ca. 1.0, resulting in approximately $1x10^8$ Colony Forming Units (CFU)/ml. Aliquots of the adjusted cell suspensions were packaged for irradiation as previously described in Chapter IV. Samples were either irradiated using a 10 MeV eBeam linear accelerator at the NCEBR or with gamma radiation using the reactor core at the NSC as previously described (Chapter IV). Dose measurements were obtained as previously described in Chapter IV. Non-irradiated samples (0 kGy) were used as controls. These samples were packaged the same way as the experimental samples and were transported to the irradiation facility to eliminate possible differences in survival due to transport and handling. Following irradiation, the sample bags were aseptically opened and 0.5 ml aliquots were transferred to sterile 15ml conical tubes containing 4.5 ml 1x TSB. The tubes were either incubated in a 37°C water bath or at RT on the bench. Tubes were monitored for growth and at appropriate time points (day 0, 1, 2, 3, 5, 7, 14) aliquots were plated on Tryptic Soy Agar (TSA) plates and incubated either at 35°C or RT for 4 days. TSB tubes and TSA plates were scored (positive or negative) for growth. To determine the starting cell numbers, the non-irradiated (control) samples were diluted in PBS and plated on TSA on the day of the irradiation.

For the first experiment, the target doses were 2.0, 3.0, 4.0, 5.0, and 6.0 kGy. The starting concentrations of *S.* Typhimurium for the eBeam and gamma irradiations were 8.90±0.10 $\log_{10}$ CFU/ml and 8.89±0.04 $\log_{10}$ CFU/ml, respectively. For all the doses tested, there were no residual survivors of *S.* Typhimurium neither for eBeam nor gamma irradiation. Based on these results, the target doses for the second experiment were lowered to 1.3, 1.5, 1.7, 2.0, and 3.0 kGy. The starting concentrations of *S.* Typhimurium for the eBeam and gamma irradiations were 8.86±0.07 $\log_{10}$ CFU/ml and 8.81±0.13 $\log_{10}$ CFU/ml, respectively. Residual survivors of *S.* Typhimurium were observed up to 1.42±0.014 kGy for gamma irradiation and up to 1.305±0.007 kGy for eBeam irradiation. The results from both experiments are summarized in Table 17 for eBeam irradiation and in Table 18 for gamma irradiation.

Table 17. Summarized results from two experiments to determine the lowest lethal eBeam irradiation dose for *S.* Typhimurium in PBS (ca. 10^8 CFU/ml).

Target Dose (kGy)			**1.3**	**1.7**	**2.0**	**2.0**	**3.0**	**3.0**	**4.0**	**5.0**	**6.0**
Absorbed Dose (kGy)			**1.31**	**1.76**	**2.01**	**2.56**	**2.99**	**3.06**	**3.92**	**5.00**	**6.23**
Day 0	Plate	RT	-	-	-	-	-	-	-	-	-
		37	-	-	-	-	-	-	-	-	-
Day 1	Tube	RT	+	-	-	-	-	-	-	-	-
		37	-	-	-	-	-	-	-	-	-
	Plate	RT/RT	+	-	-	-	-	-	-	-	-
		RT/37	+	-	-	-	-	-	-	-	-
		37/37	-	-	-	-	-	-	-	-	-
		37/RT	-	-	-	-	-	-	-	-	-
Day 2	Tube	RT	-	-	-	-	-	-	-	-	-
		37	-	-	-	-	-	-	-	-	-
	Plate	RT/RT	-	-	-	-	-	-	-	-	-
		RT/37	-	-	-	-	-	-	-	-	-
		37/37	-	-	-	-	-	-	-	-	-
		37/RT	-	-	-	-	-	-	-	-	-
Day 3	Tube	RT	-	-	-	-	-	-	-	-	-
		37	-	-	-	-	-	-	-	-	-
	Plate	RT/RT	-	-	-	-	-	-	-	-	-
		RT/37	-	-	-	-	-	-	-	-	-
		37/37	-	-	-	-	-	-	-	-	-
		37/RT	-	-	-	-	-	-	-	-	-
Day 5	Tube	RT	-	-	-	-	-	-	-	-	-
		37	-	-	-	-	-	-	-	-	-
	Plate	RT/RT	-	-	-	-	-	-	-	-	-
		RT/37	-	-	-	-	-	-	-	-	-
		37/37	-	-	-	-	-	-	-	-	-
		37/RT	-	-	-	-	-	-	-	-	-
Day 7	Tube	RT	-	-	-	-	-	-	-	-	-
		37	-	-	-	-	-	-	-	-	-
	Plate	RT/RT	-	-	-	-	-	-	-	-	-
		RT/37	-	-	-	-	-	-	-	-	-
		37/37	-	-	-	-	-	-	-	-	-
		37/RT	-	-	-	-	-	-	-	-	-
Day 14	Tube	RT	-	-	-	-	-	-	-	-	-
		37	-	-	-	-	-	-	-	-	-
	Plate	RT/RT	-	-	-	-	-	-	-	-	-
		RT/37	-	-	-	-	-	-	-	-	-
		37/37	-	-	-	-	-	-	-	-	-
		37/RT	-	-	-	-	-	-	-	-	-

RT=room temperature incubation; 37=37°C incubation; RT/RT=tube incubated at RT streaked out on TSA plate which was then incubated at RT; RT/37=tube incubated at RT streaked out on TSA plate which was then incubated at 37°C; 37/37=tube incubated at 37°C streaked out on TSA plate which was then incubated at 37°C; 37/RT=tube incubated at 37°C streaked out on TSA plate which was then incubated at RT; +=positive for growth; -=negative for growth

Table 18. Summarized results from two experiments to determine the lowest lethal gamma irradiation dose for *S.* Typhimurium in PBS (ca. 10^8 CFU/ml).

Target Dose (kGy)			**1.5**	**1.7**	**2.0**	**2.0**	**3.0**	**3.0**	**4.0**	**5.0**	**6.0**
Absorbed Dose (kGy)			**1.18**	**1.42**	**1.71**	**2.02**	**2.57**	**2.96**	**4.23**	**5.30**	**6.53**
Day 0	Plate	RT	-	-	-	-	-	-	-	-	-
		37	-	-	-	-	-	-	-	-	-
Day 1	Tube	RT	+	-	-	-	-	-	-	-	-
		37	+	-	-	-	-	-	-	-	-
	Plate	RT/RT	+	-	-	-	-	-	-	-	-
		RT/37	+	-	-	-	-	-	-	-	-
		37/37	+	-	-	-	-	-	-	-	-
		37/RT	+	-	-	-	-	-	-	-	-
Day 2	Tube	RT	-	-	-	-	-	-	-	-	-
		37	-	-	-	-	-	-	-	-	-
	Plate	RT/RT	-	-	-	-	-	-	-	-	-
		RT/37	-	-	-	-	-	-	-	-	-
		37/37	-	-	-	-	-	-	-	-	-
		37/RT	-	-	-	-	-	-	-	-	-
Day 3	Tube	RT	-	+	-	-	-	-	-	-	-
		37	+	-	-	-	-	-	-	-	-
	Plate	RT/RT	-	+	-	-	-	-	-	-	-
		RT/37	-	+	-	-	-	-	-	-	-
		37/37	+	-	-	-	-	-	-	-	-
		37/RT	+	-	-	-	-	-	-	-	-
Day 5	Tube	RT	+	-	-	-	-	-	-	-	-
		37	+	-	-	-	-	-	-	-	-
	Plate	RT/RT	+	-	-	-	-	-	-	-	-
		RT/37	+	-	-	-	-	-	-	-	-
		37/37	+	-	-	-	-	-	-	-	-
		37/RT	+	-	-	-	-	-	-	-	-
Day 7	Tube	RT	-	+	-	-	-	-	-	-	-
		37	+	-	-	-	-	-	-	-	-
	Plate	RT/RT	-	+	-	-	-	-	-	-	-
		RT/37	-	+	-	-	-	-	-	-	-
		37/37	+	-	-	-	-	-	-	-	-
		37/RT	+	-	-	-	-	-	-	-	-
Day 14	Tube	RT	+	-	-	-	-	-	-	-	-
		37	-	-	-	-	-	-	-	-	-
	Plate	RT/RT	+	-	-	-	-	-	-	-	-
		RT/37	+	-	-	-	-	-	-	-	-
		37/37	-	-	-	-	-	-	-	-	-
		37/RT	-	-	-	-	-	-	-	-	-

RT=room temperature incubation; 37=37°C incubation; RT/RT=tube incubated at RT streaked out on TSA plate which was then incubated at RT; RT/37=tube incubated at RT streaked out on TSA plate which was then incubated at 37°C; 37/37=tube incubated at 37°C streaked out on TSA plate which was then incubated at 37°C; 37/RT=tube incubated at 37°C streaked out on TSA plate which was then incubated at RT; +=positive for growth; -=negative for growth

In order to determine the lowest possible lethal irradiation dose for *Salmonella* Typhimurium in PBS (ca. 10^8 CFU/ml), post-irradiation incubation conditions were carefully chosen to ensure the detection of any and all survivors. Post-irradiation recovery conditions, such as incubation temperature and composition of growth media, are known to affect bacterial survival (7, 65, 125-127). With regards to incubation temperature, Lucht et. al. showed that incubating gamma irradiated *S*. Typhimurium at a suboptimal growth temperature of 22°C for 20 hours prior to incubation at 37°C for 24 hours resulted in an increased survival level compared to a 44 hour incubation at the optimal growth temperature of 37°C alone (65).

To ensure the detection of any and all survivors, an enrichment step in liquid growth media at both incubation temperatures (suboptimal and optimal) was included in the recovery protocol. Enrichment steps are frequently used in the recovery of bacteria from food and water (63, 128, 129). Hence, irradiated *S*. Typhimurium cells were incubated in 1x TSB for up to 14 days either at 37°C (optimal growth temperature) or at RT (suboptimal growth temperature). Following the enrichment step, cells were streaked on TSA plates which were either incubated at 37°C or RT for 4 days. The results showed that whenever there was growth (visible increase in turbidity) during the enrichment step, there was growth on the respective agar plates as well regardless of their incubation temperature. In other words, when there was no growth during the enrichment step, there was no growth on solid agar plates (Tables A.1 and A.2).

The results revealed that an absorbed dose of 2 kGy for either eBeam or gamma irradiation consistently resulted in no survivors for *S.* Typhimurium (ca. 10^8 CFU/ml) irradiated in PBS. Based on the D_{10} value for *S.* Typhimurium in PBS (ca. 170 Gy) obtained in Chapter IV, a dose of 2.0 kGy would theoretically result in an 11.76 log reduction of the organism. Considering that the starting concentrations of *S.* Typhimurium at an OD_{600} of 1.0 are typically around 8.5-9.0 $\log_{10}$ CFU/ml and taking into account the 4-8% uncertainty in dosimetry, it was decided that a target dose of 2.0 kGy provided a large enough safety margin to always result in a lethal irradiation dose for *S.* Typhimurium in PBS. Hence, a target dose of 2.0 kGy was determined to be appropriate for subsequent experiments.

Viable Cell Counts and Optical Density Measurements for *Salmonella* Typhimurium Following a Lethal Dose of Ionizing Radiation

In addition to collecting RNA samples for RNA-Seq analysis, viable cell counts (on TSA) along with optical density (OD_{600}) readings (Eppendorf Spectrophotometer) were obtained at the 0, 4, and 24 hour time points. The viable cell counts for the non-irradiated (control) *S.* Typhimurium cells incubated in PBS buffer at 4°C and TSB growth media at 37°C are depicted in Fig. 28 and Fig. 29, respectively. The OD_{600} readings for both the irradiated and non-irradiated (control) *S.* Typhimurium cells incubated in PBS buffer at 4°C and TSB growth media at 37°C are depicted in Fig. 30 and Fig. 31, respectively.

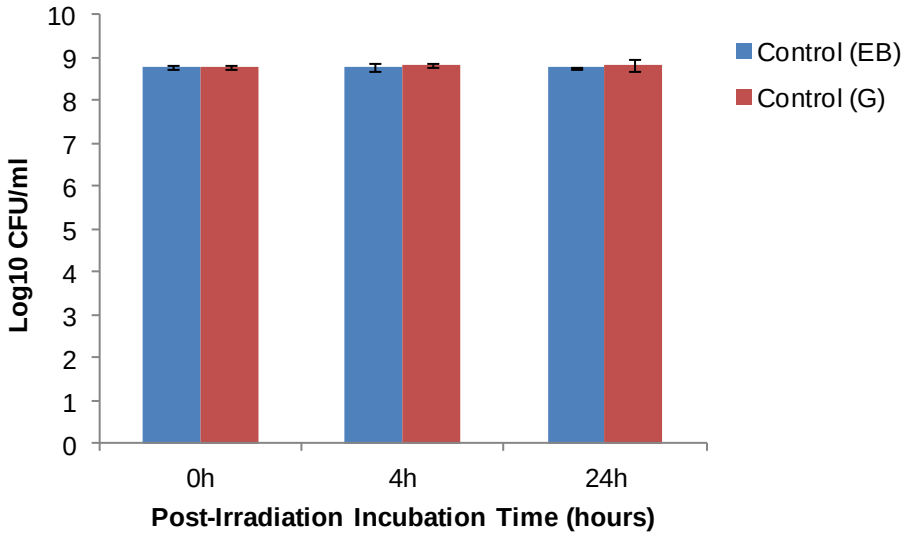

Figure 28. Viable cell counts of the non-irradiated *S.* Typhimurium (control) cells incubated at 4°C in PBS buffer. Lethally irradiated *S.* Typhimurium cells yielded no survivors. Four independent experiments were performed, with standard deviations shown. EB = eBeam; G = Gamma.

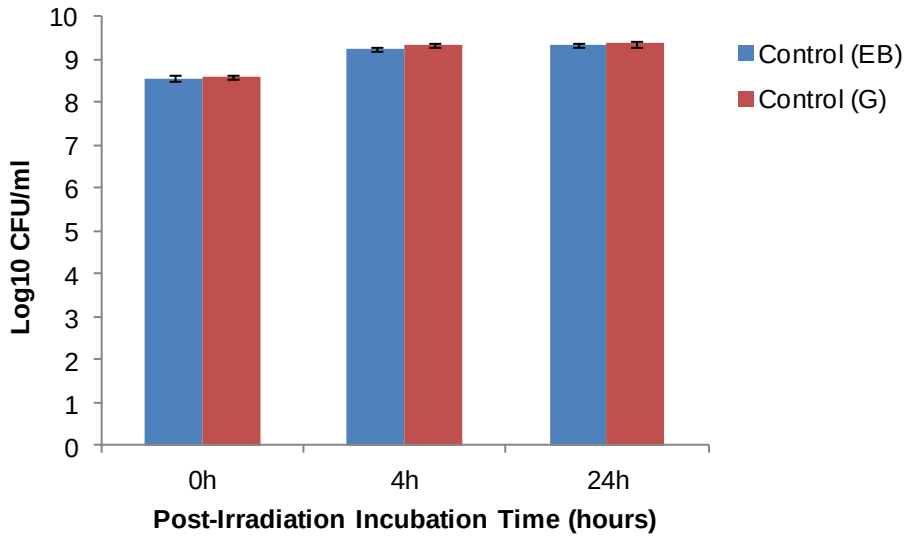

Figure 29. Viable cell counts of the non-irradiated *S.* Typhimurium (control) cells incubated at 37°C in TSB growth media. Lethally irradiated *S.* Typhimurium cells yielded no survivors. Four independent experiments were performed, with standard deviations shown. EB = eBeam; G = Gamma.

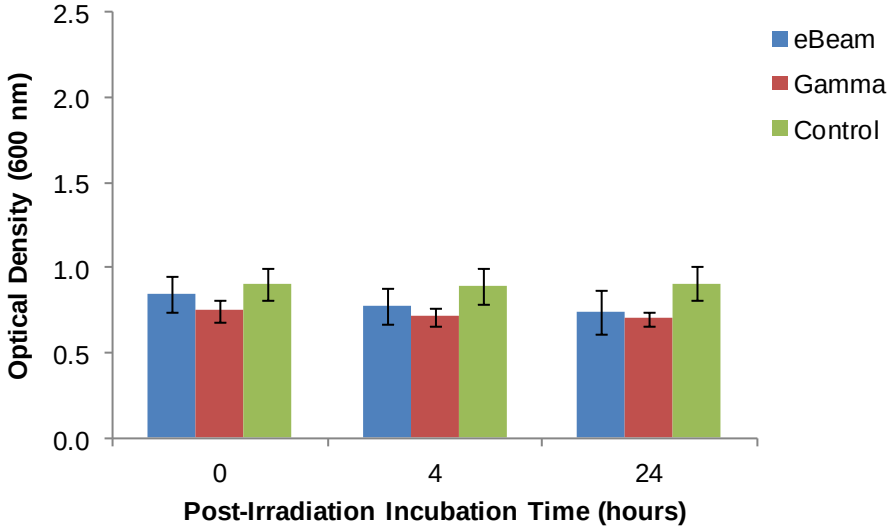

Figure 30. Optical density readings for lethally irradiated and non-irradiated *S.* Typhimurium (control) cells incubated at 4°C in PBS buffer. Four independent experiments were performed, with standard deviations shown.

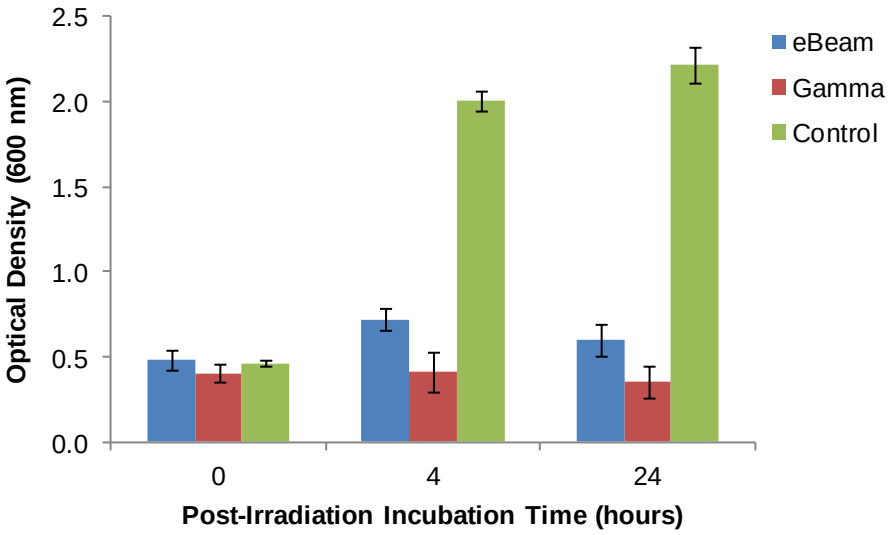

Figure 31. Optical density readings for lethally irradiated and non-irradiated *S.* Typhimurium (control) cells incubated at 37°C in TSB growth media. Four independent experiments were performed, with standard deviations shown.

The viable cell counts confirmed that the starting concentration of *S.* Typhimurium cells was ca. 8.5 $\log_{10}$ CFU/ml (Fig. A.1 and A.2). Following lethal irradiation, there were no viable survivors. The OD readings for the samples incubated in PBS at 4°C remained stable over the 24 hour study period for both irradiated and non-irradiated (control) cells (Fig. A.3). The OD readings for the non-irradiated (control) cells incubated in TSB at 37°C increased over the 24 hour study period. This was expected since these cells were able to divide and multiply. As expected, OD readings for the gamma irradiated samples did not change over the 24 hour study period. However, the eBeam irradiated samples did not behave as expected. Between the 0h and 4h time point, there was an increase in OD of 0.24 (Fig. A.4). We hypothesize that this increase may be due to eBeam irradiated cells either elongating or being able to divide into non-viable offspring (in one or more

growth cycles). The OD readings slightly decreased between the 4 and 24 hour time points. The increase in OD between 0-4 hours post-eBeam irradiation warrants further investigation to determine if cells are elongating or able to divide into truly senescent offspring. Labaw et. al. showed that heavily x-ray irradiated *E. coli* cells elongated during post-irradiation incubation. But they also observed "central pits" in these heavily x-ray irradiated cells and the authors speculate that this may represent "a first, and only, step towards cell division" (106). The dose rate for the x-ray irradiation in this paper was more similar to the gamma dose rate in this study. This phenomenon has not been investigated with eBeam irradiated cells.

APPENDIX B

SUPPORTING INFORMATION

Alanine Dosimetry

The alanine dosimetry system is considered the "gold standard" among dosimetry systems due to its accuracy in measuring absorbed dose over a wide dose range (10 Gy - 100+ kGy) (61). Alanine dosimetry is based on the irradiation of L-α-alanine followed by free radical detection with an Electron Paramagnetic Resonance (EPR) spectrometer (61). Ionizing radiation creates stable free radical with unpaired electrons in alanine (Fig. 32)

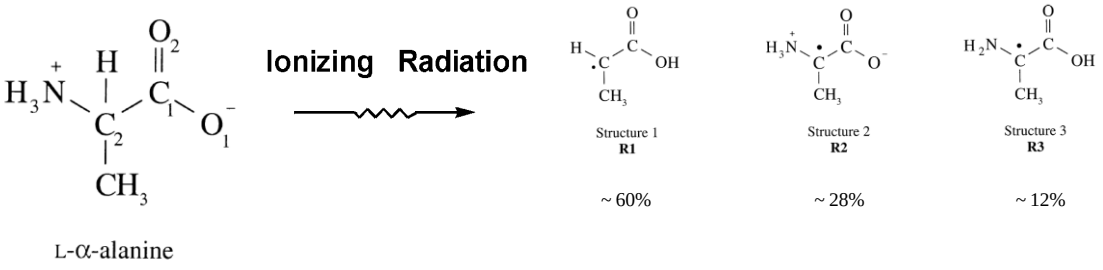

Figure 32. Ionizing radiation creates free radicals in alanine.

Every electron has an intrinsic magnetic moment (spin). When two electrons occupy an atomic or molecular orbital, the spins are opposite and cancel each other out; hence the material is not magnetic. The unpaired electrons, however, make the alanine

paramagnetic (attracted to a magnetic field). However, the alanine does not retain its magnetic properties in the absence of an external magnetic field because thermal motion randomizes the spin orientations. When an external magnetic field is applied, the unpaired electrons will align themselves either with or against this field. The interaction of unpaired electrons with a magnetic field is known as the Zeeman interaction. The Zeeman interaction produces two discrete energy levels, parallel (lowest energy state) or anti-parallel (highest energy state) to the magnetic field. An unpaired electron can move between these two energy (spin) states by either absorbing or emitting electromagnetic radiation energy. However, this movement of unpaired electrons between the two energy states only occurs at a very specific radiation energy. This movement or energy difference (between the two spin states) can be generated by either varying the electromagnetic radiation frequency while applying a constant magnetic field or varying the magnetic field while keeping the electromagnetic radiation frequency constant. For greater sensitivity, Bruker EPR spectrometers keep the electromagnetic radiation frequency constant and vary the magnetic field. When the alanine dosimeter is placed in the Bruker EPR microwave cavity (a metal box located between two magnets), it is exposed to microwave radiation at a constant frequency. By increasing the strength of the external magnetic field, the gap between the two electron spin states is increased until it equals the energy of the microwaves (field of resonance). At this point, the electrons can move between their two spin states. Since the electrons aligned parallel to the magnetic field, they are in the lowest energy spin state and have to absorb energy to

move to the higher energy spin state. This energy absorption is monitored and converted into a spectrum. This spectrum or EPR signal intensity can be correlated with dose (Gy).